

**THE SIDE EFFECTS OF DIFFERENT ANTIEMBOLIC
AGENTS ON THE FRACTURE HEALING AND
MICRO-MECHANICAL BEHAVIOR OF THE FRACTURED
BONE**

by

BURCU TUNÇ

BS., in Physics, Bogaziçi University, 2006

Submitted to the Institute of Biomedical Engineering
in partial fulfillment of the requirements
for the degree of
Master of Science
in
Biomedical Science

Bogaziçi University

June 2009

ACKNOWLEDGMENTS

First of all, I would like to express my sincere gratitude to my thesis advisor, Prof. Dr. A. Hikmet ÜÇİŞİK. This thesis would not be possible without his kind support and the remarkable patience. I would like to thank Assoc. Prof. Dr. Metin USTA from Gebze Institute of Technology for giving the opportunity to carry out my experiments in their laboratories. It is a pleasure to thank to Dr. Emin AKSOY from Ministry of Health İstanbul Health Management for his kind support and for giving the opportunity to communicate with Ministry of Health Services Metin Sabancı Baltalimanı Osteopathic Training and Research Hospital. I would like to thank head doctor Vedat ŞAHİN and Dr. Ahmet Şükrü MERCAN from Ministry of Health Services Metin Sabancı Baltalimanı Osteopathic Training and Research Hospital. I would like to express my sincere gratitude to Dr. Işıl KUTBAY and Levent Salim ALTUĞ from Gebze Institute of Technology, Mızrap CANİBEYAZ from İstanbul Technical University for their support during laboratory experiments. It is a pleasure to thank to Dr. Ramazan ÖZYURT from Ministry of Health İstanbul Health Management, Burhanettin ATAŞ from Taksim State Hospital.

Finally, I would like to dedicate this thesis to my family whose constant encouragement and never-ending love I have relied throughout my life. I am grateful to my friends especially Sırma Başak YANARDAĞ for providing moral and technical support and motivation during my thesis. And I am deeply grateful to Bahadır TÜTÜNCÜ for his love, emotional support and patience.

ABSTRACT

THE SIDE EFFECTS OF DIFFERENT ANTIEMBOLIC AGENTS ON THE FRACTURE HEALING AND MICRO-MECHANICAL BEHAVIOR OF THE FRACTURED BONE

Fracture of bone is always expected when the stress exposed to body is enough for initiation and propagation of the crack. Due to social lives, increase of life expectancy, wars and accidents the number of bone fracture has increased. One of the problem during healing of the fractured bone is hematoma formation. In order to eliminate hematoma formation, antiembolic agents injection into the body is generally imperative. In this thesis, we deal with the inorganic portion of the bone, treated with and without antiembolic agents. 16 Wistar-Albino male rats were used for the study. Scanning electron microscopy and X-ray diffraction technique were applied in order to reveal the effect of antiembolic agents on the bone fractured followed by healing. It is observed that antiembolic agents helped healing of the fractured bone without defect and crystalline nature of the inorganic part of bone showed phase transitions.

Keywords: bone, fracture, bone healing, heparin, LMWH, enoxaparin, fondaparinux, crystallinity, SEM, XRD

ÖZET

FARKLI ANTIEMBOLİK AJANLARIN KEMİK KIRIKLARI İYİLEŞMESİ ÜZERİNE ETKİLERİ VE KIRIK KEMİĞİN MİKRO-MEKANİK DAVRANIŞINA ETKİLERİ

Sosyal yaşamın değişmesi, yaşam beklentilerinin yükselmesi, savaş ve kaza sayılarının artması kemik kırıkları sayısında artışa neden olmuştur. Kırığın iyileşmesi sürecinde karşılaşılan problemlerden biri de pıhtı oluşumudur. Antiembolik ajanlar Ortopedi ve Travmatoloji pratiğinde pıhtılaşmayı engellemek için sıkça kullanılan ilaçlardır. Kemığın inorganik yapısının incelendiği bu tezde, kırık oluşturulan sıçanlar farklı antiembolik ajanlarla tedavi edilmiştir. Bu çalışmada 16 adet Wistar-albino tipi erkek sıçan kullanılmıştır. Antiembolik ajanların kırılıp tedavi edilen kemiklerin üzerine etkilerini gözlemek için, taramalı elektron mikroskop ve X-ışını kırınım teknikleri uygulanmıştır. Antiembolik ajanların kırık iyileşmesine olumlu etki gösterdiği ve kemığın inorganik kısmının kristal yapısını değiştirdiği gözlenmiştir.

Anahtar Sözcükler: kemik, kırık, kaynama, heparin, DMAH, enoxaparin, fondaparinux, kristallografik, SEM, XRD.

TABLE OF CONTENTS

ACKNOWLEDGMENTS	iii
ABSTRACT	iv
ÖZET	v
LIST OF FIGURES	viii
LIST OF TABLES	xiv
LIST OF SYMBOLS	xv
LIST OF ABBREVIATIONS	xvi
1. INTRODUCTION	1
1.1 Objective of the Thesis	1
1.2 Physiology of Bone	4
1.2.1 Macrostructure of Bone	5
1.2.2 Cortical and Cancellous Bone	6
1.2.3 Composition of Bone	8
1.3 Microstructure of Bone	8
1.3.1 Woven and Lamellar Bone	8
1.3.2 Bone Cells	9
1.4 Fracture Healing of Bone	10
1.4.1 Primary Bone Healing	11
1.4.2 Secondary Bone Healing	11
1.4.3 Stages of Bone Fracture Healing	12
1.4.3.1 Inflammatory Phase	12
1.4.3.2 Reparative phase	13
1.4.3.3 Remodelling phase	15
1.4.4 Biomechanical Stages of Fracture Healing	15
1.5 Thromboembolism	17
1.5.1 Risk Factors for Venous Thromboembolism	17
1.5.2 Prevention of Deep Venous Thrombosis and Pulmonary Embolism	19
1.6 Historical Background	22
2. EXPERIMENTAL TECHNIQUES	32

2.1	Specimen preparation	32
2.1.1	Experimental Procedure	32
2.1.2	Surgical Techniques	33
2.2	Macroscopical Studies	38
2.3	Scanning Electron Microscopy (SEM)	39
2.3.1	Introduction	39
2.3.2	Materials and Methods	41
2.3.3	Results and Discussion of the SEM Studies on the Fractured and Healed Bone Samples	41
2.3.3.1	Control group	41
2.3.3.2	Heparin-treated group	49
2.3.3.3	LMWH-treated group	57
2.3.3.4	Fondaparinux-treated group	63
2.4	X- Ray Diffractometry (XRD)	71
2.4.1	Introduction	71
2.4.2	Materials and Methods	72
2.4.3	Results and Discussion	73
3.	DISCUSSION	77
4.	CONCLUSION	82
	REFERENCES	83

LIST OF FIGURES

Figure 1.1	Schematic view of long bone demonstrating epiphysis, diaphysis, articular cartilage, endosteum and periosteum [1].	5
Figure 1.2	Hierarchical structure in human compact bone [2].	9
Figure 1.3	An approximation of the relative amounts of time devoted to the inflammation, reparative, and remodelling phases in fracture healing [3].	12
Figure 1.4	Schematic demonstration of early fracture [4].	13
Figure 1.5	Schematic demonstration of the inflammatory stage of fracture healing [4].	14
Figure 1.6	Schematic demonstration of the reparative stage of fracture healing [4].	15
Figure 1.7	Schematic demonstration of the remodelling stage of fracture healing [4].	16
Figure 2.1	Preparation of knee region of rats for operation	34
Figure 2.2	Apperance of rat femoral condoyle and preparation of intrameduller channel	34
Figure 2.3	Intramedullar location of Kirschner wire	35
Figure 2.4	View after the location of Kirschner wire	35
Figure 2.5	Suturation of femoral condyles	36
Figure 2.6	Creation of closed fracture by the Guillotine system	36
Figure 2.7	Approval of fractures by the radiographies which are obtained from rats after the operation	37
Figure 2.8	An example for an ideal rat femur fracture	37
Figure 2.9	Bone samples of control group, in formaldehyde solution	38
Figure 2.10	Bone samples of heparin-treated group, in formaldehyde solution	38
Figure 2.11	Bone samples of LMWH-treated group, in formaldehyde solution	38
Figure 2.12	Bone samples of fondaparinux-treated group, in formaldehyde solution	39

Figure 2.13	Montage-like SEM picture of lateral surface of conventionally healed bone (without injection of antiembolic agents) rat number 1 obtained with relatively low magnification	41
Figure 2.14	The SEM micrographs under various magnifications of the control sample 1, obtained far from healed region, being fractured and healed.	42
Figure 2.15	The SEM micrographs under various magnifications of the control sample 1, obtained from closed to healed region, being fractured and healed.	43
Figure 2.16	The SEM micrographs under various magnifications of the controlled sample 1, obtained almost from healed region, being fractured and healed.	43
Figure 2.17	The SEM micrographs under various magnifications of the controlled sample 1, apart from healed region, being fractured and healed	44
Figure 2.18	Montage-like SEM picture of lateral surface of the bone with conventional method (without injection of antiembolic agents), rat number 2, with relatively low magnification	44
Figure 2.19	The SEM micrographs under various magnifications of the control sample 2, obtained far from healed region, being fractured and healed.	45
Figure 2.20	The SEM micrographs under various magnifications of the control sample 2, obtained from closed to healed region, being fractured and healed being fractured and healed.	46
Figure 2.21	The SEM micrographs under various magnifications of the control sample 1, obtained from almost healed region, being fractured and healed	46
Figure 2.22	The SEM micrographs under various magnifications of the control sample 2, obtained from closed to healed region, being fractured and healed.	47
Figure 2.23	The SEM micrographs obtained from similar regions of control groups under x500 magnification	48

Figure 2.24	The SEM micrographs obtained from similar regions of control groups under x1000 magnification	48
Figure 2.25	Montage-like SEM picture of lateral surface of the fractured and healed with heparin injection sample 1, with relatively low magnification.	49
Figure 2.26	The SEM micrographs under various magnifications of the heparin-injected sample 1, obtained far from healed region, being fractured and healed.	50
Figure 2.27	The SEM micrographs under various magnifications of the heparin-injected sample 1, obtained from closed to healed region, being fractured and healed.	50
Figure 2.28	The SEM micrographs under various magnifications of the heparin-injected sample 1, obtained almost from healed region, being fractured and healed.	51
Figure 2.29	The SEM micrographs under various magnifications of the heparin-injected sample 1, obtained apart from healed region, being fractured and healed.	52
Figure 2.30	Montage-like SEM picture of lateral surface of the fractured and healed with heparin injection sample 2 obtained with relatively low magnification.	52
Figure 2.31	The SEM micrographs under various magnifications of the heparin-injected sample 2, far from healed region, being fractured and healed.	53
Figure 2.32	The SEM micrographs under various magnifications of the heparin-injected sample 2, from closed to healed region, being fractured and healed.	54
Figure 2.33	The SEM micrographs under various magnifications of the heparin-injected sample 1, from almost healed region, being fractured and healed.	54
Figure 2.34	The SEM micrographs under various magnifications of the heparin-injected sample 1, apart from healed region, being fractured and healed.	55

Figure 2.35	The SEM micrographs obtained from similar regions of heparin groups under x500 magnification	56
Figure 2.36	The SEM micrographs obtained from similar regions of heparin groups under x1000 magnification	56
Figure 2.37	Montage-like SEM picture of lateral surface of the fractured and healed with LMWH injection sample 1, with relatively low magnification.	57
Figure 2.38	The SEM micrographs under various magnifications of the LMWH-injected sample 1, closed to healed region, being fractured and healed.	58
Figure 2.39	The SEM micrographs under various magnifications of the LMWH-injected sample 1, almost healed region, being fractured and healed.	58
Figure 2.40	The SEM micrographs under various magnifications of the LMWH-injected sample 1, far from healed region, being fractured and healed.	59
Figure 2.41	Montage-like SEM picture of the fractured and healed with LMWH injection sample 2, with relatively low magnification.	60
Figure 2.42	The SEM micrographs under various magnifications of the LMWH-injected sample 2, from almost healed region, being fractured and healed.	60
Figure 2.43	The SEM micrographs under various magnifications of the LMWH-injected sample 2, from closed to healed region, being fractured and healed.	61
Figure 2.44	The SEM micrographs under various magnifications of the LMWH-injected sample 2, closed to healed region, being fractured and healed.	61
Figure 2.45	The SEM micrographs obtained from similar regions of LMWH groups under x500 magnification	62
Figure 2.46	The SEM micrographs obtained from similar regions of LMWH groups under x1000 magnification	63

Figure 2.47	Montage-like SEM picture of lateral surface of the fractured and healed with fondaparinux injection sample 1, with relatively low magnification.	63
Figure 2.48	The SEM micrographs under various magnifications of the fondaparinux-injected sample 1, obtained from closed to healed region, being fractured and healed.	64
Figure 2.49	The SEM micrographs under various magnifications of the fondaparinux-injected sample 1, obtained almost from healed region, being fractured and healed	65
Figure 2.50	The SEM micrographs under various magnifications of the fondaparinux-injected sample 1, obtained from closed to healed region, being fractured and healed.	66
Figure 2.51	The SEM micrographs under various magnifications of the fondaparinux-injected sample 1, obtained far from healed region, being fractured and healed.	66
Figure 2.52	Montage-like SEM picture of lateral section of the fractured and healed with fondaparinux injection sample 2 with relatively low magnification.	67
Figure 2.53	The SEM micrographs under various magnifications of the fondaparinux-injected sample 2, far from healed region, being fractured and healed.	68
Figure 2.54	The SEM micrographs under various magnifications of the fondaparinux-injected sample 2, closed healed region, being fractured and healed.	68
Figure 2.55	The SEM micrographs under various magnifications of the fondaparinux-injected sample 2, closed to healed region of the bone, being fractured and healed.	69
Figure 2.56	The SEM micrographs under various magnifications of the fondaparinux-injected sample 2, obtained almost from healed region of the bone, being fractured and healed.	70
Figure 2.57	The SEM micrographs obtained from similar regions of fondaparinux groups under x500 magnification	70

Figure 2.58	The SEM micrographs obtained from similar regions of fondaparinux groups under x1000 magnification	71
Figure 2.59	The X-ray diffractogram of the fractured and healed control sample	73
Figure 2.60	The X-ray diffractogram of the fractured and healed control sample and the heparin-treated sample	74
Figure 2.61	The X-ray diffractogram of the fractured and healed control sample and the LMWH-treated sample	75
Figure 2.62	The X-ray diffractogram of the fractured and healed control sample and the fondaparinux-treated sample	76
Figure 2.63	The X-ray diffractograms of the control, heparin-treated, LMWH-treated and fondaparinux-treated sample	76

LIST OF TABLES

Table 2.1	The distribution of experiment animals	33
-----------	--	----

LIST OF SYMBOLS

λ	the wavelength of X-rays, and moving electrons, protons and neutrons
θ	the angle between the incident ray and the scattering planes

LIST OF ABBREVIATIONS

ACT	Activated Clotting Time
ALP	Alkaly Phospatase
aPPT	Activated Partial Thromboplastin Time
AT	Antithrombin
BCC	Body Centered Cubic
BE	Backscattered Electrons
BEI	Backscattered Electron Imaging
BLC	Bone Lining Cell
BMD	Bone Mineral Density
cm	centimeter
COX-2	Cyclooxygenases 2
DMAH	Düşük molekül ağırlıklı heparin
DVT	Deep Venous Thrombosis
FCC	Face Centered Cubic
g	gram
HCP	Hexagonal Closed-Packed
kg	kilogram
kV	kilovolt
LMWH	Low Molecular Weighted Heparin
mA	milliampere
mg	milligram
mm	millimeter
NaCl	Sodium Chloride
nm	nanometer
NSAID	Nonsteroidal Antiflammatory Drugs
PE	Pulmonary Embolism
PYD	Pyridinoline
SE	Secondary Electrons

SEI	Secondary Electron Imaging
SEM	Scanning Electron Microscopy
UH	Unfractionated Heparin
XRD	X-Ray Diffraction
VTE	Venous Thromboembolism

1. INTRODUCTION

1.1 Objective of the Thesis

Due to rapid changes in the social lives in the world population and life expectancy increased as well as conflicts among the countries, the number of traveling people as well as terrorist activities and wars reached the level that we did not have before and early World War I. Because of the number of aged population osteoporosis in bone, which increases susceptibility to the fracture of bone. Traffic accidents, wars and terrorist activities become not only the cause of death also due to be posed to the high strain rate impacts several different type of bone fracture occurred, occur and will occur. Advanced countries have statistics on the number of bone fracture resulting in economical lost.

Mechanical behavior of material and fracture mechanics give information on the physics and the deformation of fracture generally [5]. As of early 20th century many researches help to understand crack initiation and propagation resulting in fracture in materials. However, although explanation of the fracture behavior of the single crystals, purely amorphous, crystalline with one and multi phases materials would be possible, complicated-anisotropic composite materials like human bone which is living and dynamical material needs to be paid more attention to understand how and why fracture occur.

After fracture in bone, in order to weld fractured fragments of the bone i.e. healing occurs via the manipulations and/or surgery performed by orthopaedics surgeons. Unfortunately the mechanisms of bone healing in the macro, micro and nano level are not clear. To our knowledge it is not paid attention to the thermodynamics of healing and the contribution of both inorganic and organic parts to the healing. Besides that during healing one important discrepancy is formation of hematoma.

Antiembotic agents are routinely used in orthopaedics and traumatology clinics, especially after arthroplastic operations, in case of having tumor and major trauma in order to decrease the potential clinical problems that are caused by embolism. This study was designed to evaluate the side effects of different antiembolic agents on the bone fracture healing.

In order to get rid off hematoma formation certain medicines are advised, but effect of medicine inserted into the body during bone healing, to our knowledge, is not known in terms of what happens in the bone in micro and nano level, which in turn alter crack initiation and propagation mechanisms of the bone. To study and to reach satisfactory conclusions on this subject it is necessary to design various research programmes.

The aim of this research is to start to reveal the effect of agents on the structure of inorganic part of bone. Since bone is consisting of organic and inorganic parts, during current study it is concentrated only on the inorganic part. The rest would be studied by another researches to complete whole picture.

After using an experimental animal model, where "enoxaparin", "fondaparinux" and "heparin" are used as antiembolic agents, fractured and healed bones are studied micro-structurally by the help of x-ray diffraction (XRD) and scanning electron microscopy (SEM).

To reach this idea, initially, rat, which was used as experimental animal was injected by different antiembolic agents. After sacrifice (with the permission of ethical committee) of animal, the bones were studied in material laboratories to reveal structural changes. XRD studies were performed to reveal, if there is any change in the crystallinity of bone. SEM studies also were performed in order to reveal micro-structural and morphological features.

Bone fracture is not only a medical condition but it is also a well known physical time and rate dependent phenomenon, in which cohesive strength in bone locally or

totally becomes zero. Certainly the main cause of the fracture is the exceeding the amount of stress over the value, which can be carried by the material [6, 7]. Since bone is time dependent and easily remodeled material addition to its highly anisotropic composite structure, mechanism of bone fracture behavior is too complex. After injecting antiembolic agents mentioned above all the physiological conditions like the transport phenomena, piezoelectrical properties of the bone, type of collagen and texture of minerals inside the bone may be affected and may cause mechanically weakening of bone [8, 9, 10, 11].

Due to traffic accidents, wars, sportive activities, some chronic illnesses affecting bone metabolism, rapid changes in living environment may cause sudden fracture and also weakening of bone, so that economical impact of bone failure to the society may drastically increase.

Compact bone behaves like a ceramic/polymer composite with discontinuous fibers. Stress-strain behavior of bone depends on the types of bone, the age, the directionality and accompanying illnesses if there is any [7]. However generally it is accepted in tension bone exhibits a stress-strain curve that is initially linear and then shows a departure from linearity that is called yielding. It is characterized by micro-structural damage that is actually the beginning of the fracture, which finally occurs after a further increase in stress [6, 7]. There is a certain amount of toughness in compact bone, partly due to collagen fibers, which can stabilize micro-cracks in the mineral phase until their number becomes overwhelming. The quantitative value of the toughness is related with accumulation of damage, crack initiation and crack propagation [7].

The effect of antiembolic agents on the bone and fracture healing is an issue with different opinions from medical researchers. While the negative effects of heparin on bone healing is a well known issue, the other medical agents for replacing heparin like LMWH (low molecular weighted heparin) and fondaparinux are considered as antiembolic agents having no effects on bone healing [12, 13, 14].

The objective of this study is to reveal the side effects of the antiembolic agents used extensively to get rid of embolism on the structural changes in bone. By using these agents, it would be possible to avoid embolism, but on the other hand there are debates remained about the effects of these antiembolic agents on successful healing of fractured bone [15, 16].

Fracture healing is a kind of welding, which is affected by interactions of the cells, micro-fluidics, diffusion, transport phenomena that are quantitatively, according to our knowledge, unknown. Injecting any kind of medicine certainly influence on the parameters mentioned above. Antiembolic agents are one of the externally injected liquids which certainly play an important role on the physiological behavior. Combining material science and engineering methods with medical sciences especially with the orthopaedics will help to understand the mechanisms occurring in the system being, here, process of bone healing after injecting antiembolic agents.

1.2 Physiology of Bone

Bone is as a connective tissue, and it is unique among the connective tissues because it is hard. It is one of the most dynamic and metabolically active tissue in the body. Blood circulation makes it most evident that bone is a living tissue. As a highly vascular tissue it has an extensive capacity for self repair and also it can alter its properties and configuration [1].

The skeleton serves eight functions: (i) support: framework for the body; (ii) protection: for internal organs and bone marrow; (iii) mechanical: provides kinematic links and attachment sites for muscles for locomotion; (iv) metabolic: acts as a mineral reservoir, playing a vital role in the maintenance of steady-state levels of ions in the body, especially calcium and phosphate; and (v) hematopoiesis: the formation and development of blood cells, especially in the bone marrow, (vi) growth factor storage: mineralized bone matrix stores important growth factors such as insulin-like growth factors, transforming growth factor, bone morphogenic proteins and others, (vii) fat

storage: the yellow bone marrow acts as a storage reserve of fatty acids (vii) acid-base balance: bone buffers the blood against excessive pH changes by absorbing or releasing alkaline salts [17].

1.2.1 Macrostructure of Bone

Bones can be classified according to their shapes as: long (e.g. femur and humerus), short (e.g. tarsus and carpus), flat (e.g. the ribs and the bones of the skull), and irregular (e.g. the vertebrae along the spine). The long bones serve as a classical model for describing the general macroscopic structure of bone (Figure 1.1).

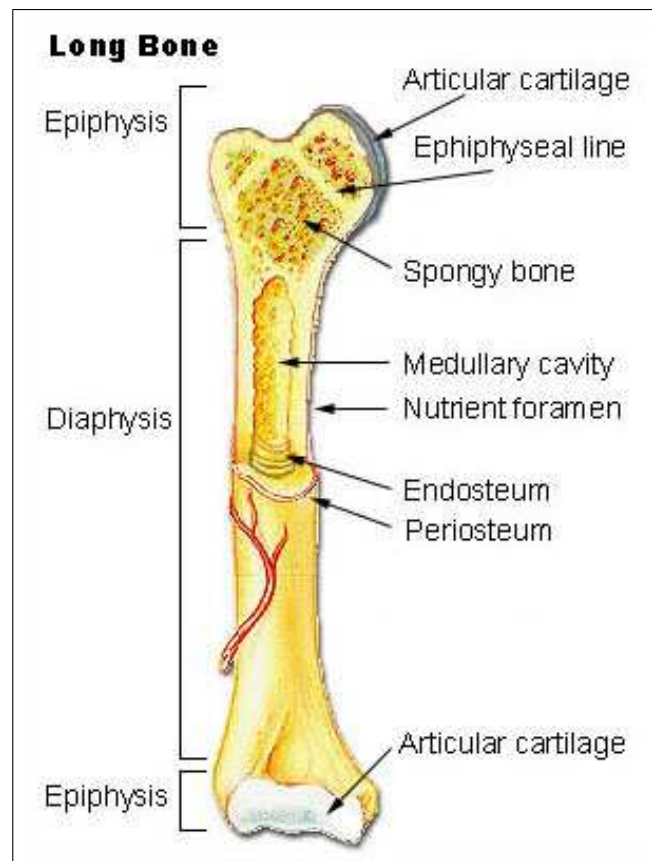


Figure 1.1 Schematic view of long bone demonstrating epiphysis, diaphysis, articular cartilage, endosteum and periosteum [1].

A typical long bone has a cylindrical like shaft called diaphysis, near the middle of the shaft is comprised mostly of compact bone that is resistant to bending stresses and usually has its maximum thickness, two wider and rounded ends, the epiphysis,

which are at the extreme ends of the bone are composed of cancellous bone. The surface of the cortical bone is covered by a thin layer; metaphysis. During growth, the metaphysis is surrounded by an epiphysis united to its metaphysis by a cartilaginous growth plate. The growth plate is where calcification of cartilage occurs. During maturity, the cartilage of the epiphysis has been replaced by cancellous bone [1].

1.2.2 Cortical and Cancellous Bone

At the macroscopic level, cortical bone accounts for 80 % of the skeleton and is composed of tightly packed osteons or haversian systems that are connected by transverse volkmann's canals which contain blood vessels, lymphatic tissue, nerves and connective tissue. Volkmann's canals communicate with the longitudinally like orientated haversian systems. Interstitial lamellae lie between the osteons. Along the boundaries of each lamella there are small cavities called lacunae, each of which contains one bone cell, an osteocyte. Small channels called canaliculi connect the lacunae of adjacent lamellae and finally reach the haversian canal. These channels allow nutrients from the blood vessels to reach the osteocytes. Canaliculi do not cross cement lines. Cement lines define the outer border of the osteons and it is the weakest portion of the bone. Cortical bone is characterized by a slow turnover rate a relatively high Young's Modulus (E) and a higher resistance to torsion and bending than cancellous bone.

Cancellous (spongy, trabeculae) bone which is the remaining 20% part of the skeleton has higher turnover rate and has more porous architecture than cortical bone [18]. It is composed of thin plates or trabeculae arranged into a loose mesh structure. The space between the trabeculae is filled with red marrow. Cancellous bone tissue is arranged in lacunae-containing lamellae but it does not contain haversian canals. The osteocytes receive nutrients through canaliculi from blood vessels passing through the red marrow.

Both cortical or cancellous bone constituted by the same cells and the same extracellular matrix components, but there are architectural and functional differences

[4]. The differences in structure depend on the amount of solid matter, as well as the size and number of spaces; in the compact tissue, the cavities are small and the solid matter between them is abundant, on the other hand in the cancellous tissue, the spaces are large and the solid matter is in smaller quantity. The functional differences are a consequence of these structural differences and vice versa. The structural composition of cortical bone mainly provides the mechanical and protective functions of bone, on the other hand, trabecular bone provides the metabolic function.

Long bones consist of a diaphysis with an expansion referred to as metaphysis. Diaphysis is the shaft of bone. It is a hollow tube and its walls are composed of dense cortex. Towards the epiphysis and metaphysis the cortex becomes progressively thinner and the internal space contains mostly cancellous bone with a thin shell of cortical bone [19]. The spaces enclosed by these thin trabecular are interconnecting pores that are filled with hematopoietic bone marrow [20].

The sizes of the pores vary considerably throughout the bone interior and thus present a structure of variable porosity. The arrangement of the trabeculae is functional. Their orientation closely parallels the trajectories of maximum stress and thus gives the skeleton maximum rigidity and resistance to mechanical stresses and strains [1].

The external surface of a bone is completely covered by periosteum. This membranous tissue has two layers, an outer fibrous layer (periosteum) and an inner osteogenic or cambium layer (endosteum) [21]. The outer fibrous layer is permeated by blood vessels and nerve fibres and acts in a supportive capacity. The inner layer contains highly active cells. During growth, these cells produce circumferential enlargement and remodeling of bone [22]. Therefore they form an osteogenic layer. After maturity, this layer consists mainly of a capillary blood vessel network. The endosteum is a membrane consists of bone surface cells (osteoclasts, osteoblasts, osteocytes and bone lining cells) and lines the cavities of cortical and cancellous bone and the marrow cavity of the diaphysis [1].

1.2.3 Composition of Bone

Bone is a composite material, which consists of 65 % mineral salts, 35 % organic matrix (mainly collagen), cells and water. Bone mineral consists mainly of calcium phosphate in the form of crystalline hydroxyapatite, $Ca_{10}(PO_4)_6(OH)_2$, responsible for the compressive strength of the bone, but also contains other mineral ions such as magnesium, strontium, carbonate, citrate and fluoride [23]. The hydroxyapatite crystals arranged along the length of the collagen fibers forming a composite material.

Organic matrix includes collagen, proteoglycans, noncollagenous matrix proteins (glycoproteins, phospholipids, phosphoproteins) and growth factors and cytokines. Collagen, which accounts for about the 90 % of organic matrix (predominantly collagen type 1), is responsible for tensile strength of bone and it gives mechanical integrity [24]. It is the main load carrying element in blood vessels, skin, tendons, bone, fascia etc. Therefore, the mechanical properties of collagen are very important to biomechanics.

Proteoglycans are partially responsible for the compressive strength and they inhibit mineralization. Although the function of noncollagenous matrix proteins such as osteocalcin, bone sialoprotein, osteonectin and osteopontin is not yet fully understood, it is believed that they promote mineralization and bone formation [25]. Growth factors and cytokines are present in small amounts in bone matrix, and they have an important regulatory role in bone remodelling; differentiation, activation, growth and turnover.

1.3 Microstructure of Bone

1.3.1 Woven and Lamellar Bone

Woven bone with high proportion of osteocytes, is the first bone to appear in embryonic development and is also seen in the initial stages of fracture healing and in biologic implant fixation [26]. Woven bone is weaker, with a small number of randomly

oriented collagen fibers, but laid down very quickly. It is replaced by lamellar bone, which is highly organized in concentric sheets with a low proportion of osteocytes. In contrast, lamellar bone is stronger and laid down slower. It is comprised of fine fibre bundles, and the collagen and associated mineral as they are arranged in parallel, concentric curving sheets [20].

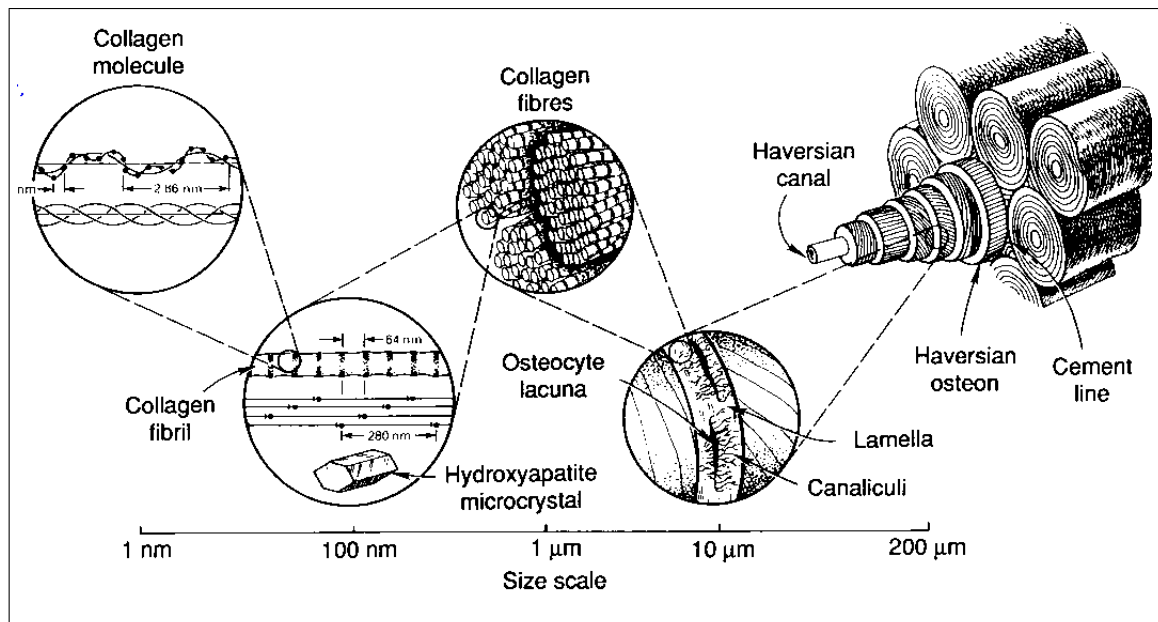


Figure 1.2 Hierarchical structure in human compact bone [2].

1.3.2 Bone Cells

Four major types of cells are involved in bone turnover; bone modeling and bone remodelling, namely osteoblasts, bone lining cells, osteocytes, and osteoclasts.

Osteoblasts are the bone-forming cells, derived from mesenchymal stem cells located in the bone marrow. Their functions are to synthesize and secrete unmineralised bone matrix; osteoid and produce the majority of the organic components of bone, including collagen, proteoglycans, and other non-collagenous proteins [21]. Osteoblasts are mononucleate. Osteoblasts participate in the calcification and resorption of bone, and regulate the flux of calcium and phosphate in and out of bone [1].

More differentiated metabolically active cells line at bone surfaces and less active

cells found in resting region called resting osteoblasts or bone-lining cells [27]. Bone lining cells (BLCs) share a common lineage with osteogenic (bone forming) cells may regulate mineral homeostasis with the complex of osteoblasts and osteocytes [1]. They function as a barrier for certain ions induced osteogenetic cells. They are flattened, mononucleate cells which line bone.

Osteocytes originate from osteoblasts, which have become embedded within the bone matrix. Osteocytes are located in the lacunae and are interconnected by long cytoplasmic processes to other osteocytes and osteoblasts. The role of the osteocyte is not yet fully understood. Their functions include to varying degrees: formation of bone, matrix maintenance and calcium homeostasis. They possibly act as mechanosensory receptors-regulating the bones' response to stress [27].

The fourth type of specialised bone cell is the osteoclast. Osteoclasts are the cells responsible for bone resorption. Osteoclasts are large, multinucleated cells located on bone surfaces in what are called Howship's lacunae [27].

1.4 Fracture Healing of Bone

Fracture healing is a complex biological cascade of cellular and molecular processes. The primary aim of fracture healing is actual reconstitution of the injured bone without a scar becoming almost identical to its original shape. The fracture healing process has been under investigation for many years.

The process of fracture healing can occur in two ways. Direct or primary bone healing occurs without callus formation. Indirect or secondary bone healing occurs with a callus precursor stage [21, 28, 29].

1.4.1 Primary Bone Healing

Primary fracture healing, also known as direct or osteonal healing, involves intramembranous bone formation and a direct attempt by the cortex to re-establish itself after interruption across a fracture line or osteotomy. This process primarily occurs between rigidly opposed cortical fracture ends to re-establish mechanical continuity such that no internal or external callus is formed [30].

Primary healing seems to process only when there is a combination of anatomical reduction, stabilization and compression of the fracture.

During primary healing, the periosteum is left intact and the blood supply is not disrupted. Under these conditions, bone-resorbing cells on one side of the fracture show a tunnelling resorptive response, whereby they re-establish new haversian systems by providing pathways for the penetration of blood vessels [21, 28, 29]. There is a direct reconstruction of the fragment edges by haversian remodelling [29]. Primary bone healing consists of simultaneous remodelling and formation of new bone at the fracture site [28]. However, intermittent cartilaginous stage, as seen in secondary bone healing, is bypassed. There is no relevant amount of callus visible on radiographs. Fragment resorption does not occur; thus there is no fragment end shortening. Also primary healing is a slow process which will continue months to years [28].

1.4.2 Secondary Bone Healing

Secondary (indirect) healing of bone dominates when less rigid forms of internal and external fixation are used e.g. conservative treatment using a cast. The process of bone repair by secondary healing can be divided into three overlapping stages. Healing begins with inflammation which is followed by the formation of hard callus by intramembranous ossification and bridging is achieved by endochondral ossification of the soft callus reparative stage and finally the callus is resorbed during callus remodelling [21, 30, 28].

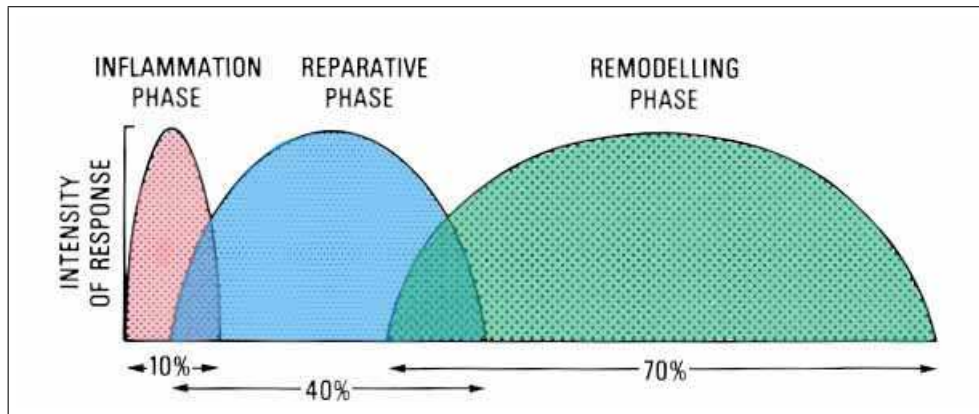


Figure 1.3 An approximation of the relative amounts of time devoted to the inflammation, reparative, and remodelling phases in fracture healing [3].

Healing with callus formation is the hallmark of secondary bone healing [30]. It serves as a bridge between the bone fragments and helps to eliminate motion between them.

1.4.3 Stages of Bone Fracture Healing

1.4.3.1 Inflammatory Phase. The inflammatory stage, the shortest stage in the repair process, begins immediately after fracture and lasts between 2 and 3 weeks after injury (Figure 1.5). Healing begins with bleeding from the trauma which disrupts the fracture surfaces, the periosteum and the surrounding soft tissues and results in the formation of the fracture haematoma. The haematoma forms an important source of haematopoietic cells and platelets that initiate the inflammatory process. The haematoma releases a large number of signalling molecules, including cytokines and growth factors [1, 17, 18]. Disruption of the haversian system results in the death of osteocytes at the immediate ends of the bone fragments. These dead osteocytes releases lysosomal enzymes that trigger the destruction of the organic matrix [30].

Macrophages and osteoclasts are found early in the inflammatory phase and begin the process of resorption and removal of dead bone. The necrotic tissue chemotactically attracts primitive mesenchymal elements from the cambium layer of the

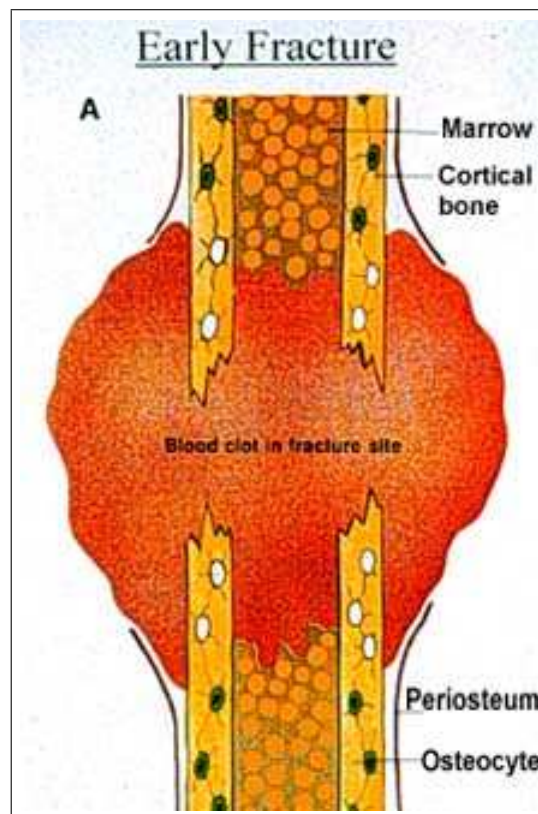


Figure 1.4 Schematic demonstration of early fracture [4].

periosteum, endosteum, bone marrow, and the endothelium. Mesenchymal cells and inflammatory cells differentiate into osteoblasts and chondrocytes, begin producing the elements of the soft periosteal callus, granulation tissue, between fracture ends [1, 17, 18]. The resulting proliferation of woven bone tissue will produce a hard fracture callus, thus bridging the fracture gap.

1.4.3.2 Reparative phase. In all fractures, the reparative phase of healing begins by appositional growth of new woven bone between days 3 and 5, when a majority of the callus still consists of granulation tissue (Figure 1.6) [30].

The second stage of healing is the reparative phase where the cellular synthesis of new bone, organic matrix, and the ossification of the matrix occurs to form new woven bone.¹¹ Bone growth in fracture callus proceeds via two routes: intramembranous and endochondral growth. During the reparative phase, the configuration of fracture

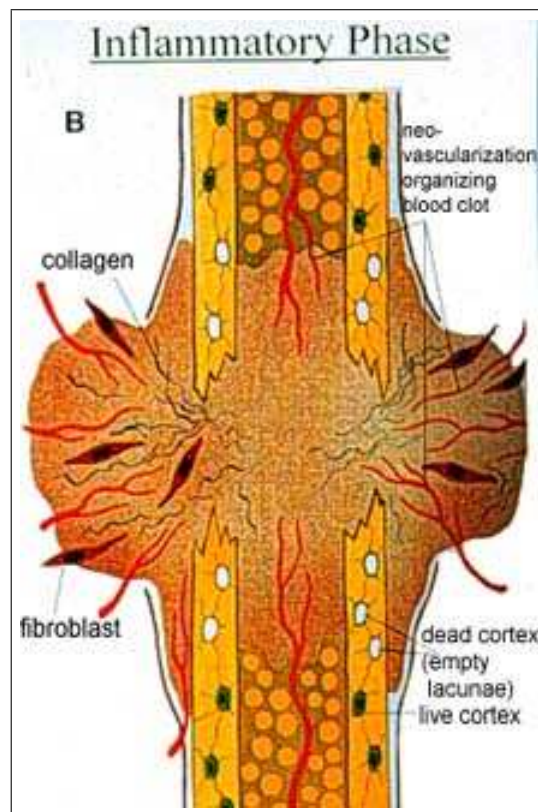


Figure 1.5 Schematic demonstration of the inflammatory stage of fracture healing [4].

healing is highly susceptible to mechanical factors and degree of immobilization. If the bone fragments are well immobilized, intramembranous growth dominates. On the other hand, if the bone fragments are not well immobilized, endochondral bone formation dominates.

The undifferentiated periosteal callus begins to undergo rapid chondrogenic transformation and proliferation; an increase in collagen type I, II and III collagen, but during the latter stages of repair as the process continues, type I collagen predominates [1] and an accumulation of hydroxyapatite crystals [4] in the matrix [28]. The cartilaginous callus mineralizes and envelopes the bone ends, leading to an increase in stability between the bone fragments [30]. Blood vessels begin to pass through the fibrous callus of one fracture fragment to reunify with those of other fragments. The combination of osteoblasts, cartilaginous matrix, and woven bone is the fracture callus. Formation of a bony bridging callus is the final step in the reparative phase of the fracture healing.

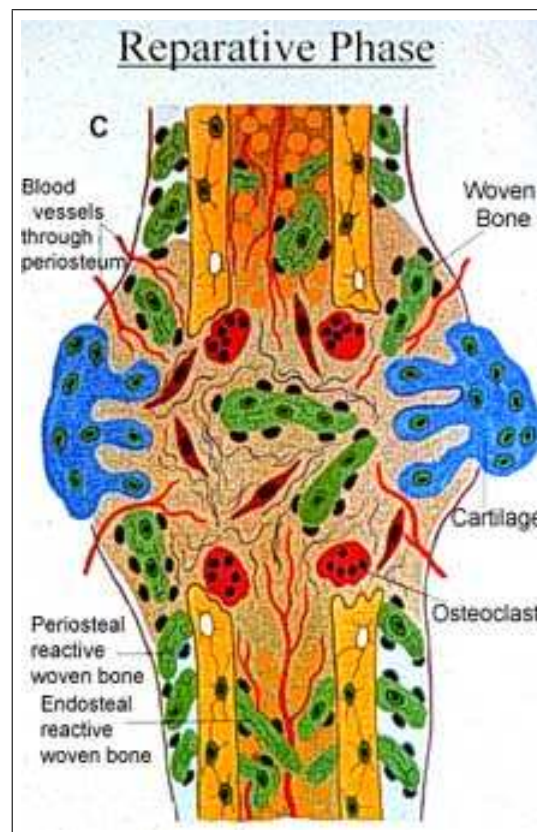


Figure 1.6 Schematic demonstration of the reparative stage of fracture healing [4].

1.4.3.3 Remodelling phase. Remodeling is the third and longest biological stage of fracture healing, suggested to last 6 to 9 years after the initial trauma in humans begins when the fracture is bridged by callus (Figure 1.7) [17, 25]. During this phase, the mineralized cartilage is transformed into woven bone, then the woven bone laid down in converted to lamellar bone [17]. Bone remodeling is predominantly regulated by the mechanical environment and the resultant piezoelectricity generated in the crystalline environment of the bone [17, 29, 28]. The final result of the remodeling stage is a bone whose organic and mineral phases are better aligned to resist local stresses [25].

1.4.4 Biomechanical Stages of Fracture Healing

The biomechanical stages of fracture healing were described by White and his coworkers (1977) using an externally fixed rabbit tibial osteotomy model [31]. Rabbit tibias were tested in torsion and the maximum torque, angle, energy and stiffness

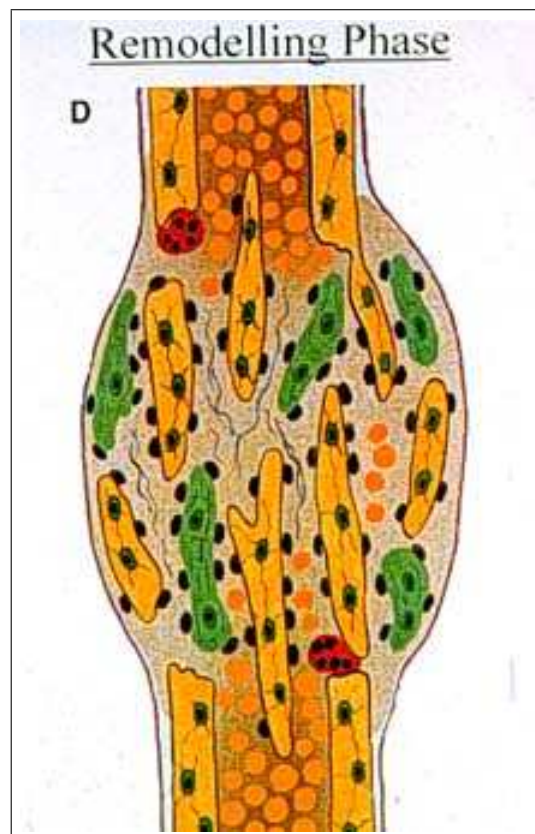


Figure 1.7 Schematic demonstration of the remodelling stage of fracture healing [4].

(slope) were determined. This work provided the first objective measurement of healing bone and proposed 4 biomechanical stages.

Stage 1 The bone fails through the original experimental fracture site with a low stiffness; the fracture site has low stiffness and low strength.

Stage 2 The bone fails through the original fracture site with a high stiffness; the fracture site has normal bone stiffness but low strength.

Stage 3 The bone fails partially through the original fracture site and partially through the surrounding bone; the fracture has normal bone stiffness and medium strength.

Stage 4 The site of failure is not related to the original fracture site; the fracture site has normal bone stiffness and normal bone strength.

1.5 Thromboembolism

Thrombosis is the formation or presence of a blood clot, or thrombus, in an artery or vein. An embolism is an occlusion of a blood vessel by a thrombus. A thromboembolism is caused by a piece of a thrombus that breaks off and travels through the blood to become lodged in a smaller blood vessel perfusing a particular organ, such as the lung (pulmonary embolism), brain (stroke), or heart (myocardial ischemia or heart attack) [32, 33].

Venous thromboembolism (VTE) is a complex vascular disease with a multifactorial pathogenesis that results in two major clinical manifestations. The first and more common manifestation is deep venous thrombosis (DVT). Deep venous thrombosis most often originates in the deep veins of the major calf muscles. Pulmonary embolism (PE), the second and more serious manifestation, occurs if a fragment of the venous thrombosis is released and travels through the right ventricle of the heart and becomes lodged in the pulmonary artery [32, 33, 34].

Symptomatic PE occurs in approximately 30% of patients with DVT. If one counts asymptomatic events, some 50-60% of patients with DVT develop PE [35, 32]. Venous thromboembolism occurs in approximately 1 in 1,000 persons, with over 200,000 cases of deep vein thrombosis and pulmonary embolism occurring annually in the United States Heit et al [35]. Up to 30% of patients die from the disorder and one fifth experience sudden death from pulmonary embolism, which alone accounts for 50,000 deaths per year.

1.5.1 Risk Factors for Venous Thromboembolism

Primary risk factors [32]

- Deficiency of antithrombin

- Congenital dysfibrinogenemia
- Thrombomoduline
- Hyperhomocystinemia
- Anticardiolipin
- Excess plasminogen activator inhibitor
- Prothrombin 20210A mutation
- Deficiency of protein C
- Factor V Leiden (APC-R)
- Deficiency of plasminogen
- Dysplasminogenemia
- Deficiency of protein S
- Deficiency of Factor XII

Secondary risk Factors [32]

- Trauma/Fracture
- Surgical intervention
- immobilization
- Malign disease
- Obesity
- Palsy
- Age
- Center venous catheter

- Smoking
- Pregnancy
- Long journey
- Oral contraceptive administration
- Lupus anticoagulants
- Crohn's disease
- Nephrotic syndrome
- Polistemia

1.5.2 Prevention of Deep Venous Thrombosis and Pulmonary Embolism

The method for preventing DVT or PE must be effective to some or all mechanisms of Virchow' triad. Furthermore methods with non or negligible side effects, practicable, cost-effective should be preferred. In preventing from DVT there are two different principles [32, 33]:

Primary prevention: With medical treatment and physical methods or both, preventing is targeted, before formation of DVT. It is most preferred and more suitable in terms of cost-effectiveness.

Secondary prevention: It stands on the principle that surgically intervened patients with sensitive and objective diagnosis methods or the early diagnosis of subclinic DVT and treatment. It is suggested for the patients on whom the primary protection is contraindicated or ineffective.

- Low dose standard heparin
- Adjusted-dose heparin

- Low molecular weighted heparin (LMWH)
- Oral anticoagulants
- Fondaparinux
- Intermittent pneumatic compression boots
- Vascular compression stockings
- Aspirin
- Hirudin
- Inferior vena cava filter

These treatment methods do not exactly vanishes the risk of VTE, but greatly decreases. To decide which method will be used to prevent DVT, side effects, values, risk groups must be taken into account.

Heparin: Heparin, a heterogeneous mixture of branched glycosaminoglycans, was discovered to have antithrombotic properties by McLean almost 90 years ago. Its molecular weight ranges from 3,000 to 30,000, with a mean molecular weight of 15,000 (approximately 45 monosaccharide chains). Only one third of heparin molecules contain the high-affinity pentasaccharide required for anticaogulant activity.

Heparin is synthesized in the mast cells of many tissues, such as the liver, lung, and gastrointestinal tract.

Heparin binds to the plasma protein antithrombin III (AT-III), indirectly producing an anticoagulant effect. In the absence of heparin, AT-III slowly inhibits thrombin and clotting factor Xa. Once bound to a specific pentasaccharide sequence on heparin, AT-III undergoes a conformational change at an arginine reactive site increasing its inhibitory activity against thrombin and factor Xa up to 1000-fold. Inhibition of factor Xa requires that heparin bind only to AT-III. However, for there to be inhibitory

activity against thrombin, heparin must bind simultaneously to AT-III through its pentasaccharide and thrombin through 13 additional saccharide residues.

It inhibits coagulation by binding to and increasing the activity of antithrombin III (AT-III), a plasma protein that inhibits factor IIa (thrombin), factor Xa, and several other clotting factors.

Heparin is administered by deep subcutaneous or intravenous injection. Heparin has no effect on a preexisting thrombus, it prevents their enlargement and propagation.

Doses of heparin must be individualized and adjusted, if necessary, based on the activated partial thromboplastin time (aPTT). The dose of heparin is considered appropriate when aPTT values are 1.5 to 2 times normal. Measurement of the activated clotting time (ACT) can be used in conjunction with very high doses of heparin [32, 33].

Low molecular weighted heparin (LMWH): Low molecular weight heparins (LMWHs) (enoxaparin, dalteparin, ardeparin, tinzaparin, danaparoid) are produced by chemical depolymerization of unfractionated heparin to yield polysaccharide chains of m.w. 2,000 to 9,000. LMWH fractions prepared from standard commercial grade heparin. These drugs interact with antithrombin III (AT-III) but not required for attaching the thrombin. These agents are factor Xa selective, and display a 2- to 4-fold greater anti-factor Xa activity than antithrombin activity. LMWHs can be administered subcutaneously. LMWHs can be administered once a day and are more specific for factor Xa Majerus and Tollefsen (2001), they have better bioavailability and longer half-lives than UH, and their anti-thrombotic effects are more predictable [32, 33]. In this thesis, enoxaparin was used as LMWH.

Fondaparinux: Fondaparinux is a heparin-like anticoagulant that has a selective and indirect anti-factor Xa activity. Fondaparinux is a synthetic pentasaccharide. It functions by binding reversibly, but with high affinity, to anti-thrombin III Samama and Gerotziatas (2003), thereby increasing the affinity of antithrombin (AT) for Factor Xa by about 300-fold. It is administered by subcutaneous injection [32, 33].

1.6 Historical Background

Although anticoagulants must be routinely used in patients presenting risk factors to deep venous thrombosis, as well as in those experiencing fractures at pelvic region, at lower limbs and in cases of multiple traumas, the effect of antiembolic agents on bone healing is not a well-known issue. Heparin is an effective antithrombotic agent, but various studies shows that it has limitations and side effects on bone as causing osteoporosis, stimulating bone resorption, increasing calcium loss, decreasing bone mineral density. Some of these limitations of unfractionated heparin are overcome by the use of LMWH preparations. Nevertheless studies shows that they have also negative effect on bone metabolism less than unfractionated heparin. Recently, fondaparinux, at low dosages, is being used for replacing the traditional non-fractionated heparin. Although studies about the fondaparinux are limited, no negative effect on bone metabolism is stated. Besides, in these studies, it is claimed that the negative effects of heparin and similar agents can be prevented by the usage of fondaparinux.

Matzsch et al. studied the effects of heparin in inducing osteoporosis on a rat model. The animals were divided into two groups and were treated with daily injections of 2 IU heparin/g body weight for 33 and 65 days and compared with rats acting as controls. The mineral bone mass in the femora of the animals was measured quantitatively. They found a significant reduction in bone mineral mass in the heparin-treated animals. This effect was present to the same degree after 33 days as after 65 days of treatment [36].

Ginsberg et al. in order to provide estimates of the risks of symptomatic osteoporosis and reduced bone density in premenopausal women treated with long-term (greater than 1 month) heparin therapy, they evaluated a cohort of 61 consecutive premenopausal women previously treated with long-term heparin (cases) and a group of controls matched for age, parity and duration between the last pregnancy and evaluation. All patients' bone densities of the lumbar spine and the wrist were analysed and compared to control group, reduction in bone density was seen in premenopausal women treated with long-term heparin therapy. Although none of the patients suffered

symptomatic fractures, they stated that, it is possible that the reduction in bone density predisposes women to fractures, and this potential risk should be considered when treating women with long-term heparin [37].

The relation of heparin therapy to osteoporosis was assessed in women; treated with subcutaneous heparin during and after pregnancy for thromboembolism prophylaxis. De Swiet et al. found that the phalangeal cortical area ratio was significantly less after long term therapy (greater than 25 weeks) compared with that after short term therapy (less than 7 weeks) in a retrospective analysis. The findings indicate a dose-related demineralization process associated with prophylactic heparin therapy in pregnancy [38].

Barbour et al. as a prospective study, compared the bone densitometry of 14 pregnant women requiring heparin therapy and 14 pregnant controls matched for age, race, and smoking status was identified by 20 weeks' gestation to evaluate the subclinical occurrence of heparin-induced osteoporosis in pregnancy. Proximal femur bone density measurements were taken at baseline, immediately post partum, and 6 months post partum in the cases and controls. Reduction in bone density by 10 % of 36 % case was seen in women treated with heparin therapy, this difference continued to be statistically significant 6 months post partum [39].

Dahlman published an extensive study about the effect of long-term treatment during gestation with heparin. 184 pregnant women was treated with the mean dosage of heparin 19,100 IU per 24 hours, for 25 weeks. Symptomatic vertebral fractures were found in 2.2 % of the women, and a relationship to the amount of heparin was indicated [40].

Similar results was indicated by Douketis et al too. In this study the effects of long-term heparin therapy on lumbar spine bone density was investigated. Twenty-five women who received heparin during pregnancy, and 25 matched controls was compared. Heparin-treated patients had lower bone density compared to untreated controls. It was indicated that long-term heparin therapy was associated with a significant reduction

in bone density [41].

Von Mandach et al. was claimed that the short-term low-dose heparin plus bed rest in pregnancy damage the bone metabolism. Serum ionised calcium, 1.25-dihydroxyvitamin D(3), osteocalcin, and urinary calcium/creatinine ratio were determined three times at 2-week intervals. They concluded that short-term low-dose heparin plus bed rest suppresses 1.25-dihydroxyvitamin D(3) and osteocalcin levels in pregnancy [42].

Since the first suggestion of heparin-induced osteoporosis in 1963, a large body of work has been published. The mechanism can be explained by the effect of heparin as a cofactor for physiological stimulators of osteoclasts [43]. LMWH which are designated because of the possible complications of UH has been also searched in similar osteoporosis studies. Sivakumaran et al. reported that although LMWHs have a lower potential to cause osteopenia than the unfractionated preparations, still there is a potential risk of this complication with the prolonged use of LMWH preparations [44].

Casele et al. serially measured bone density in the proximal femur, in 16 women receiving enoxaparin sodium (40 mg daily) for a mean duration of 25 weeks, during pregnancy to evaluate changes in bone density. Measurements were taken within 2 weeks of starting therapy and then at 6-8 weeks postpartum and 6 months postpartum. There was no significant change in mean bone density measurement from baseline measurements to the conclusion of therapy at 6 weeks postpartum and no patient experienced a decrease in bone mass at 6 weeks postpartum. By 6 months postpartum, there was a significant mean decrease in bone density and 14 % patients evaluated experienced an overall bone loss of > 10 % [45].

Pettila et al. was performed an open study; 44 pregnant women with confirmed thromboembolism were randomised to receive either low-molecular-weight heparin (dalteparin) or unfractionated heparin for thromboprophylaxis during pregnancy and puerperium. Bone mineral density in the lumbosacral spine was measured in 1, 6,

16, 52 weeks. Bone mineral density values were also compared with those of healthy, control group. Mean bone mineral density values of the lumbar spine was significantly lower in the unfractionated heparin group compared with the dalteparin and with the control groups. Bone mineral density values in the dalteparin group did not differ from of healthy delivered women [46].

To determine and compare the effects of long-term secondary venous thromboembolic prophylaxis with LMWH or acenocoumarol on bone mineral density, Wawrzynska et al. studied on 86 patients receiving LMWH or acenocoumarol for 3-24 months. They reported a mean decrease in BMD of the femur was 1.8 % and 2.6 % in patients given acenocoumarol and 3,1 and 4,8 % in patients given enoxaparin, respectively, at 1 and 2 years of follow-up. Decrease in BMD, more evident in patients on LMWH than on acenocoumarol. To perform densitometry before starting long-term anticoagulation and to repeat it every 12 months, especially in patients with concomitant risk factors for osteoporosis in order to identify patients in need of its prophylaxis was suggested. ref

The effects of heparin and LMWH were investigated in a variety of animal experiments. Matzsch et al. divided the rats into 4 groups and treated with UH (2 IU/g bw) (the first group), LMWH in 2 doses; 2 XaI U/g (the second group), 0.4 XaI U/g (third group) and placebo (saline) (the final group) for 34 days. Studied variables were the bone mineral mass in femora; fragility of humera; zinc and calcium levels in serum and bone ash and albumin in plasma. An expressive reduction in bone mineral mass was found in all heparin-treated rats. There was no difference between UH and LMWH in this aspect, but in LMWH-treated rats, this effect was found to be dose-dependent. A reduction in zinc content in bone ash was found in all heparin-treated animals compared to control groups, though the fragility of the humera did not differ between all heparin-treated group and control group. Researchers concluded that, if dosed according to similar factor Xa inhibitory activities, there would be no difference between LMWH and UH in inducing osteoporosis aspect [47].

A similar research was done by Monreal et al. in an animal model, to determine

the effect of a high dose of UH(2 IU/g s.c. twice a day) and LMWH (Dalteparin, 1 anti-Xa U/g once a day) was compared with that of placebo on the mineral bone mass in the femur of rats. After 33 days of treatment no differences were found in the weight of the femur. Though heparin-treated rats had a lower density compared to control rats and also LMWH-treated rats. They claimed that LMWH may have a lower osteopenic effect than that of UH [48].

Hurley et al. studied the effect of LMWH on collagen synthesis in 21-day fetal rat calvariae and claimed that LMWH compounds were just as inhibitory as native heparin on collagen synthesis and offer no protection against heparin-induced osteoporosis. Moreover, the size and sulfation of a heparin-derived oligosaccharide contribute to its ability to inhibit collagen synthesis in bone [49].

Murray et al. studied whether heparin-induced osteoporosis is influenced by the molecular weight of heparin on rabbits and compared LMWH-treated, UH-treated or high molecular weight heparin-treated rabbits. A reduction in cortical and trabecular bone density was seen in UH and HMWH-treated rabbits but not in LMWH-treated rabbits, compared to the control group. A significant increase was seen in femoral fragility in HMWH-treated rabbits. Authors concluded that HMWH and UH can induce some osteoporotic changes, but LMWH did not cause toxic skeletal effects [50].

Shaughnessy et al. in a study on rats, stated that unfractionated heparin stimulates the process of bone resorption and that the LMWHs, enoxaparin, fragmin, logiparin, and ardeparin produce significantly less calcium loss than UH [51].

Muir et al. has studied the effects of UH on trabecular bone histomorphometrically. Rats were treated with once daily subcutaneous injections of heparin (0.25 to 1.0 U/g) or saline for 8 to 32 days and the effects on bone were monitored both histomorphometrically and biochemically by measuring urinary type I collagen cross-linked pyridinoline (PYD) and serum alkaline phosphatase, markers of bone resorption and formation, respectively. They found that heparin induces both a time- and dose-dependent decreased in trabecular bone volume, with the majority of trabecular bone

loss occurring within the first 8 days of treatment. They showed that heparin doses of 1,0 U/g/d resulted in a 32 % loss of trabecular bone. Moreover, a 37 % and 75 % decrease was seen in osteoblast surface and osteoid surface in heparin-treated rats, respectively. Based on these observations, they conclude that heparin decreases trabecular bone volume both by decreasing the rate of bone formation and increasing the rate of bone resorption. In contrast, LMWH, causes less osteopenia than heparin because it only decreases the rate of bone formation [52]. In another research included LMWH [53], Muir et al. found that both heparin and LMWH decrease cancellous bone volume in a dose-dependent fashion, but that heparin causes significantly more cancellous bone loss than does LMWH. They concluded that heparin decreases cancellous bone volume both by decreasing the rate of bone formation and increasing the rate of bone resorption. In contrast, LMWH, causes less osteopenia than heparin because it only decreases the rate of bone formation [53].

Bhandari et al. studied the the relative effects of UH and LMWH on osteoblast function, and used an in vitro bone nodule assay. For this aspect, with bone nodule formation, alkaline phosphatase (ALP) activity was measured. They stated that both agents inhibited bone nodule formation and alkaly phospatase (ALP) activity in a concentration-dependent manner, but 6 to 8-fold higher concentrations of LMWH were required to achieve equivalent effects. They cited that the risk of osteoporosis is lower with LMWH than with heparin [54].

In an another research, Shaughnessy et al. studied whether heparin-induced bone loss is reversible when heparin treatment is stopped and heparin was found to be retained in bone for at least 56 days after stopping heparin treatment. To their findings, they claimed that heparin-induced osteoporosis is not rapidly reversible because heparin is sequestered in bone for an extended period [55].

Kock et al. in a standardized in vitro model, studied the effects of UH and LMWHs on osteoblast growth were studied at the same dose, on human osteoblast cell cultures and analyzed 4 different LMWHs (nadroparin, enoxaparin, dalteparin, certoparin). They emphasized that, LMWHs caused a significant inhibition of osteoblast

growth and an increase in bone resorption, compared to control groups [56].

Various studies about the effect of LMWHs on bone histomorphometry on rats, found that LMWHs inhibits the bone formation and stimulates the bone resorption [57].

The negative effects of anticoagulants especially heparin on fracture repair was shown in different studies also. In 1956 Stinchfield et al. found that daily injection of UF and warfarin significantly inhibites the fracture repair in rabbit and dog experiment model [58].

Street et al. found that LMWH, enoxaparin, significantly attenuated the bone repair, on the healing of a closed rabbit rib fracture model. In enoxaparin-treated rabbits, on the 3.,7. and 14. days, less increase of cells in medullar callus and less turnover rate of perist was observed. In comparison to control groups, a decrease in bone repair on enoxaparin-treated rabbits on the 7. and 14. days was observed and biomechanical testing assessed after 21 days showed that mechanical properties of bone weaken [59].

Kock et al. applied a standardized bone defect to both femur condyles to evaluate the effects of UH and LMWH on fracture healing. Three groups of ten rabbits received subcutaneous injections of an UH, a LMWH (certoparin), or normal saline over a period of 6 weeks. After therapy with LMWH, there was no inhibition of defect healing compared to control group [60].

Hak et al. studied on dalteparin, to evaluate the effect of LMWH on fracture healing in a standard stabilized rat femur fracture model. Following the treatment with dalteparin for 2 weeks, radiological, histological and mechanical measurements taken in the 2., 3., and 6. weeks were compared. Dalteparin did not show a meaningful effect on fracture healing in comparison to control group [61].

Through LMWHs have faster effect than oral anticoagulants, it is not a surprise

that in LMWH-treated patients preventing from sore side hematoma is significantly greater after surgery. In early period treatment with LMWH due to fracture can may be cause a greater fracture side hematoma. It is believed that fracture side hematoma has a positive effect on fracture healing. Muzino et al. have revealed that fracture side hematoma has a osteogenic potential [62].

Hawkins et al. found that fondaparinux may be a safe and effective alternative to UH and LMWH in women who require anticoagulation during pregnancy on long-term therapy. They claimed that heparin induced osteoporosis can be reduced with fondaparinux treatment [63, 64].

Fracture healing always has been studied detailly in Orthopaedics and Traumatology clinics. Bone healing and speeding up effects of nonsteroidal anti-inflammatory drugs (NSAIDs) and different agents on bone healing has been investigated on various experimental animal model. It has been found that most of the NSAIDs have a negative effect on fracture healing [65, 66, 67].

It has been showed that NSAID diclofenac, reduces appearance of osteoblasts in bone defect healing in rats [68]. In an another study , it has been found that tenoxicam, a NSAID, delays fracture healing process in rat tibia [69]. In a different study it has been found that NSAIDs adversely effect fracture union [70].

In an another research it was found that nonsteroidal anti-inflammatory drugs inhibit cyclooxygenases (COX-2). NSAIDs have been reported to delay fracture healing and cause non-union, possibly due to the drug-induced inhibition of osteoblast recruitment and differentiation [71, 72, 73].

Simvastatin is an agent for reducing cholesterol levels. It was found that simvastatin promotes fracture healing [74, 75, 76] and increases the formation and differentiation of osteoprogenitor cells [77].

In an animal model experiment, it was found that Levodopa, an agent used in

the treatment of Parkinson Disease, has a positive effect on fracture repair [78].

Glutamin, an aminoacid, histologically increases the fracture healing minimally, hyaluronic acid has also shown similar positive effects on fracture healing [79]. It was found that nitric oxide, increases the healing rate radiographically and histologically [80]. Turk et al. evaluated the effects of vitamin E on the fracture healing and stated that vitamin E has positive effects [81].

In a study, evaluating the effect of human amniotic fluid on bone healing, calvarial defects was created in rabbits and defects were injected with human amniotic fluid and the defects treated with human amniotic fluid had superior ossification in comparison to the control group defects [82].

In an in vivo study, it is found that colchicine inhibits fracture union and reduces bone strength [83]. Long-term systemic use of corticosteroids causes osteoporosis and increased risk of fracture, however no inhibitory effects were seen following short-term corticosteroid treatment [84].

The effects of antibiotic usage because of infection prophylaxis on fracture healing has been researched in literature. In a study that has been designated to evaluate the effects of cefazolin and ciprofloxacin on bone healing, it was concluded that in cefazolin group fracture union was closed to control group, on the other hand, ciprofloxacin has delayed fracture union [85]. In an another study it was found that Levofloxacin and trovofloxacin has adverse effects on fracture healing [86]. There are also studies about the negative effect of Gentamicin on fracture healing [87].

The effects of pulsed electromagnetic fields [88] and ultrasound on fracture healing has been evaluated and generally it was claimed that they speed the healing process [89].

Various agents and factors have been searched to speed fracture healing. Recombinant human vascular endothelial growth factor enhances bone healing, was es-

established in an experimental nonunion model [90]. In an another study it was found that; growth hormone accelerates bone healing, biomechanically and histologically [91].

2. EXPERIMENTAL TECHNIQUES

In this thesis mainly it is concentrated on the inorganic part of bone. X-ray diffraction tools and SEM analysis which will be explained below well characterisation methods used.

Bones, on which characterisation applied where bones obtained from albino male rats prepared in Ministry of Health Services Metin Sabancı Baltalimanı Osteopathic Training and Research Hospital.

2.1 Specimen preparation

2.1.1 Experimental Procedure

In this study 16 Wistar-Albino male rats (Istanbul University Cerrahpaşa Faculty of Medicine Experimental Research Laboratory) were used. Before this study, all required permission was obtained from Ministry of Health Services Metin Sabancı Baltalimanı Osteopathic Training and Research Hospital Ethic Commission and Istanbul University Cerrahpaşa Faculty of Medicine Test Animals Ethic Commission. This study is performed at Istanbul University Cerrahpaşa Faculty of Medicine Test Animals Research Laboratory.

All test animals in this study are average 2.9 months old (2.5-3.2 month) and mean weights of these rats were 190 grams (172-273 gram). Rats were randomly classified into 4 groups and in laboratory environment as such 4 rats in each cage preoperative 48 hours along were monitored. During the study all rats are fed with unlimited rodent feed and tap water. Rats that remained 12 hours in the light and 12 hours in the dark were followed at the temperature 22 centigrade degrees. All animals were operated in the same day by the same surgeon. Antibiotic prophylactic therapy wasn't done during or after operations. No infection in any rat was observed around the

wound. Four cages were named A,B,C and D (Table 2.1). 1cc subcutaneous isotonic sodium chloride solution was injected once a day for 2 weeks to Group A rats. 1000 antiXa IU/Kg subcutaneous enoxaparin was injected once a day for two weeks to Group B rats [14]. To Group C rats 0.2 mg/Kg [14, 15, 16] subcutaneous fondaparinux was injected once a day for two weeks and finally 1000 antiXa IU/Kg subcutaneous heparin [12] was injected once a day for two weeks again to Group D rats. Injections of the agents were done to the right groin area with an insulin injector by the same person. All rats were sacrificed after 14 days. Cervical dislocation was used as a euthanasia method. After the rats were euthanized, their left femurs were disarticulated from hip and knee-joint. The soft tissue on the femur was grazed gently to prevent callus tissue deformation.

Table 2.1
The distribution of experiment animals

	Group Name	# of Animals
Control	A	2
Enoxaparin	B	3
Fondaparinux	C	2
Heparin	D	2

2.1.2 Surgical Techniques

The rats that all necessary preparation and follow-ups had been done were took in the operating room. The weight of each rat was weighed with an electronic weighing scale in order to calculate the anesthetic drug doses. Ketamin (Ketalar@, Pfizer, Turkey) and Turkey) 50 mg/kg and Xyrazinne (Rompun@, Bayer, Türkiye) 10 mg/kg combination was used as an anesthetic. Anesthetic combination is applied from the right groin area intraperitoneally. Method defined by Bonnarens [92] was used as surgical technique. Povidone iodine (Batticon@, ADEKA, Turkey) was applied after shaving the left knee region of the rats (Figure 2.1).

A 2-cm longitudinal incision was made through skin. Through the patella me-



Figure 2.1 Preparation of knee region of rats for operation

dial, joint capsule detached. Translation of the patella in the frontal plane was pointed laterally furthered knee flexion. Rat femoral condyle appeared (Figure 2.2).



Figure 2.2 Appearance of rat femoral condyle and preparation of intramedullary channel

Rat femoral condyle appeared. A 1 mm diameter sterile Kirschner steel wire was drilled with an electrical drill, through the femoral condyles, femur channel was prepared. Later on a 0.8 mm diameter sterile Kirschner steel wire was located to this channel (Figure 2.3).

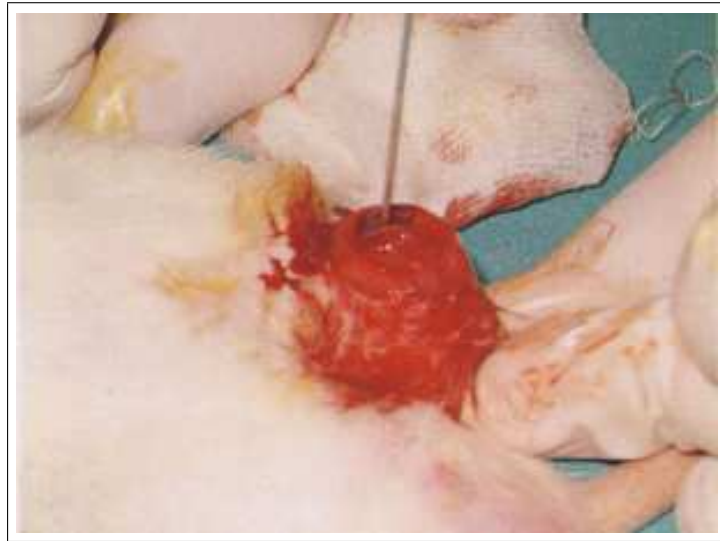


Figure 2.3 Intramedullar location of Kirschner wire

Kirschner wire was folded, and cut at the level of femoral condyles (Figure 2.4).



Figure 2.4 View after the location of Kirschner wire

By the extension of knee patella was reduced. Femoral condyles suture with 3/0 Vicryl (Atramat®, Mexico, Mexico) (Figure 2.5).

Skin suture with 2/0 silk (Sterisilk®, Turkey). Following the wound was cleaned with povidone iodine and rats were taken from operating table. To create a standard closed fracture, Bonnarens and Einhorn [92] procedure was used. The fracture ap-

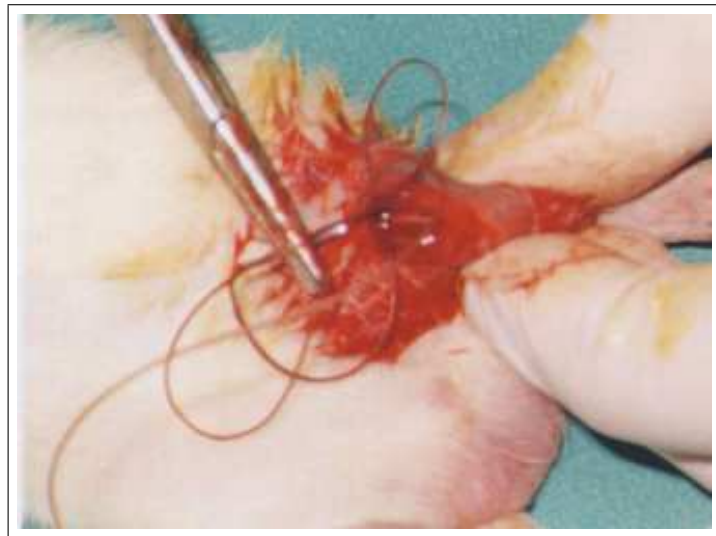


Figure 2.5 Suturation of femoral condyles

paratus consists of four component parts: (a) a frame which was designated for left femur; (b) an animal support system; (c) a guillotine ramming system; and (d) a 500 g steel weight. 500 grams of weight from a height of 35 centimeters was left free fall to create a closed fracture. Only 1.5 mm movement of obtuse guillotine was allowed by the Guillotine system screws settings (Figure 2.6).



Figure 2.6 Creation of closed fracture by the Guillotine system

Radiographies obtained to document the fracture (Figure 2.7). After the radio-

logical study; isotonic NaCl, enoxaparin, standard heparin and fondaparinux injection were done.

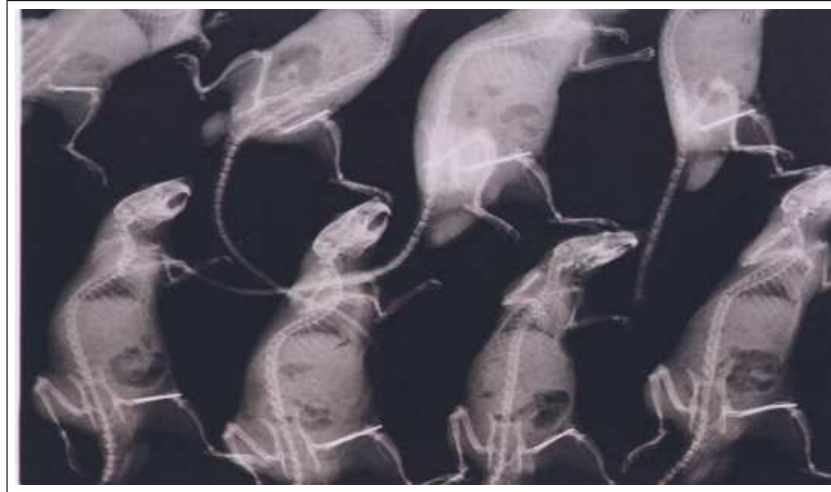


Figure 2.7 Approval of fractures by the radiographies which are obtained from rats after the operation



Figure 2.8 An example for an ideal rat femur fracture

2.2 Macroscopical Studies

Experimental techniques described above performed at Ministry of Health Services Metin Sabancı Baltalimanı Osteopathic Training and Research Hospital (Ahmet Şükrü Mercan). Bone samples obtained from Ministry of Health Services Metin Sabancı Baltalimanı Osteopathic Training and Research Hospital were studied in this thesis.

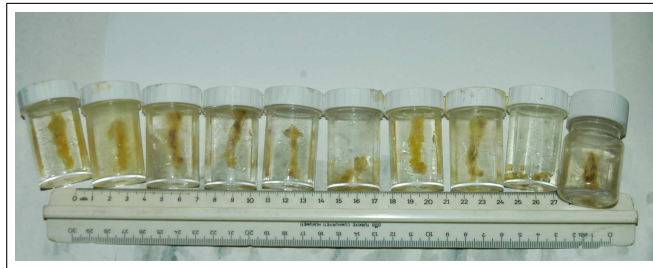


Figure 2.9 Bone samples of control group, in formaldehyde solution

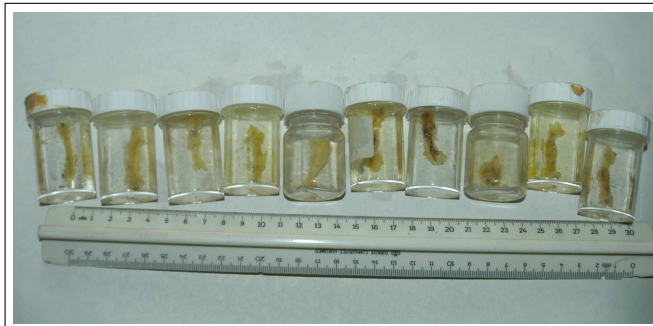


Figure 2.10 Bone samples of heparin-treated group, in formaldehyde solution

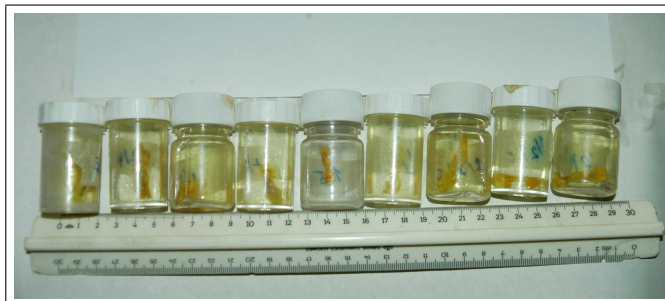


Figure 2.11 Bone samples of LMWH-treated group, in formaldehyde solution

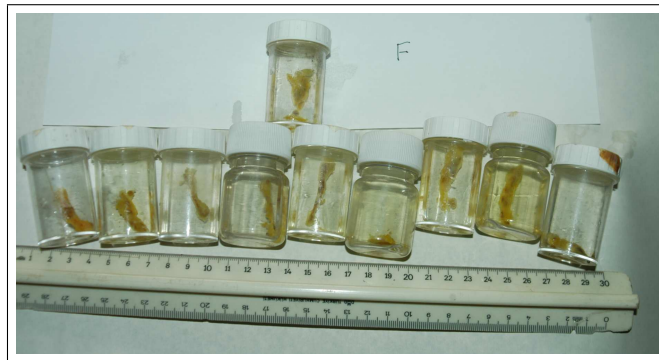


Figure 2.12 Bone samples of fondaparinux-treated group, in formaldehyde solution

2.3 Scanning Electron Microscopy (SEM)

SEM is one of the most common methods in today's laboratories in order to get a high resolution surface investigation although it gives information about the surface topography. One of the best methods to study surface feature and the fracture healed surfaces of the bones is scanning electron microscopical techniques. By the help of SEM together available features microstructurally that bone has the effect of antiembolic agent on the fracture healed areas and the areas far from the fracture healed region can be studied, so that comparisons among the antiembolic agents and control group are possible. SEM studies were performed on both control group (Group A) and antiembolic agent injected rats' bones (Group B-C-D).

2.3.1 Introduction

The first SEM image was obtained by Max Knoll, 1935, however, commercial SEM's appeared in 1965, based on the work of C, W. Oatley et al. of Cambridge University [93].

In a typical SEM, an electron beam is thermionically emitted from an electron gun is accelerated by holding the tungsten filament at a large negative potential between 1kV and 50kV and whilst the specimen is grounded. The types of signals produced by an SEM include secondary electrons (SE), back scattered electrons (BE), characteristic

x-rays, when the electron beam impinges on the material surface. Detectors connect the signal-producing and the signal-processing system of an SEM. They convert the signals produced (electrons) into electrical signals. Each signal requires a special detector. SE is captured by the detector, amplified and displayed for producing the images (SEI) [93, 94] which comprising all essential information on topography, produces electron-micrographs of high resolution. Backscattered electron imaging (BEI) is a utility for analyzing material composition, density, and surface geometry [93]. Depending on the instrument, the resolution can fall somewhere between less than 1 nm and 20 nm and a wide range of magnifications is possible, from about $\times 10$ to about $\times 350,000$ [95].

Small samples of up to several millimeters and sometimes even larger can be investigated directly in the SEM. For conventional imaging in the SEM, specimens must be electrically conductive, at least at the surface, and electrically grounded to prevent the accumulation of electrostatic charge at the surface and, a specimen is normally required to be completely dry, since the specimen chamber is at high vacuum. However, SEM observation of nonconductive samples, such as bones, is not possible without drying and a metallic or carbon conductive layer on their surface. Such a coating avoids build-up of an electric negative charge in the specimen, which would induce "imaging artifacts" [93]. In this study, since bones require conductive coating, gold was selected as coating material due to its ease to vapor deposit and on bombardment with high energy electrons it gives a high secondary yield. Generally, the thickness of gold coating is around 25 nm [94].

The main advantages of SEM are the high lateral resolution (1- 10 nm), large depth of focus (typically 100 μm at 1000x), the numerous types of electron specimen interactions that can be used for imaging or chemical analysis purposes, wide magnification range (e. g. 10x to 105x or higher) [93].

The principal limitations of SEM are cost and instrumental complexity because a vacuum system is required. Problems in analysis of biological materials by SEM are also related to sample preparation, beam penetration effects, charging, beam damage and outgassing of low molecular weight components [93].

2.3.2 Materials and Methods

JEOL JSM-6060L V scanning electron microscope was used to study side and fracture surfaces of the bones at the Material Laboratory of Gebze Institute of Technology. To view the fracture surfaces of the normally healed and antiembolic agent injected femurs in SEM, 1.5 cm lengths of the bone were fixed to a sample puck using double sided adhesive conductive carbon tapes. The samples were firstly coated with gold by using a Polaron SC7620 SEM sputter coater with CA 7625 carbon accessory (Quorum Technologies Ltd.) and a RV3 model vacuum pump (Edwards Ltd.). All samples were studied under SEM from 250x up to 2,000x magnification.

2.3.3 Results and Discussion of the SEM Studies on the Fractured and Healed Bone Samples

2.3.3.1 Control group. SEM studies on the fractured and healed bone; control sample 1

Montage-like SEM picture of lateral surface of the conventionally healed bone (without injection of antiembolic agents) rat number 1 obtained with relatively low magnification is shown in Figure 2.13.



Figure 2.13 Montage-like SEM picture of lateral surface of conventionally healed bone (without injection of antiembolic agents) rat number 1 obtained with relatively low magnification

Figure 2.14 shows the scanning electron micrographs under various magnifications (34x, 250x, 500x, 1000x, 2000x) on the lateral surface of the fractured and normally healed sample 1, which are obtained far from healed region. Haversian channels

are visible. There are no defects.

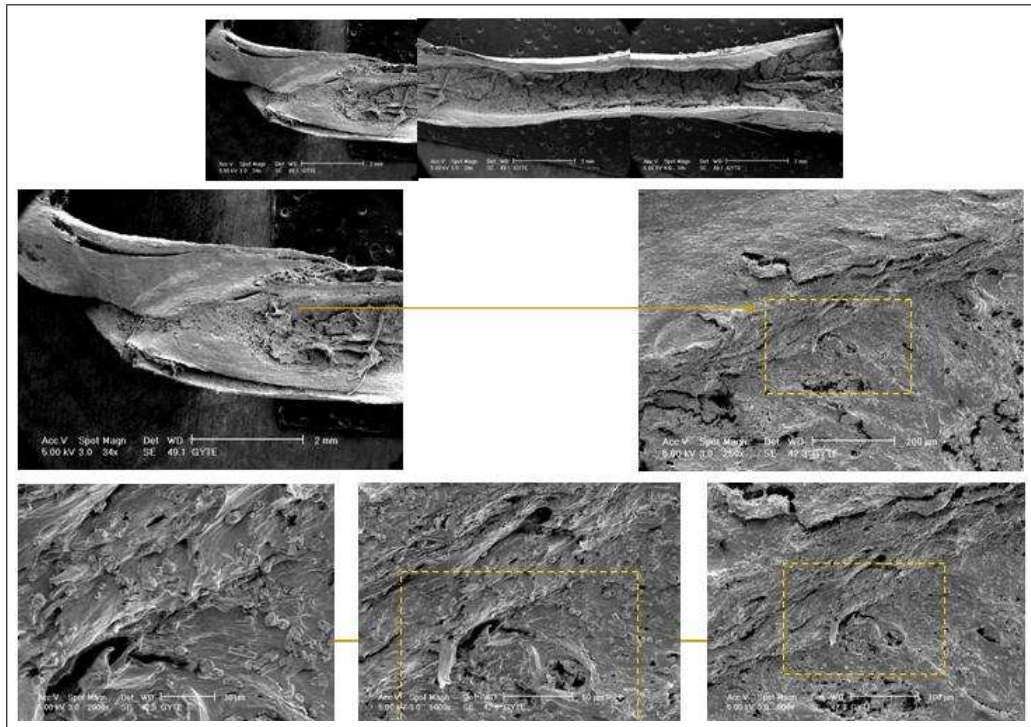


Figure 2.14 The SEM micrographs under various magnifications of the control sample 1, obtained far from healed region, being fractured and healed.

Scanning electron micrographs obtained under various magnifications (34x, 250x, 500x, 1000x, 2000x) on the lateral surface of the fractured and conventionally healed sample 1, obtained from closed to healed region are shown in Figure 2.15. It is clear, that, while coming close to healed region, defects (holes) were formed.

Scanning electron micrographs obtained under various magnifications (34x, 250x, 500x, 1000x, 2000x) on the lateral surface of the fractured and normally healed sample 1, obtained almost from healed region showing relatively more defects in micro level, see Figure 2.16.

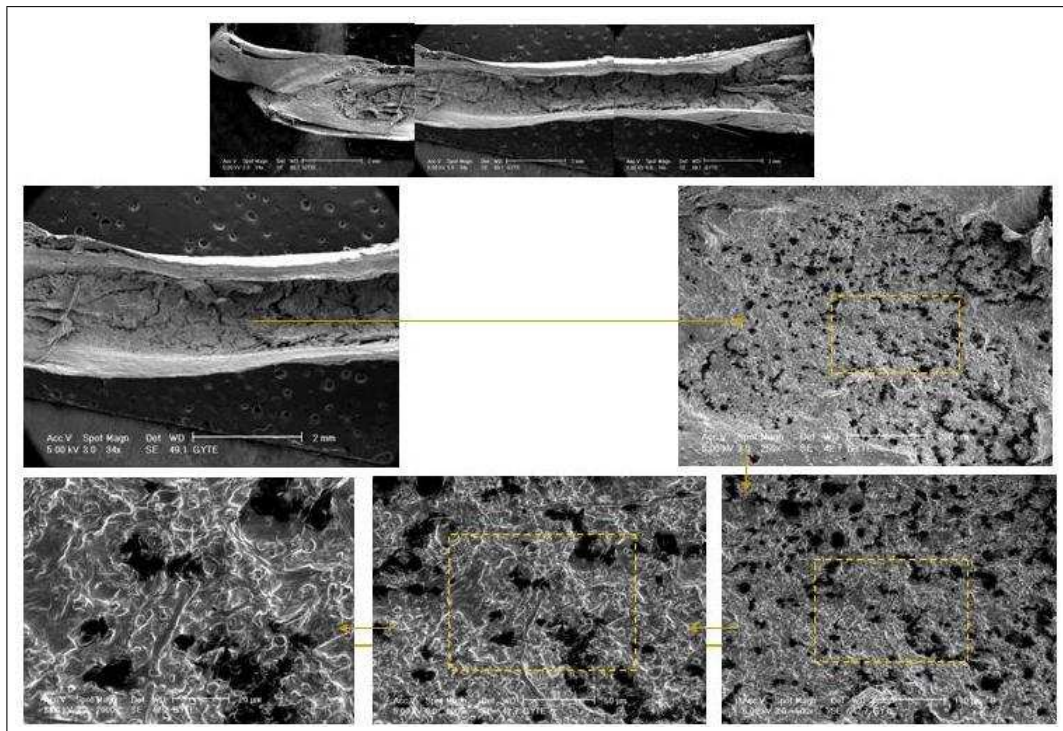


Figure 2.15 The SEM micrographs under various magnifications of the control sample 1, obtained from closed to healed region, being fractured and healed.

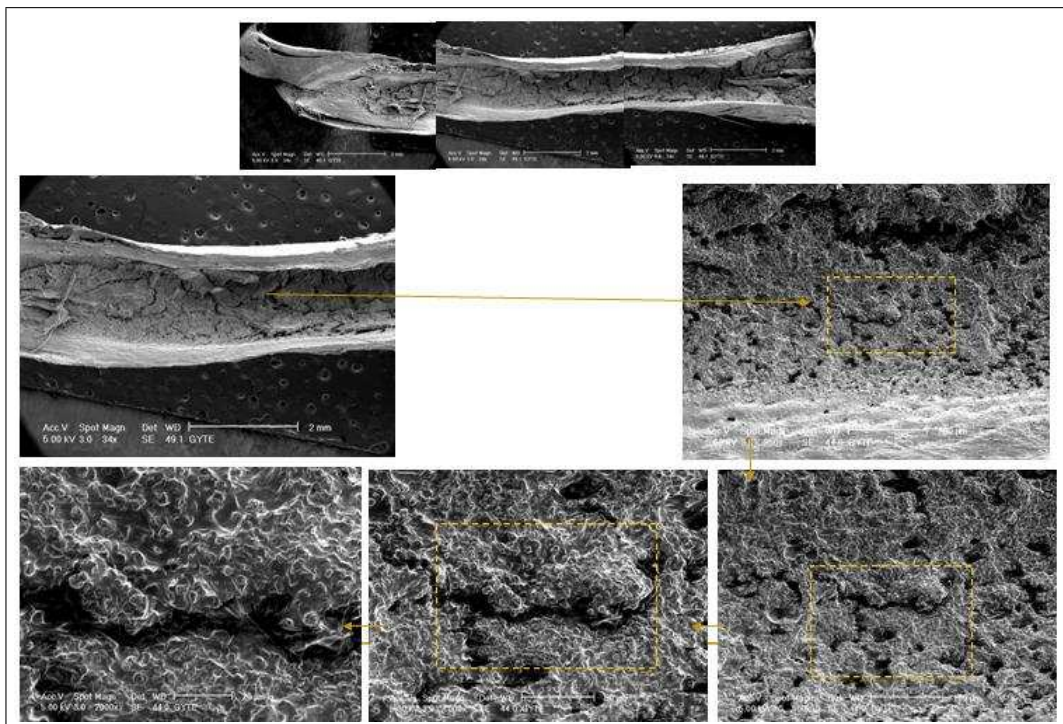


Figure 2.16 The SEM micrographs under various magnifications of the controlled sample 1, obtained almost from healed region, being fractured and healed.

The lateral surfaces of the fractured and normally healed sample 1 obtained far from the healed region are visualized with different magnifications (125x, 250x, 500x, 1000x) in Figure 2.17. Less and almost no defects are visible.

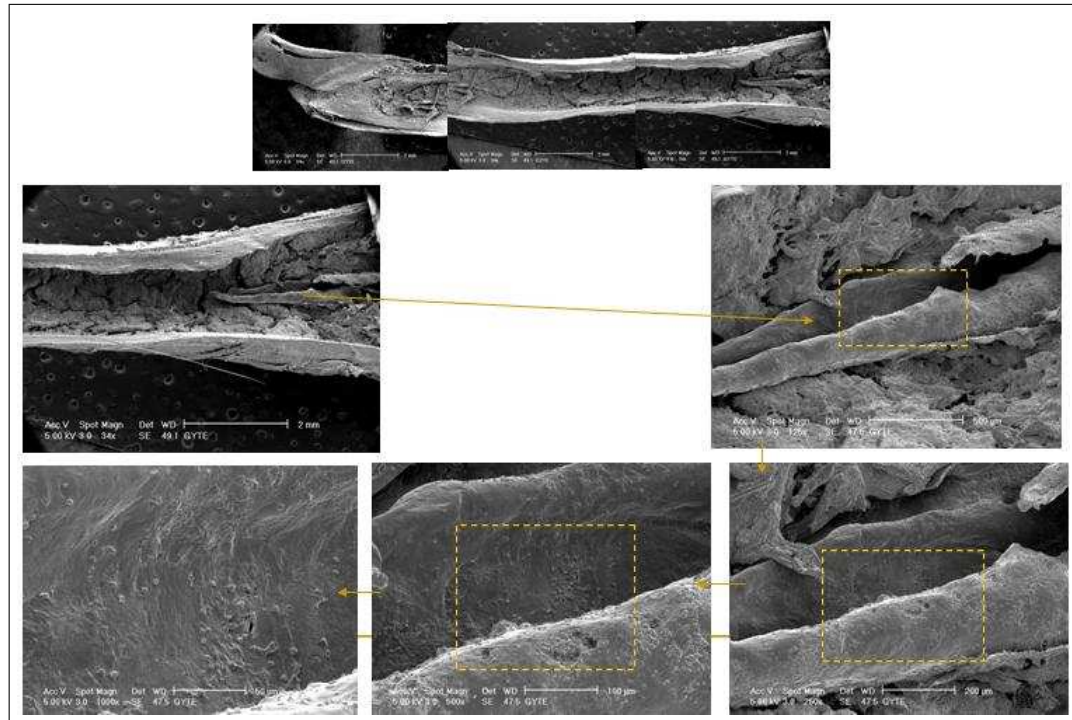


Figure 2.17 The SEM micrographs under various magnifications of the controlled sample 1, apart from healed region, being fractured and healed

SEM studies on the fractured and healed; control sample 2

Montage-like SEM picture of lateral surface of the bone with conventional method (without injection of antiembolic agents), rat number 2, with relatively low magnification is shown in Figure 2.18.

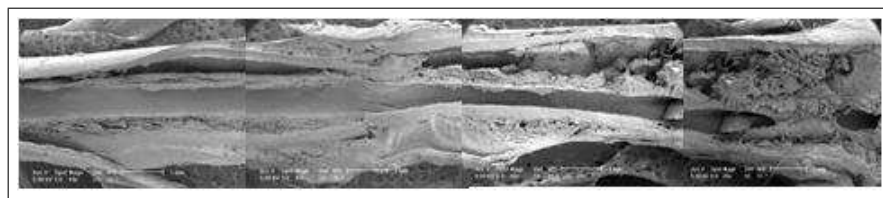


Figure 2.18 Montage-like SEM picture of lateral surface of the bone with conventional method (without injection of antiembolic agents), rat number 2, with relatively low magnification

Figure 2.19 shows the scanning electron micrographs under various magnifi-

cations (34x, 250x, 500x, 1000x, 2000x) on the lateral surface of the fractured and normally healed sample 2, obtained far from the healed region. It is obvious that defect feature is almost same with control 1 sample (Figure 2.14).

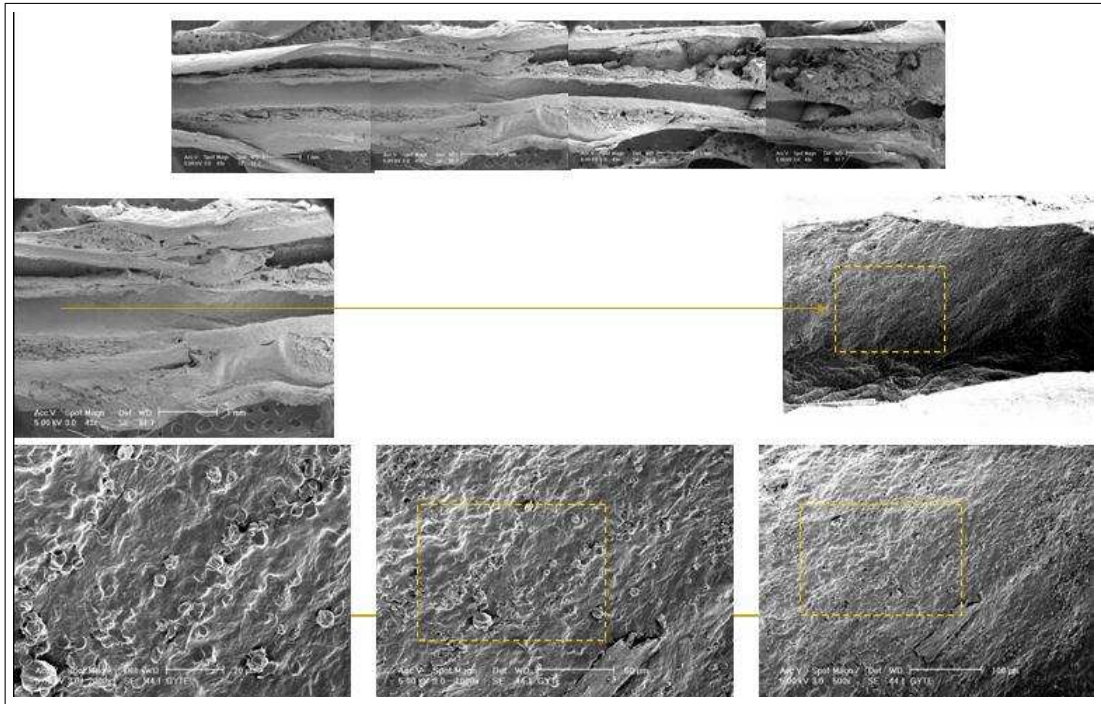


Figure 2.19 The SEM micrographs under various magnifications of the control sample 2, obtained far from healed region, being fractured and healed.

Scanning electron micrographs obtained under various magnifications (34x, 250x, 500x, 1000x, 2000x) on the lateral surface of the fractured and normally healed sample 2, obtained from closed to healed region are shown in Figure 2.20. It is clear, that, while coming close to healed region, defects (holes) were formed.

The lateral surface of the fractured and normally healed sample 2 obtained almost healed are visualized with different magnifications (34x, 250x, 500x, 1000x, 2000x) in Figure 2.21. It is clear that defects in micro level are visible like control sample 1, Figure 2.16).

Scanning electron micrographs obtained under various magnifications (34x, 250x, 500x, 1000x, 2000x) on the lateral surface of the fractured and normally healed sample 2, obtained from closed to healed region are shown in Figure 2.22. To see the similar-

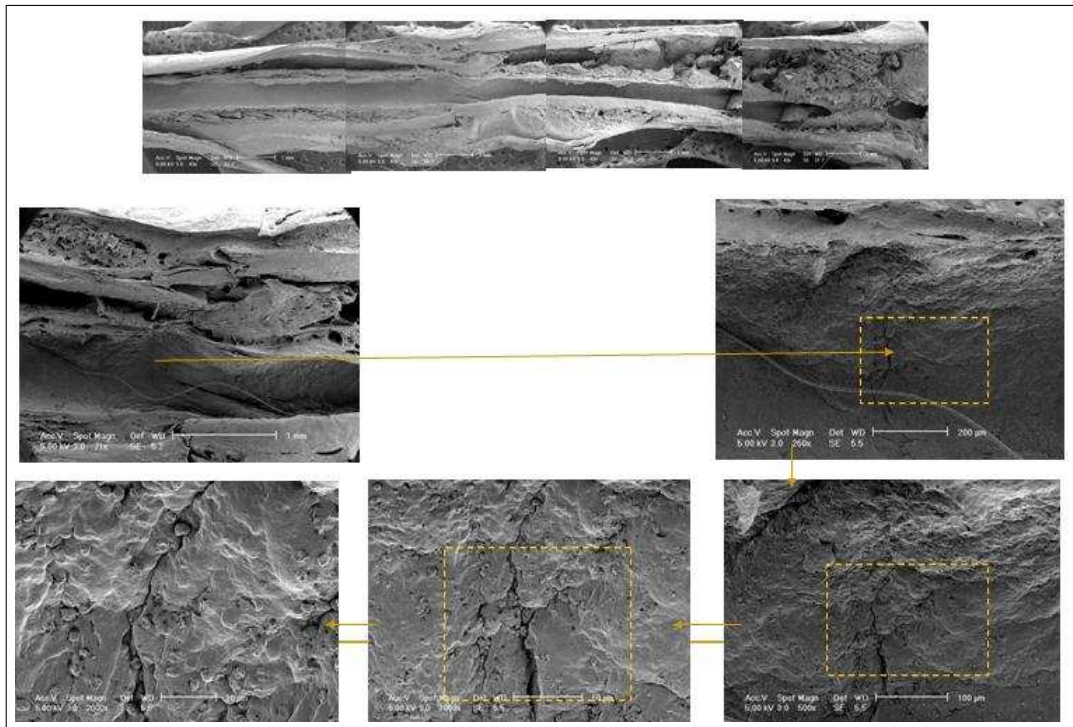


Figure 2.20 The SEM micrographs under various magnifications of the control sample 2, obtained from closed to healed region, being fractured and healed being fractured and healed.

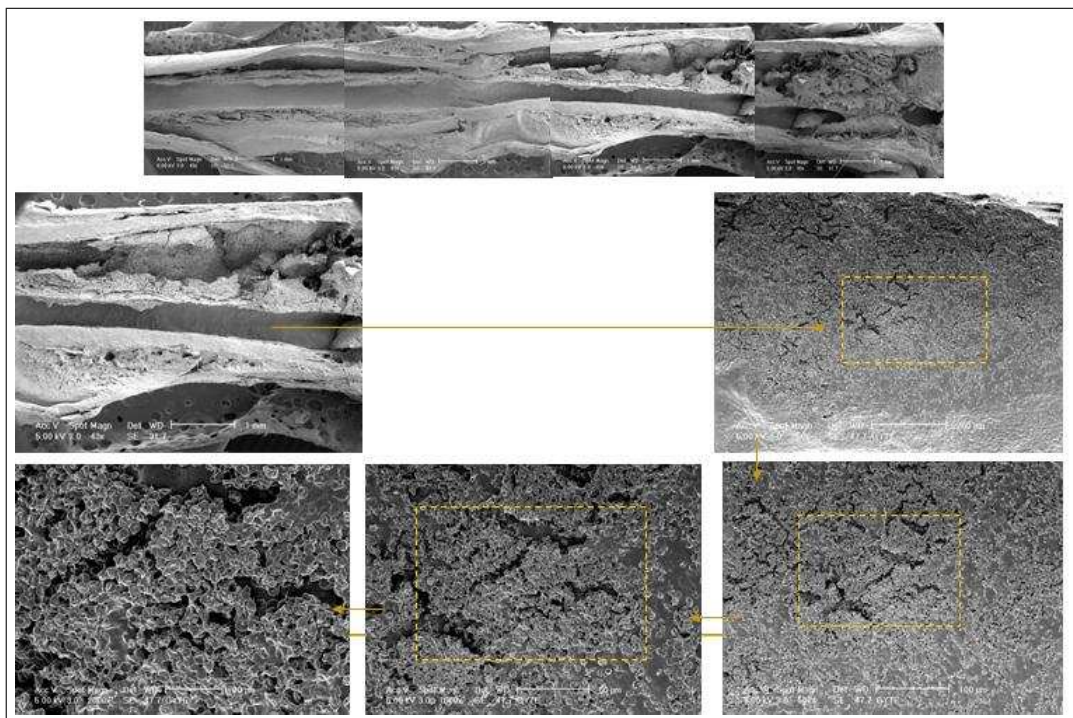


Figure 2.21 The SEM micrographs under various magnifications of the control sample 1, obtained from almost healed region, being fractured and healed

ities of control sample 1 and 2, see Figure 2.15. It is clear that while coming close to healed region, defects (holes) were formed.

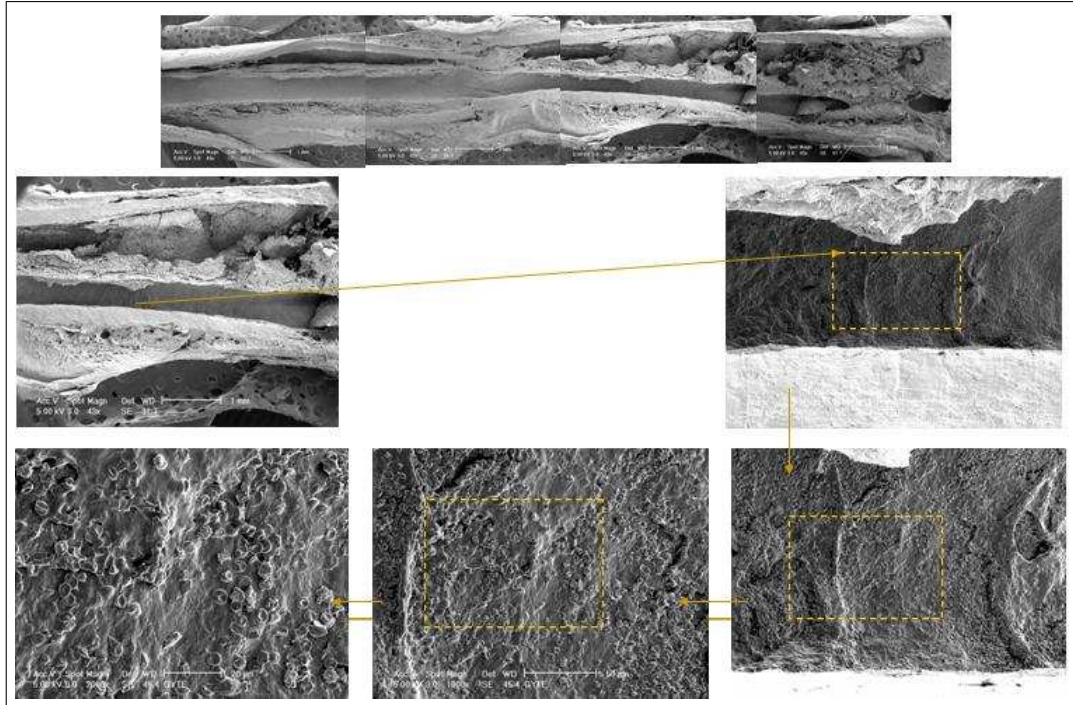


Figure 2.22 The SEM micrographs under various magnifications of the control sample 2, obtained from closed to healed region, being fractured and healed.

Figure 2.57 and Figure 2.58 are the micrographs showing microstructural changes from one end of the sample 1 and 2, to the region where fracture occurred and followed by conventional healing, with 500x and 1000x magnification respectively.

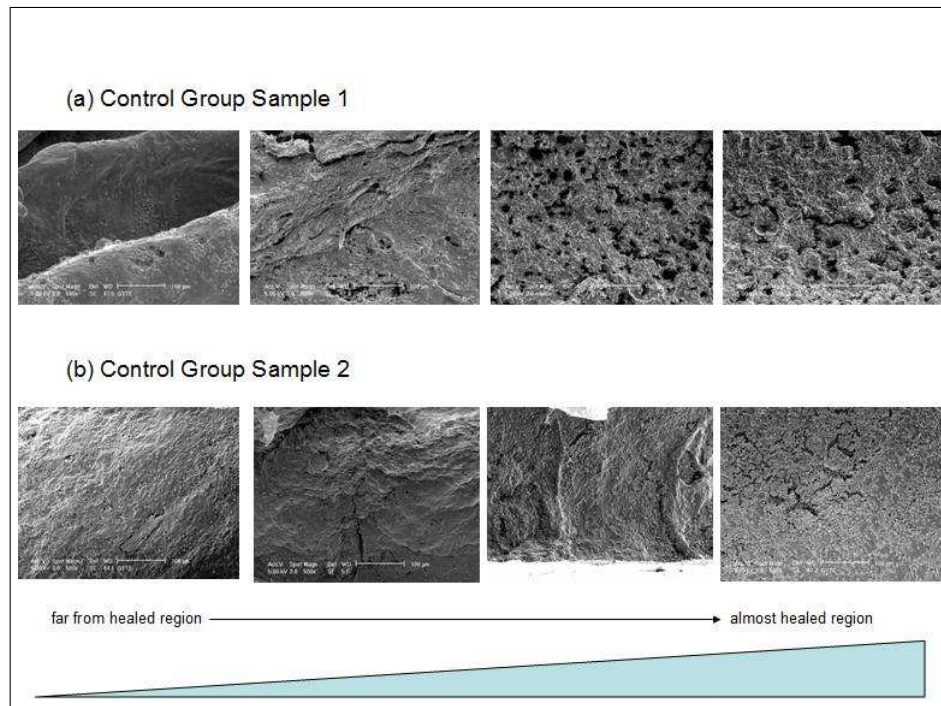


Figure 2.23 The SEM micrographs obtained from similar regions of control groups under x500 magnification

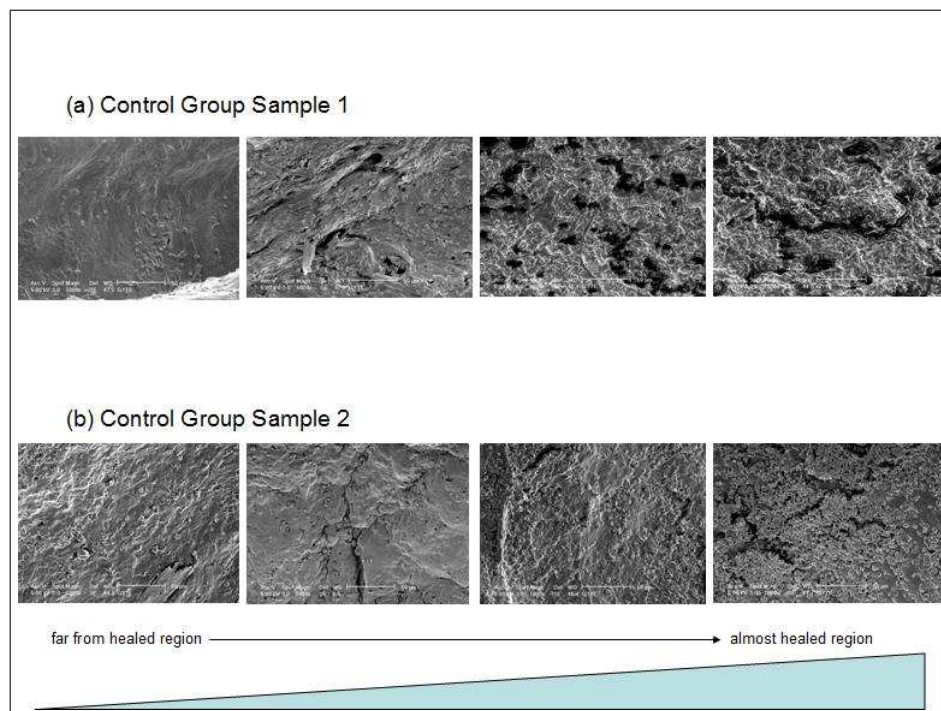


Figure 2.24 The SEM micrographs obtained from similar regions of control groups under x1000 magnification

2.3.3.2 Heparin-treated group. SEM studies on the fractured and healed; heparin-treated sample 1

Montage-like SEM picture of lateral surface of the fractured and healed with heparin injection sample 1, with relatively low magnification is shown in Figure 2.25.

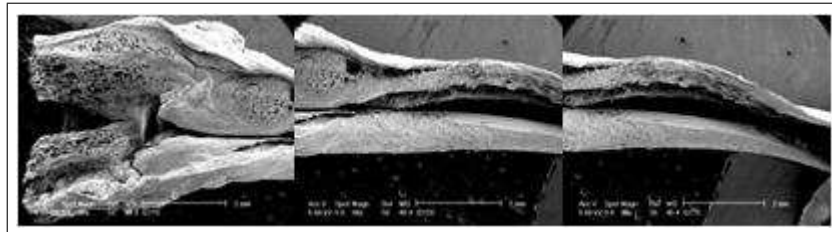


Figure 2.25 Montage-like SEM picture of lateral surface of the fractured and healed with heparin injection sample 1, with relatively low magnification.

Figure 2.26 shows the scanning electron micrographs under various magnifications (34x, 250x, 500x, 1000x, 2000x) on the lateral surface of the fractured and healed with heparin injection sample 1, obtained far from healed region. There are no defects as control sample 1. See Figure 2.14 and Figure 2.17 to observe the similarities of the morphology of the samples. We can conclude that, heparin treatment has no significant effect on the morphology of the bone when coming far from the healed region compared to control group.

Scanning electron micrographs obtained under various magnifications (34x, 500x, 1000x, 2000x) on the lateral surface of the fractured and healed with heparin injection sample 1, which magnified closed to the healed region are shown in Figure 2.27. There are almost no visible defects. Defect feature is different from control samples. To see and compare the effects of heparin on bone morphology, see Figure 2.15, Figure 2.20 and Figure 2.22, which were obtained almost from the same regions of the control samples.

Scanning electron micrographs obtained under various magnifications (34x, 250x, 500x, 1000x, 2000x) on the lateral surface of the just healed region of the fractured and heparin-treated sample 1, which magnified just to the healed region are shown

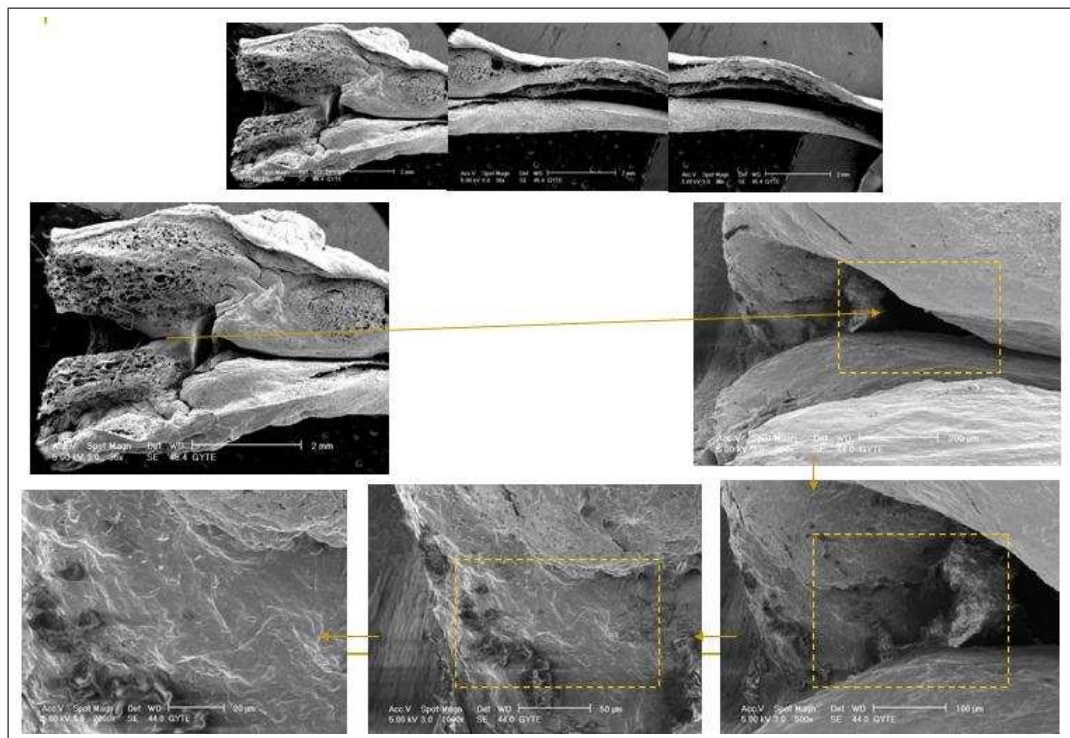


Figure 2.26 The SEM micrographs under various magnifications of the heparin-injected sample 1, obtained far from healed region, being fractured and healed.

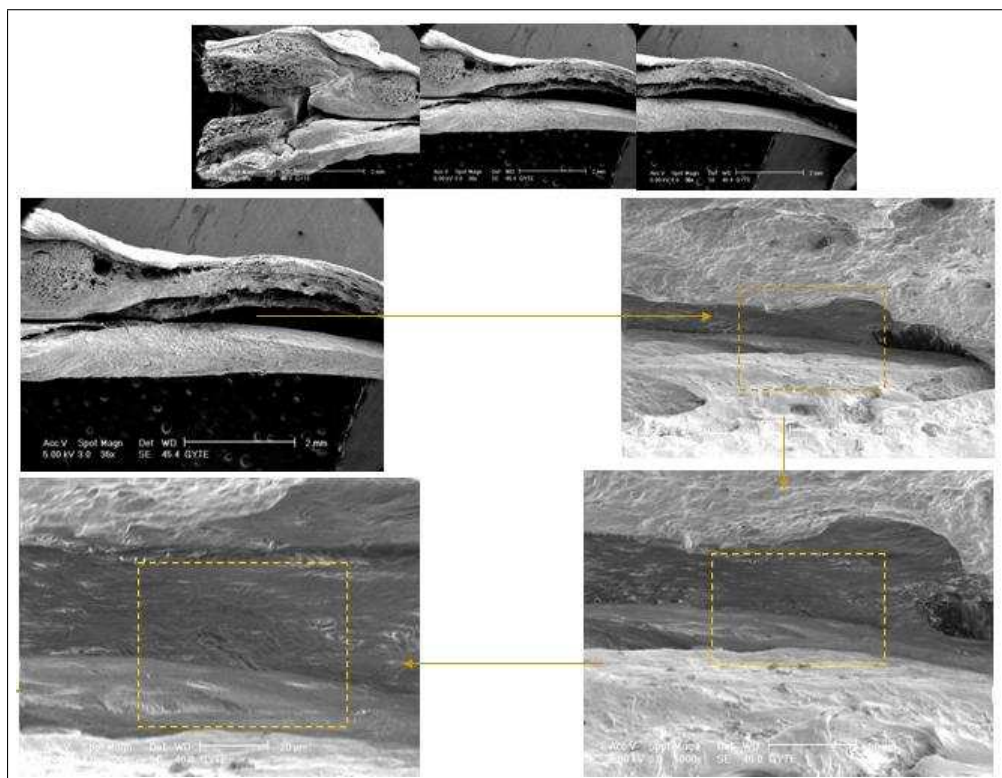


Figure 2.27 The SEM micrographs under various magnifications of the heparin-injected sample 1, obtained from closed to healed region, being fractured and healed.

in Figure 2.28, showing same defect feature in micro level with previous micrographs obtained from heparin sample 1, see Figure 2.26 and Figure 2.27. There is a significant difference between the micrographs, which are obtained from same region of the control group and heparin-injected sample 1 (Figure 2.16 and Figure 2.21).

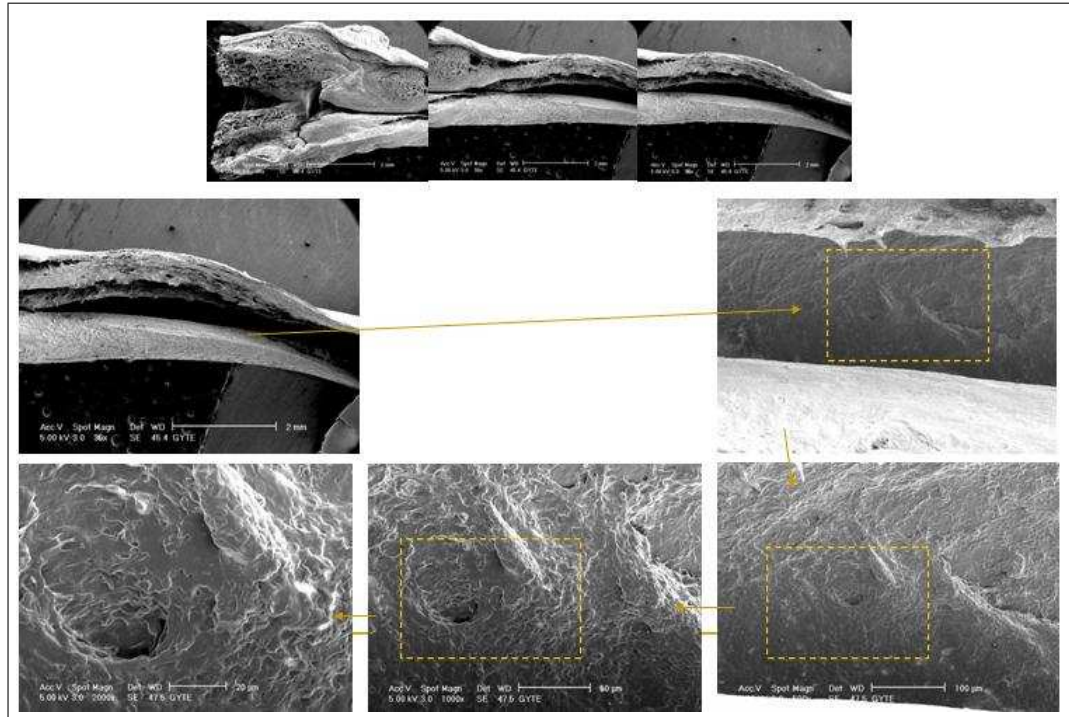


Figure 2.28 The SEM micrographs under various magnifications of the heparin-injected sample 1, obtained almost from healed region, being fractured and healed.

The lateral surfaces of the fractured and healed with heparin injection sample 1, obtained far from the healed region are visualized with different magnifications (34x, 250x, 500x, 1000x, 2000x) in Figure 2.29. Less and almost no defects are visible as previous scanning electron micrographs obtained from heparin-injected sample 1 (Figure 2.26, Figure 2.27 and Figure 2.28).

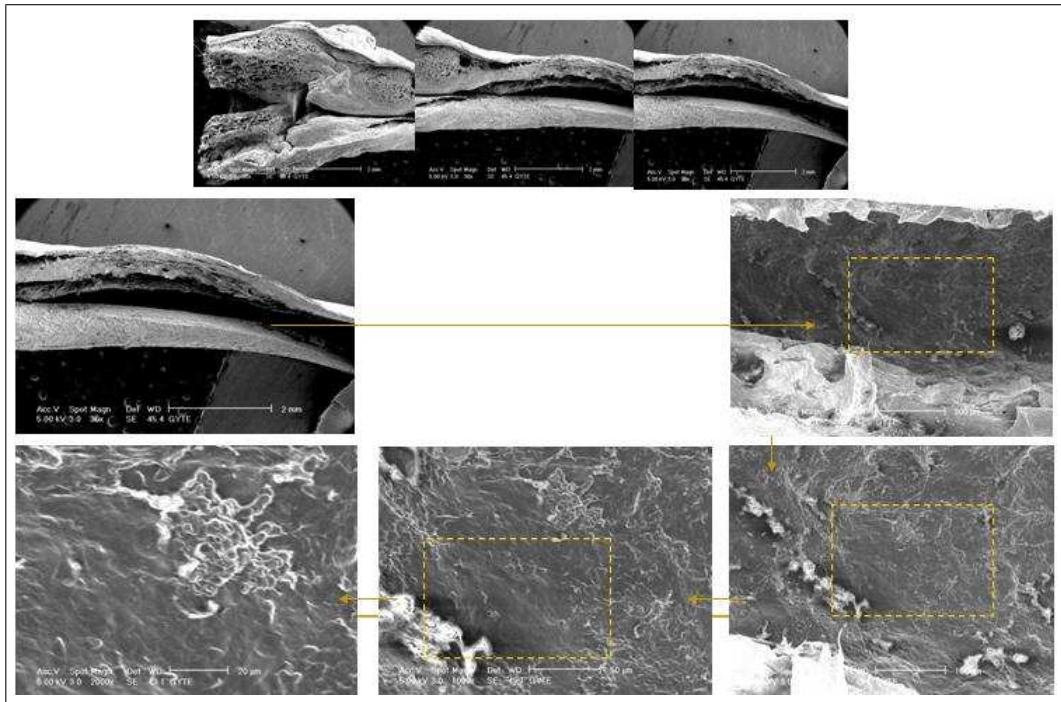


Figure 2.29 The SEM micrographs under various magnifications of the heparin-injected sample 1, obtained apart from healed region, being fractured and healed.

SEM studies on the fractured and healed; heparin-treated sample 2

Montage-like SEM picture of lateral surface of the fractured and healed with heparin injection sample 2, with relatively low magnification is shown in Figure 2.30.

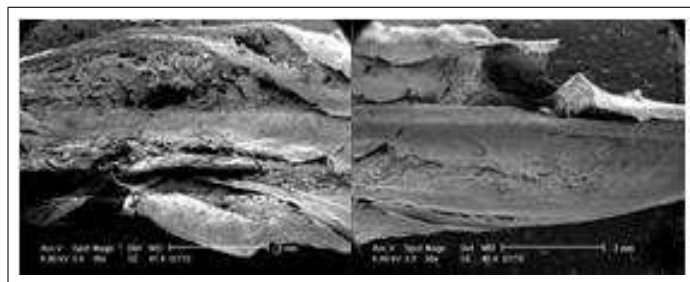


Figure 2.30 Montage-like SEM picture of lateral surface of the fractured and healed with heparin injection sample 2 obtained with relatively low magnification.

Figure 2.31 shows the scanning electron micrographs under various magnifications (34x, 250x, 500x, 1000x, 2000x) on the lateral surface of the fractured and healed with heparin injection sample 2, obtained far from healed region. There are almost no defects as micrographs obtained from the same regions of the heparin-injected sample

1 and control samples, Figure 2.26, Figure 2.29, Figure 2.14, Figure 2.17 and Figure 2.19.

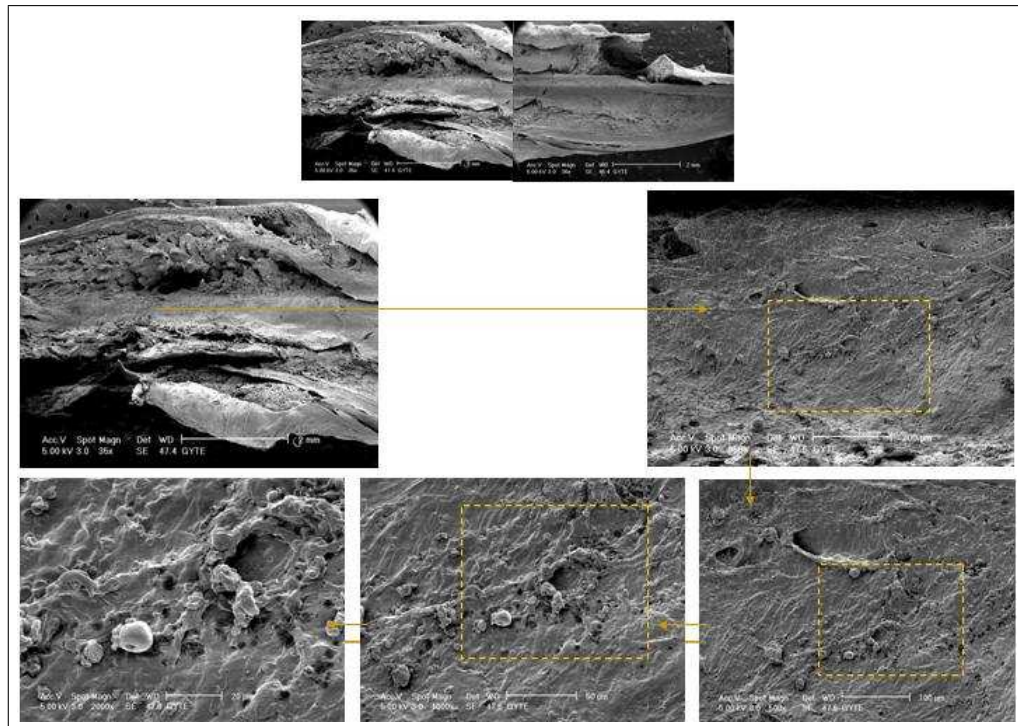


Figure 2.31 The SEM micrographs under various magnifications of the heparin-injected sample 2, far from healed region, being fractured and healed.

Scanning electron micrographs obtained under various magnifications (34x, 250x, 500x, 1000x, 2000x) on the lateral surface of the fractured and healed with heparin-injection sample 2, which were magnified closed to healed region are shown in Figure 2.32. It is clear, that, defect feature is almost same with heparin-injected sample 1 (Figure 2.27). To compare the effect of heparin on the morphology of the bone see Figure 2.15, Figure 2.20 and Figure 2.22, which were obtained almost from same regions of the control samples.

The lateral surface of the fractured and healed with heparin injection, sample 2, obtained from the healed region are visualized with different magnifications (34x, 250x, 500x, 1000x, 2000x) in Figure 2.33. Less and almost no defects are visible, as previous micrographs obtained from heparin samples (Figure 2.28). To compare the effects of heparin on bone morphology see Figure 2.16, Figure 2.21 and Figure 2.28.

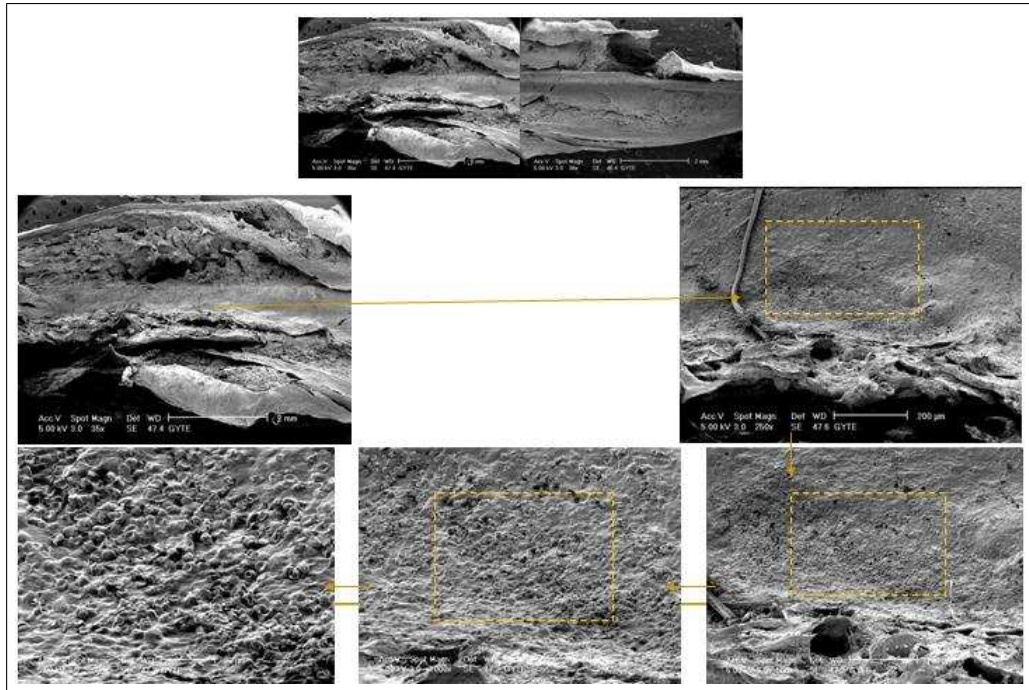


Figure 2.32 The SEM micrographs under various magnifications of the heparin-injected sample 2, from closed to healed region, being fractured and healed.

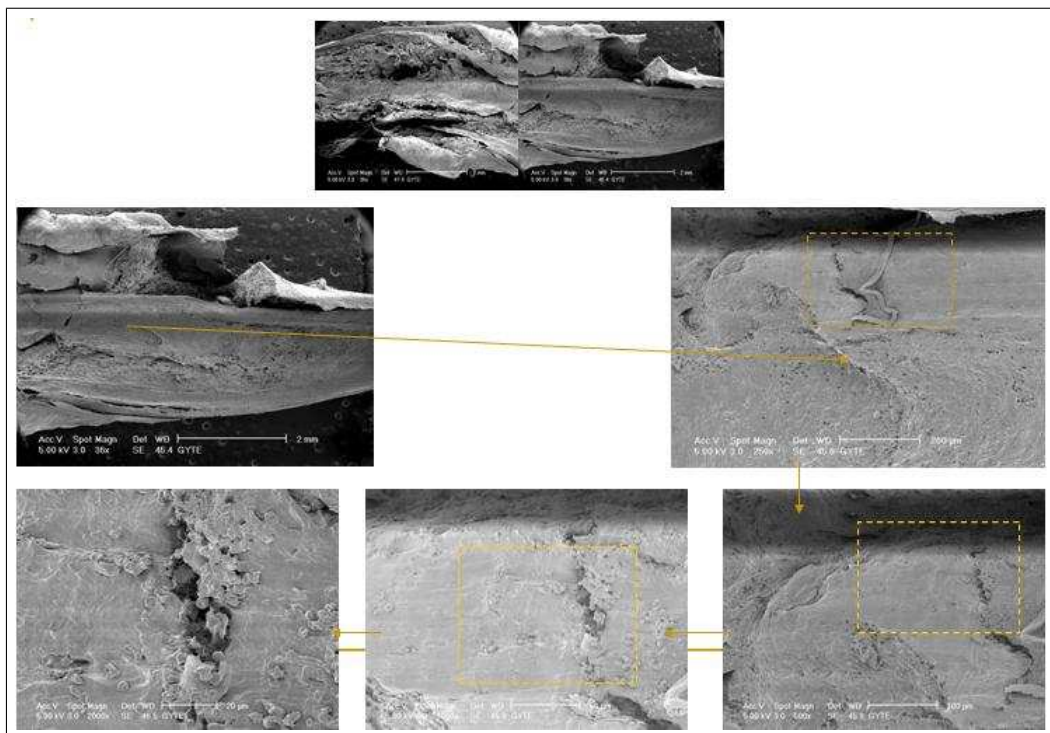


Figure 2.33 The SEM micrographs under various magnifications of the heparin-injected sample 1, from almost healed region, being fractured and healed.

Figure 2.34 shows the scanning electron micrographs under various magnifications (34x, 250x, 500x, 1000x) on the lateral surface of the fractured and healed with injection of heparin, sample 2, obtained far from healed region. These micrographs showing more defects in micro level compared to heparin-treated sample 1 (Figure 2.26 and Figure 2.29).

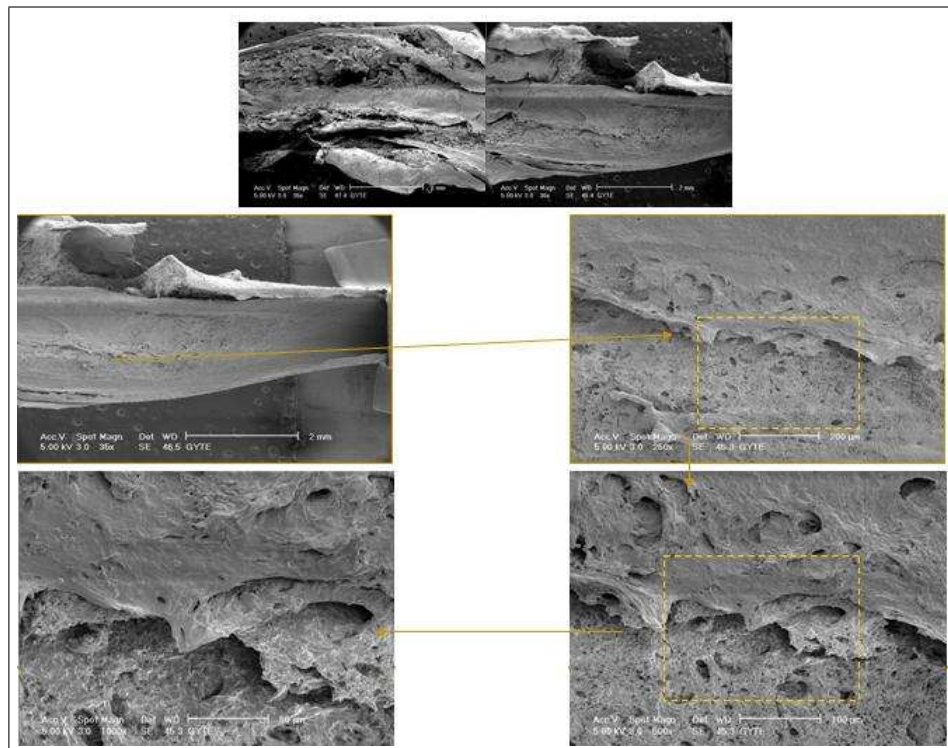


Figure 2.34 The SEM micrographs under various magnifications of the heparin-injected sample 1, apart from healed region, being fractured and healed.

Figure 2.57 and Figure 2.58 are the micrographs showing microstructural changes from one end of the sample 1 and 2, to the region where fracture occurred and followed by heparin treatment, with 500x and 1000x magnification respectively. To conclude, comparing to control group micrographs belonging to heparin-treated sample 1 and 2 are showing less almost no defect with respect to control group where no agents were injected.

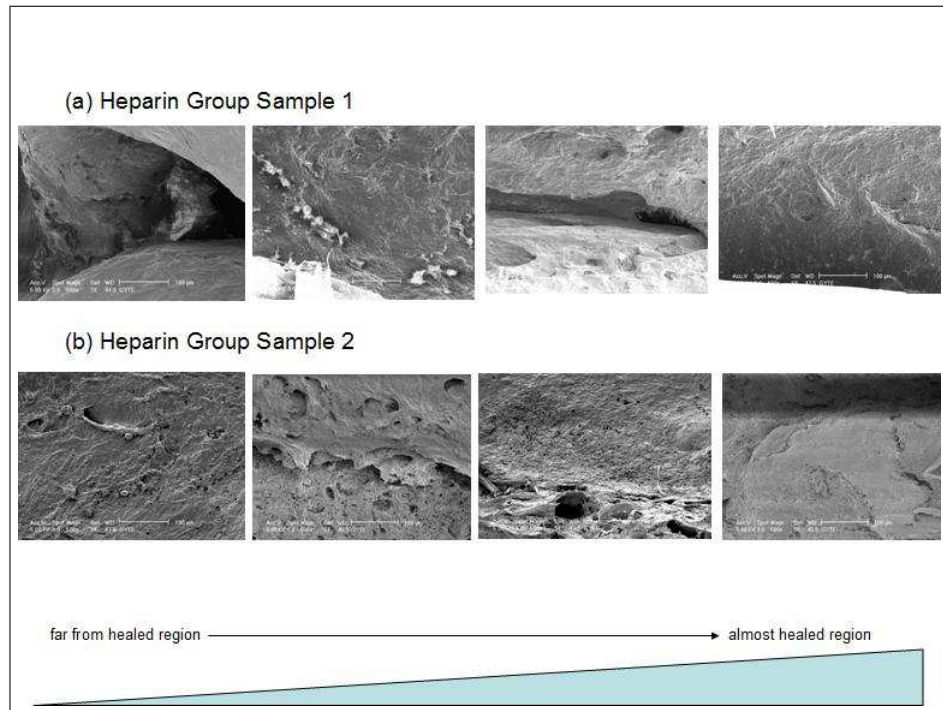


Figure 2.35 The SEM micrographs obtained from similar regions of heparin groups under x500 magnification

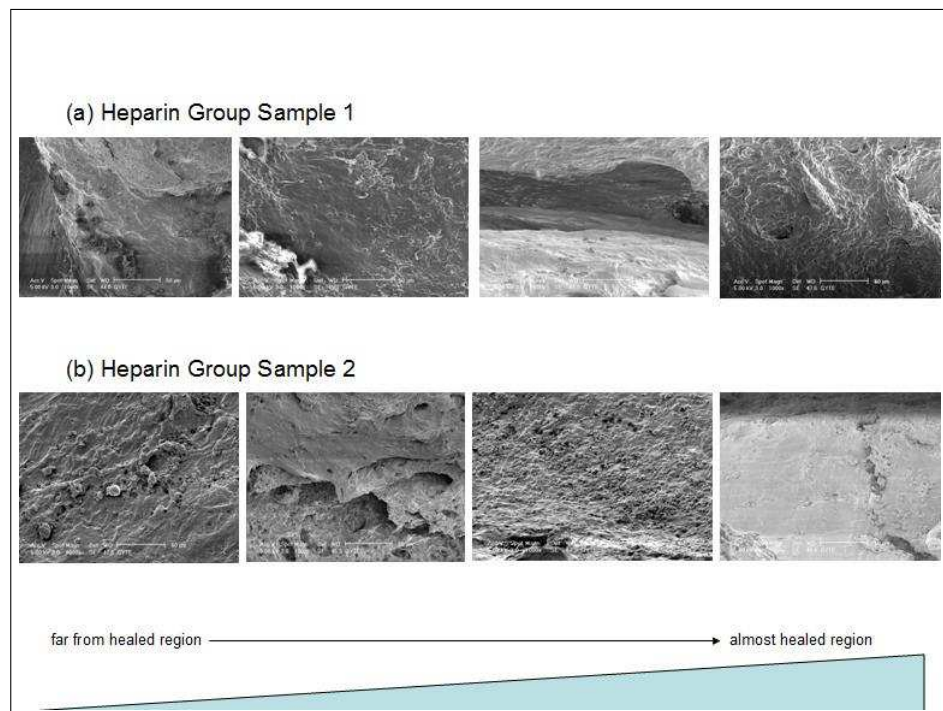


Figure 2.36 The SEM micrographs obtained from similar regions of heparin groups under x1000 magnification

2.3.3.3 LMWH-treated group. SEM studies on the fractured and healed; LMWH-treated sample 1

Montage-like SEM picture of lateral surface of the fractured and healed with LMWH injection sample 1, with relatively low magnification is shown in Figure 2.37.

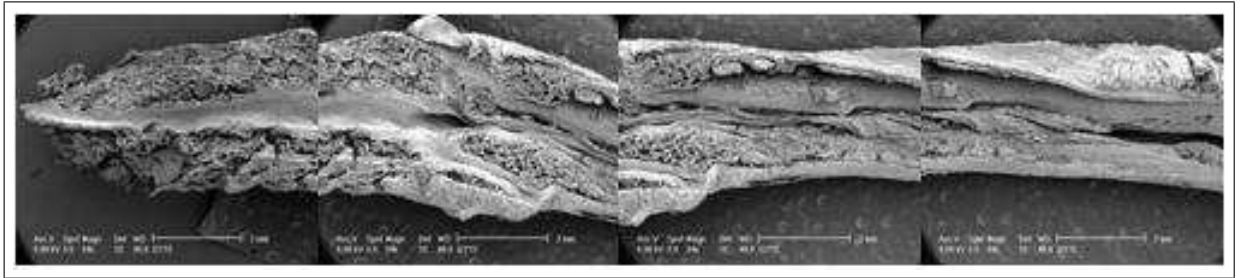


Figure 2.37 Montage-like SEM picture of lateral surface of the fractured and healed with LMWH injection sample 1, with relatively low magnification.

Figure 2.38 shows the scanning electron micrographs under various magnifications (34x, 250x, 500x, 1000x, 2000x) on the lateral surface of the fractured and healed with LMWH injection sample 1, which were magnified closed to the healed region. There are almost no defects as previous micrographs obtained from the same region of the control samples and heparin samples (Figure 2.15, Figure 2.20, Figure 2.22, Figure 2.27 and Figure 2.32).

Scanning electron micrographs obtained under various magnifications (34x, 250x, 500x, 1000x, 2000x) on the lateral surface of the fractured and healed with LMWH injection sample 1, just healed region are shown in Figure 2.39. There are no almost no defects as previous scanning electron micrographs obtained from the same region of the heparin samples (Figure 2.28 and Figure 2.33).

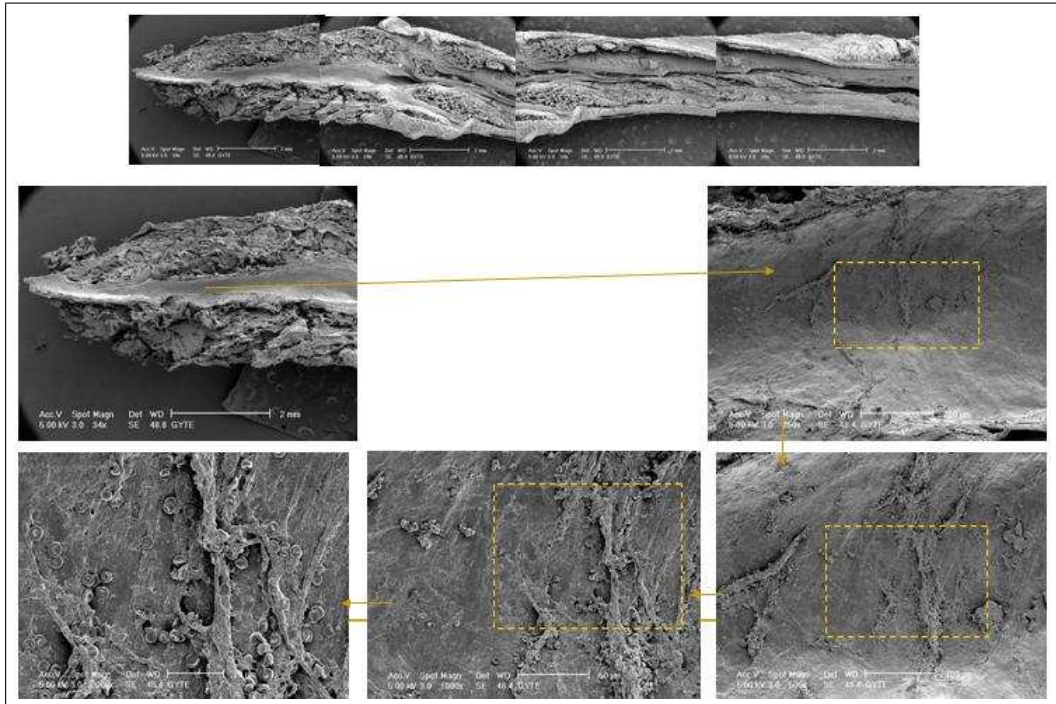


Figure 2.38 The SEM micrographs under various magnifications of the LMWH-injected sample 1, closed to healed region, being fractured and healed.

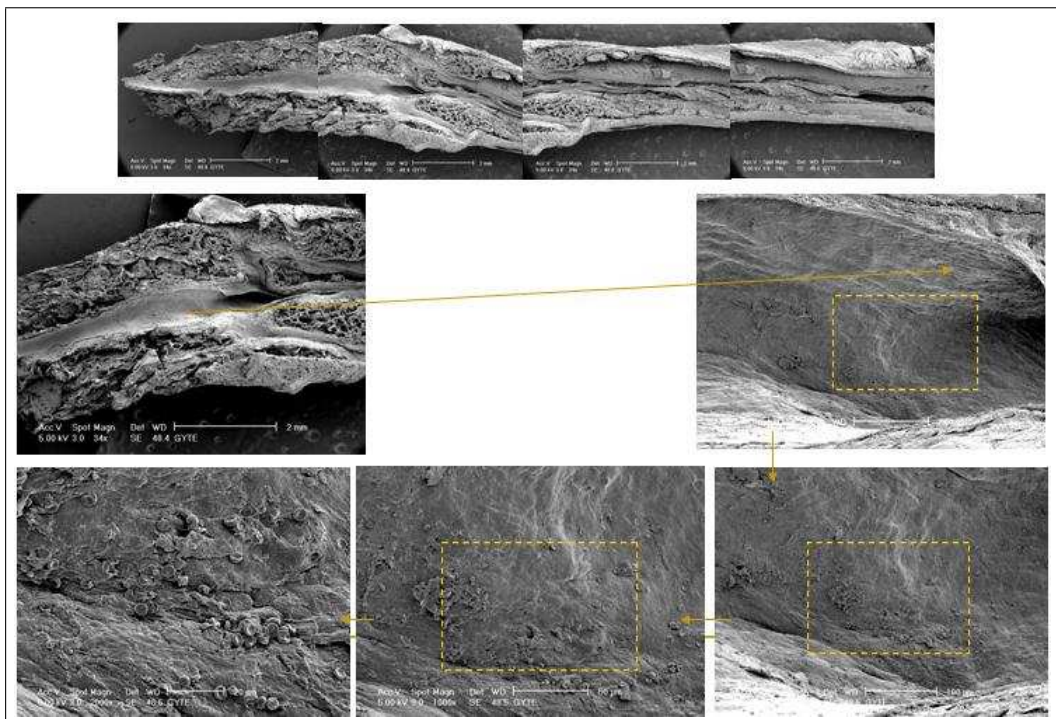


Figure 2.39 The SEM micrographs under various magnifications of the LMWH-injected sample 1, almost healed region, being fractured and healed.

The lateral surfaces of the fractured and healed with LMWH injection sample 1 obtained far from the healed region are visualized with different magnifications (34x, 250x, 1000x, 2000x) in Figure 2.40. Less and almost no defects are visible. Defect feature is same as control samples and heparin-injected samples. There are almost no defects as previous micrographs obtained from the same region of the control samples and heparin samples (Figure 2.14, Figure 2.17, Figure 2.19, Figure 2.26, Figure 2.29, Figure 2.31 and Figure 2.34)

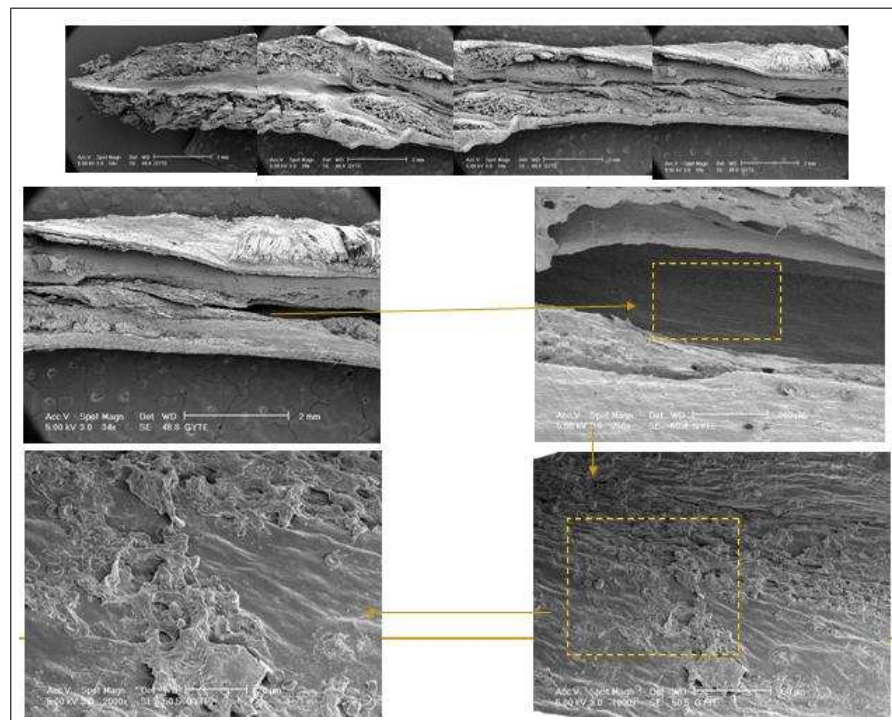


Figure 2.40 The SEM micrographs under various magnifications of the LMWH-injected sample 1, far from healed region, being fractured and healed.

SEM studies on the fractured and healed; LMWH-treated sample 2

Montage-like SEM picture of lateral surface of the fractured and healed with LMWH injection sample 2, with relatively low magnification is shown in Figure 2.41.

Scanning electron micrographs obtained under various magnifications (34x, 250x, 500x, 1000x, 2000x) on the lateral surface of the fractured and healed with LMWH injection sample 2, from almost healed region showing almost no defects in micro level, see Figure 2.42. To compare the effect of LMWH and heparin on the morphology of

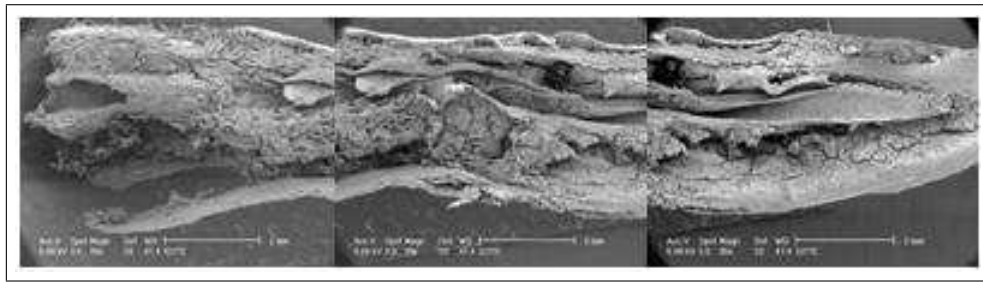


Figure 2.41 Montage-like SEM picture of the fractured and healed with LMWH injection sample 2, with relatively low magnification.

the bone, see Figure 2.16, Figure 2.21, Figure 2.28, Figure 2.33 and Figure 2.39 which were obtained almost from same regions of the control samples, heparin samples and LMWH samples.

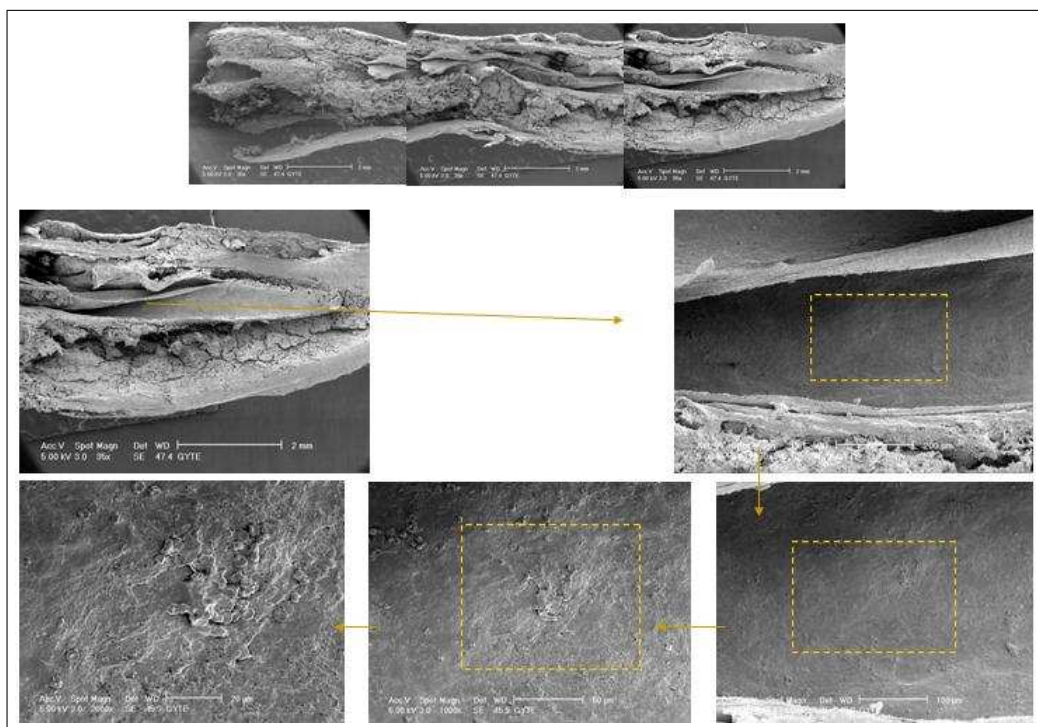


Figure 2.42 The SEM micrographs under various magnifications of the LMWH-injected sample 2, from almost healed region, being fractured and healed.

Figure 2.43 shows the scanning electron micrographs under various magnifications (34x, 250x, 500x, 1000x, 2000x) on the lateral surface of the fractured and healed with LMWH injection sample 2, from closed to healed region. There are no defects as previous scanning electron micrographs obtained from same regions of the LMWH-injected and heparin-injected samples (Figure 2.38, Figure 2.27 and Figure 2.32).

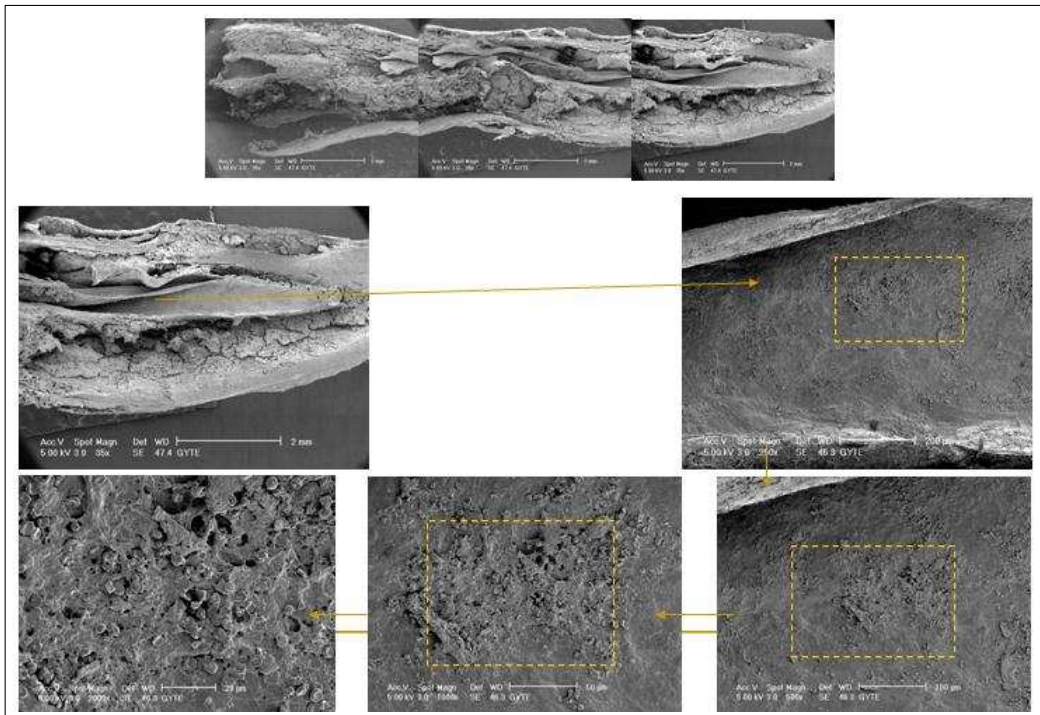


Figure 2.43 The SEM micrographs under various magnifications of the LMWH-injected sample 2, from closed to healed region, being fractured and healed.

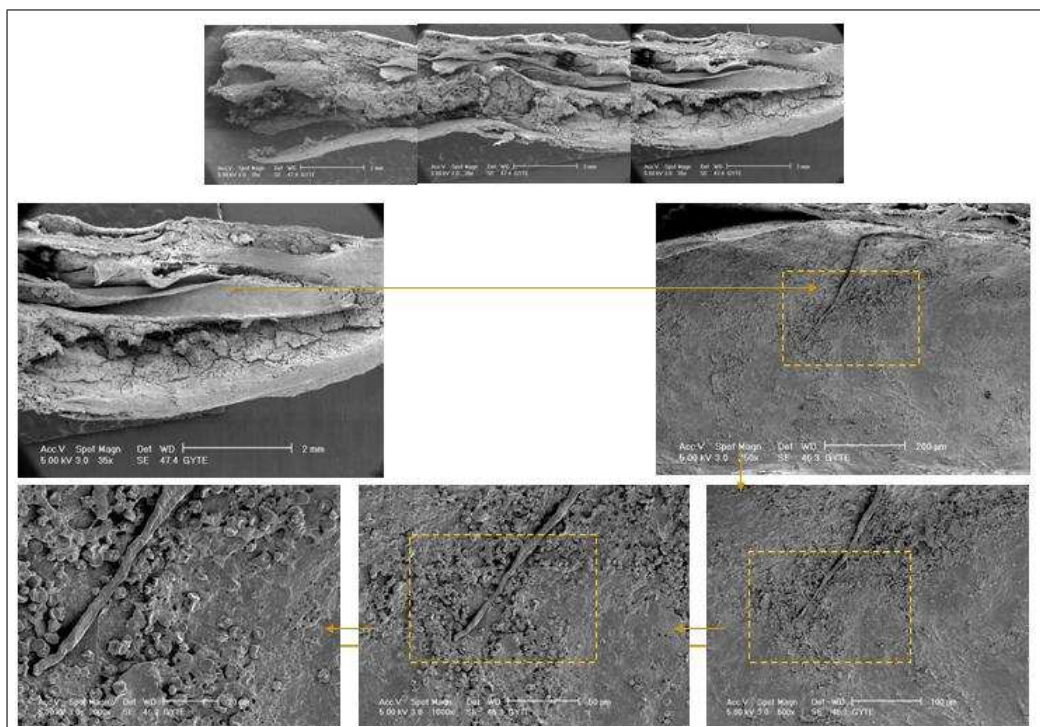


Figure 2.44 The SEM micrographs under various magnifications of the LMWH-injected sample 2, closed to healed region, being fractured and healed.

The lateral surfaces of the fractured and healed with LMWH injection sample 2, obtained from closed to the healed region are visualized with different magnifications (34x, 250x, 500x, 1000x, 2000x) in Figure 2.44. Less and almost no defects are visible as previous scanning electron micrographs obtained almost from same region of the LMWH-injected sample 1 and 2 (Figure 2.38 and Figure 2.43).

Figure 2.45 and Figure 2.46 are the micrographs showing microstructural changes from one end of the sample 1 and 2, to the region where fracture occurred and followed by LMWH treatment, with 500x and 1000x magnification respectively.

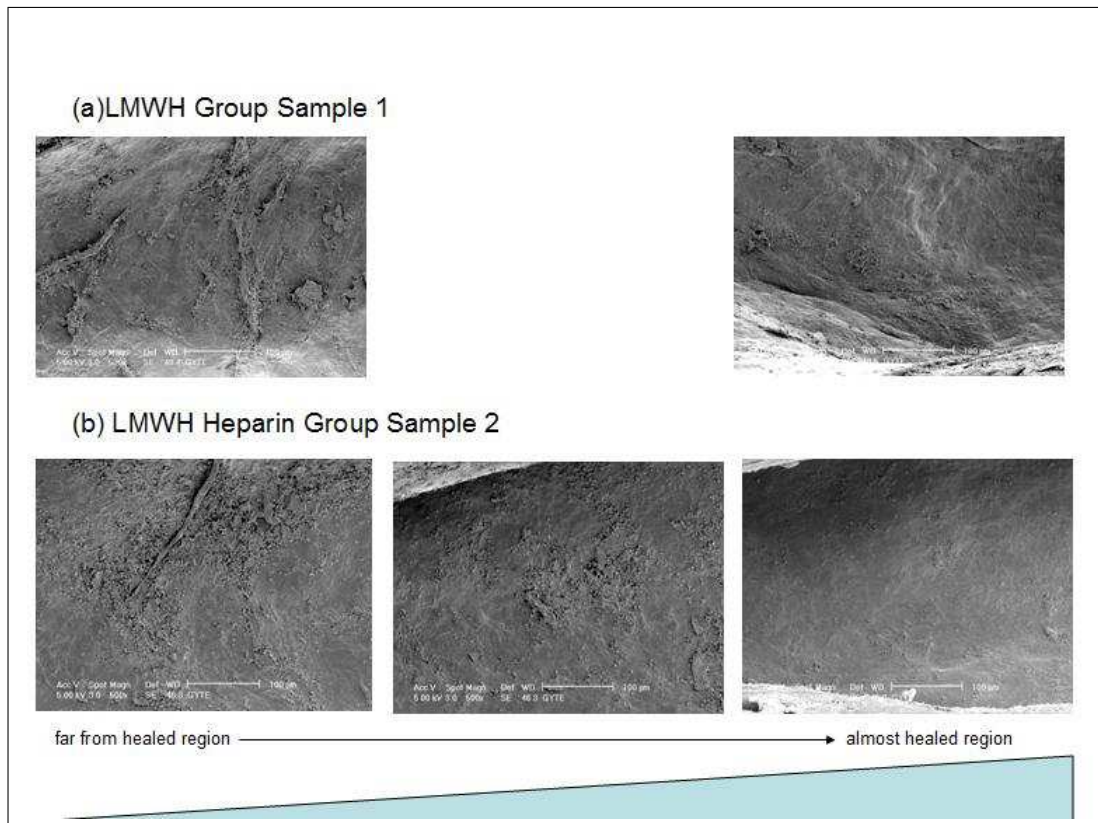


Figure 2.45 The SEM micrographs obtained from similar regions of LMWH groups under x500 magnification

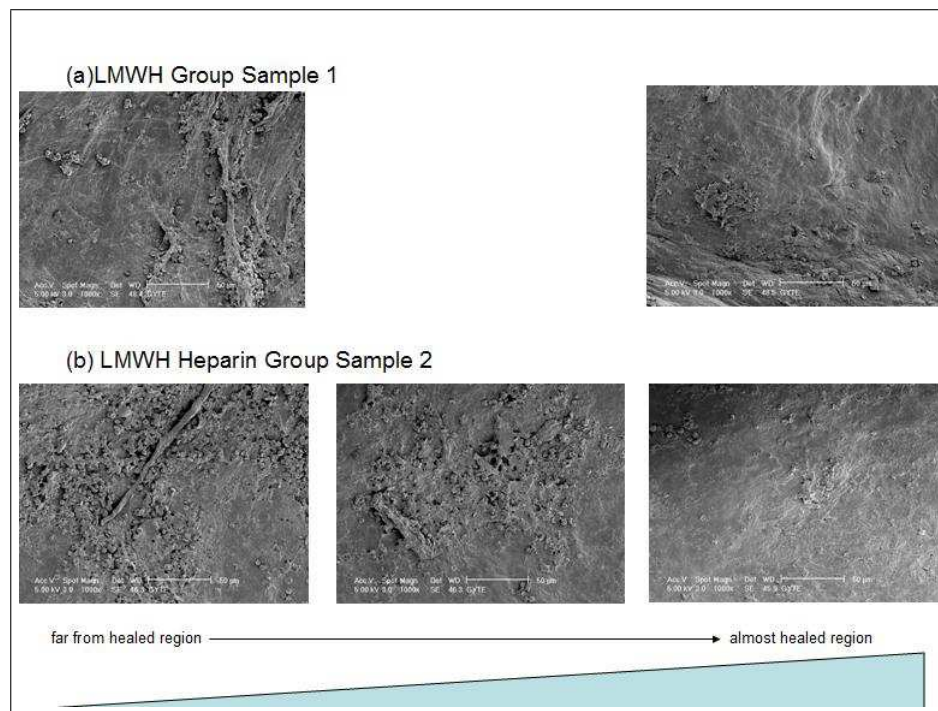


Figure 2.46 The SEM micrographs obtained from similar regions of LMWH groups under x1000 magnification

2.3.3.4 Fondaparinux-treated group. SEM studies on the fractured and healed; Fondaparinux-treated sample 1

Montage-like SEM picture of lateral surface of the fractured and healed with fondaparinux injection sample 1, with relatively low magnification is shown in Figure 2.47.

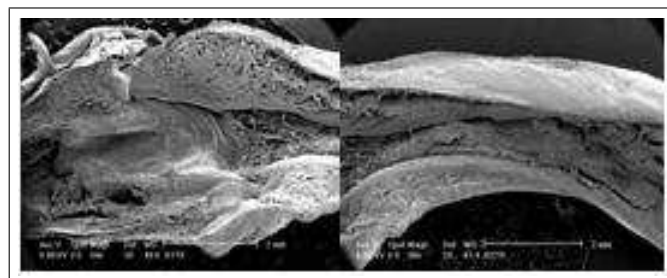


Figure 2.47 Montage-like SEM picture of lateral surface of the fractured and healed with fondaparinux injection sample 1, with relatively low magnification.

Figure 2.48 shows the scanning electron micrographs under various magnifica-

tions (34x, 250x, 500x, 1000x, 2000x) on the lateral surface of the fractured and healed with fondaparinux injection sample 1, obtained from closed to healed region. There are no defects as previous micrographs obtained from almost same regions of the control group, heparin-injected group and LMWH-injected group (Figure 2.27, Figure 2.32, Figure 2.38, Figure 2.43 and Figure 2.44).

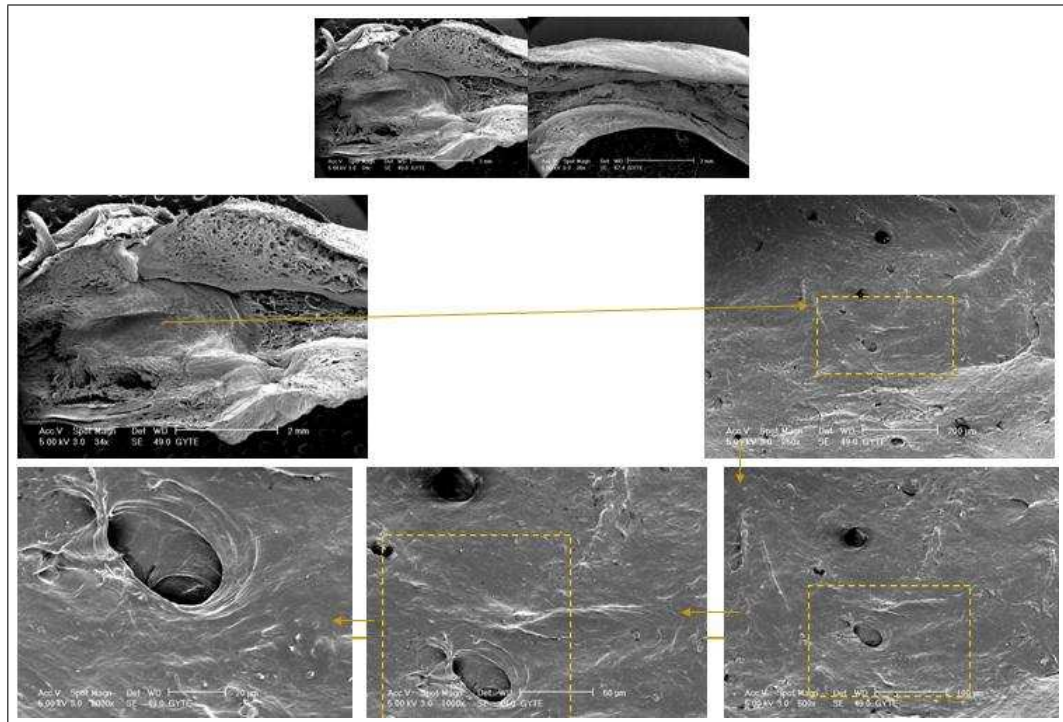


Figure 2.48 The SEM micrographs under various magnifications of the fondaparinux-injected sample 1, obtained from closed to healed region, being fractured and healed.

The lateral surface of the fractured and healed with fondaparinux injection sample 1, obtained almost from healed region are visualized with different magnifications (34x, 250x, 500x, 1000x, 2000x) in Figure 2.49. Almost no defects are visible as previous scanning electron micrographs obtained from almost same region of the heparin-injected samples and LMWH-injected samples (Figure 2.28, Figure 2.33, Figure 2.39 and Figure 2.42).

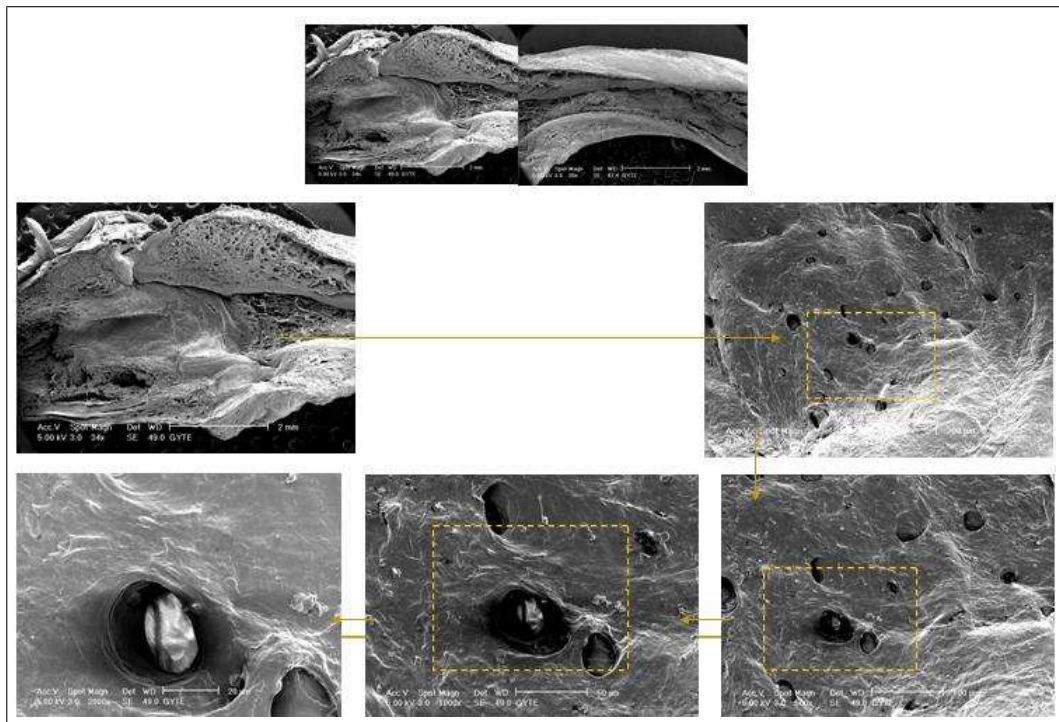


Figure 2.49 The SEM micrographs under various magnifications of the fondaparinux-injected sample 1, obtained almost from healed region, being fractured and healed

Scanning electron micrographs obtained under various magnifications (34x, 250x, 500x) on the lateral surface of the fractured and healed with fondaparinux injection sample 1, from almost healed region showing almost no defects in micro level, see Figure 2.50. These micrographs obtained from the cancellous part of the whole bone.

Figure 2.51 shows the scanning electron micrographs under various magnifications (34x, 250x, 500x, 1000x) on the lateral surface of the fractured and healed with fondaparinux injection sample 1, obtained far from healed region. There are less or almost no defects as previous scanning electron micrographs obtained almost from same regions of the control group, heparin-injected group and LMWH-injected group (Figure 2.14, Figure 2.17, Figure 2.19, Figure 2.26, Figure 2.29, Figure 2.31, Figure 2.34 and Figure 2.40).

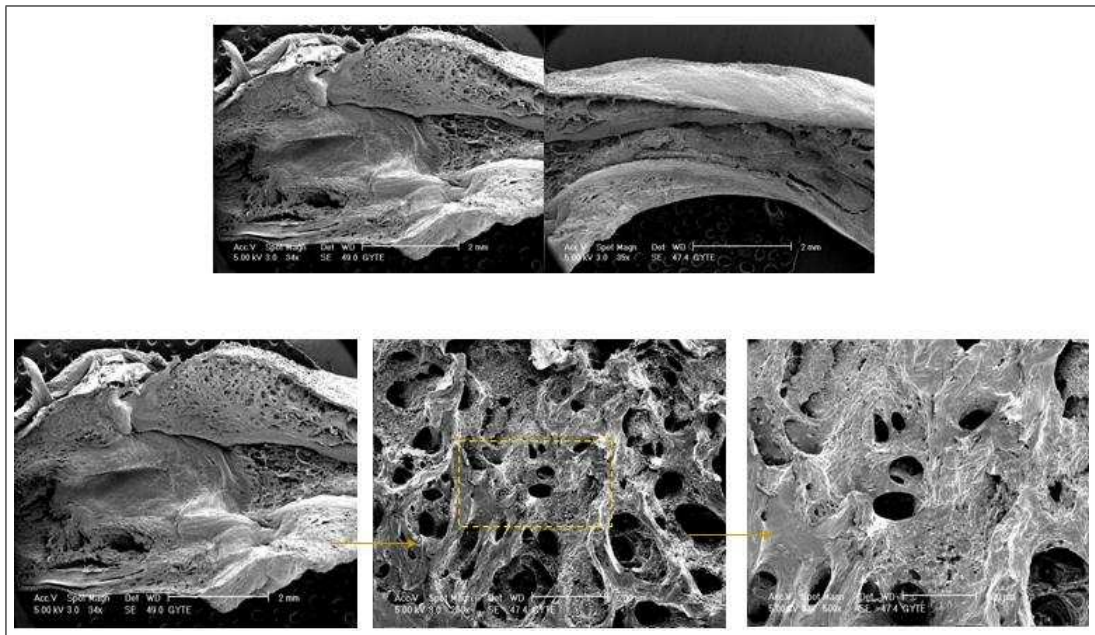


Figure 2.50 The SEM micrographs under various magnifications of the fondaparinux-injected sample 1, obtained from closed to healed region, being fractured and healed.

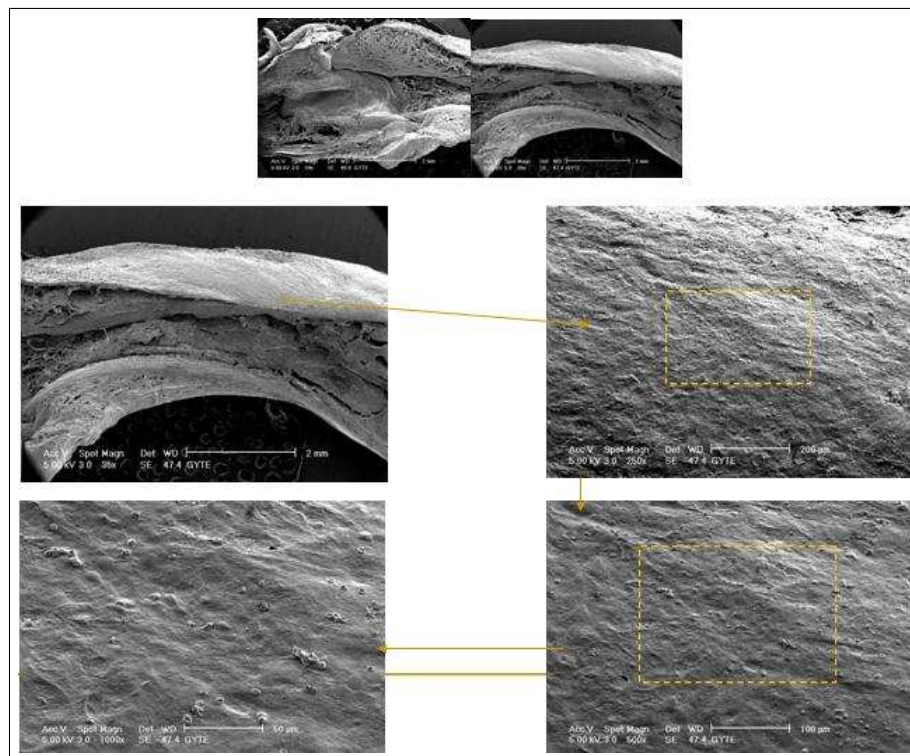


Figure 2.51 The SEM micrographs under various magnifications of the fondaparinux-injected sample 1, obtained far from healed region, being fractured and healed.

SEM studies on the fractured and healed; Fondaparinux-treated sample 2

Montage-like SEM picture of lateral surface of the fractured and healed with fondaparinux injection sample 2, with relatively low magnification is shown in Figure 2.52.

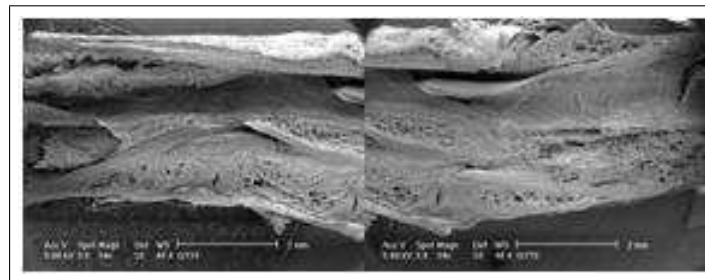


Figure 2.52 Montage-like SEM picture of lateral section of the fractured and healed with fondaparinux injection sample 2 with relatively low magnification.

The lateral surface of the fractured and healed with fondaparinux injection sample 2, obtained far from the healed region are visualized with different magnifications (34x, 250x, 500x, 1000x, 2000x) in Figure 2.53. There are almost no defects as previous scanning electron micrographs obtained almost from same regions of the control group, heparin-injected group, LMWH-injected group and fondaparinux-injected sample 1 (Figure 2.14, Figure 2.17, Figure 2.19, Figure 2.26, Figure 2.29, Figure 2.31, Figure 2.34, Figure 2.40 and Figure 2.51).

Figure 2.54 and Figure 2.55 shows the scanning electron micrographs under various magnifications (34x, 250x, 500x, 1000x, 2000x) on the lateral surfaces of the fractured and healed with fondaparinux injection sample 2, closed to healed region. There are no defects as previous scanning electron micrographs obtained almost from same regions of the control group, heparin-injected group and LMWH-injected group and fondaparinux injected sample 1 (Figure 2.27, Figure 2.32, Figure 2.38, Figure 2.43, Figure 2.44 and Figure 2.48). Layered structures are visible in these micrographs.

The lateral surface of the fractured and healed with fondaparinux injection sam-

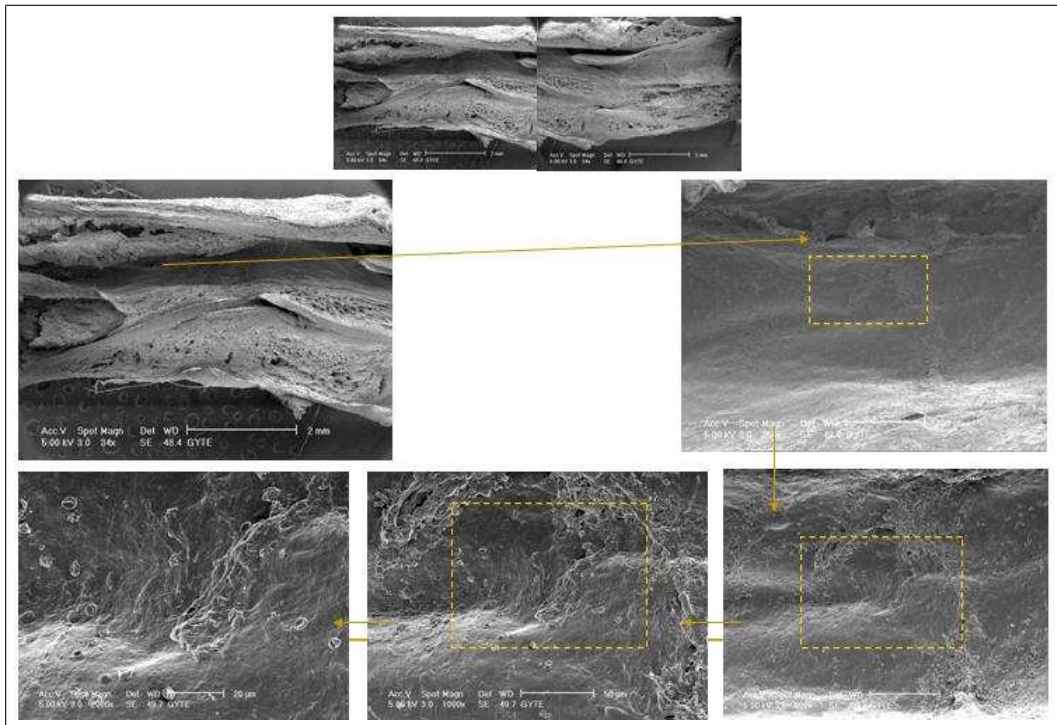


Figure 2.53 The SEM micrographs under various magnifications of the fondaparinux-injected sample 2, far from healed region, being fractured and healed.

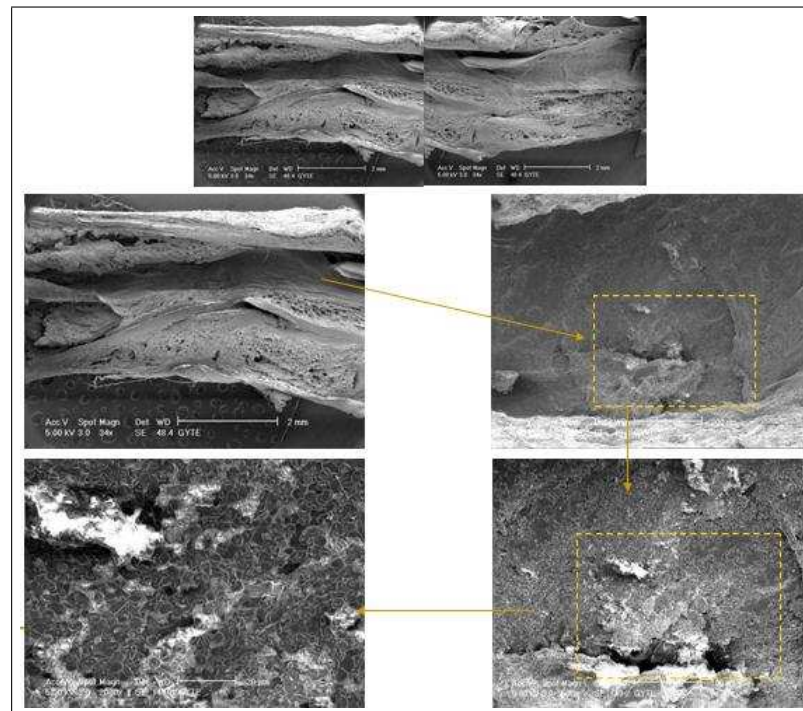


Figure 2.54 The SEM micrographs under various magnifications of the fondaparinux-injected sample 2, closed healed region, being fractured and healed.

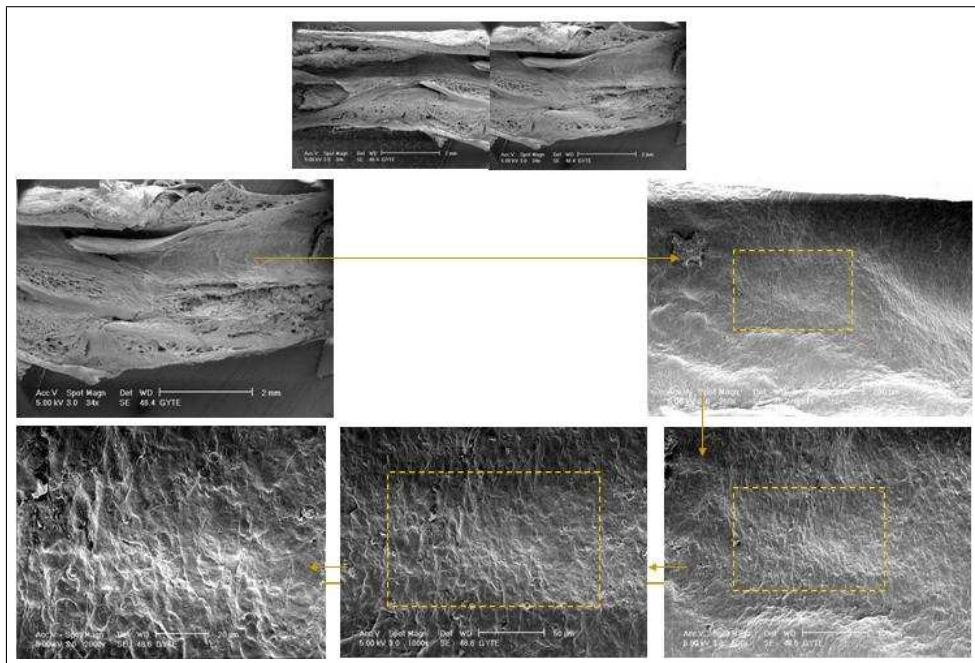


Figure 2.55 The SEM micrographs under various magnifications of the fondaparinux-injected sample 2, closed to healed region of the bone, being fractured and healed.

ple 2, obtained almost from healed region are visualized with different magnifications (34x, 250x, 500x, 1000x, 2000x) in Figure 2.56. There are almost no defects as previous scanning electron micrographs obtained from almost same regions of the heparin-injected group, LMWH-injected group and fondaparinux-injected sample 1 (Figure 2.28, Figure 2.33, Figure 2.39, Figure 2.42 and Figure 2.49). Moreover, formation of layered structure can be seen easily in fondaparinux-injected samples.

Figure 2.57 and Figure 2.58 are the micrographs showing microstructural changes from one end of the sample 1 and 2, to the region where fracture occurred and followed by fondaparinux treatment, with 500x and 1000x magnification respectively.

To conclude that, defect features of antiembolic agents; heparin, LMWH, and fondaparinux are similar and different compared to control group. There are almost no defects like micrographs obtained from control group. On the other hand, in fondaparinux-injected samples layered structures are visible in the micrographs obtained from scanning electron microscopy which are magnified closed to the healed region.

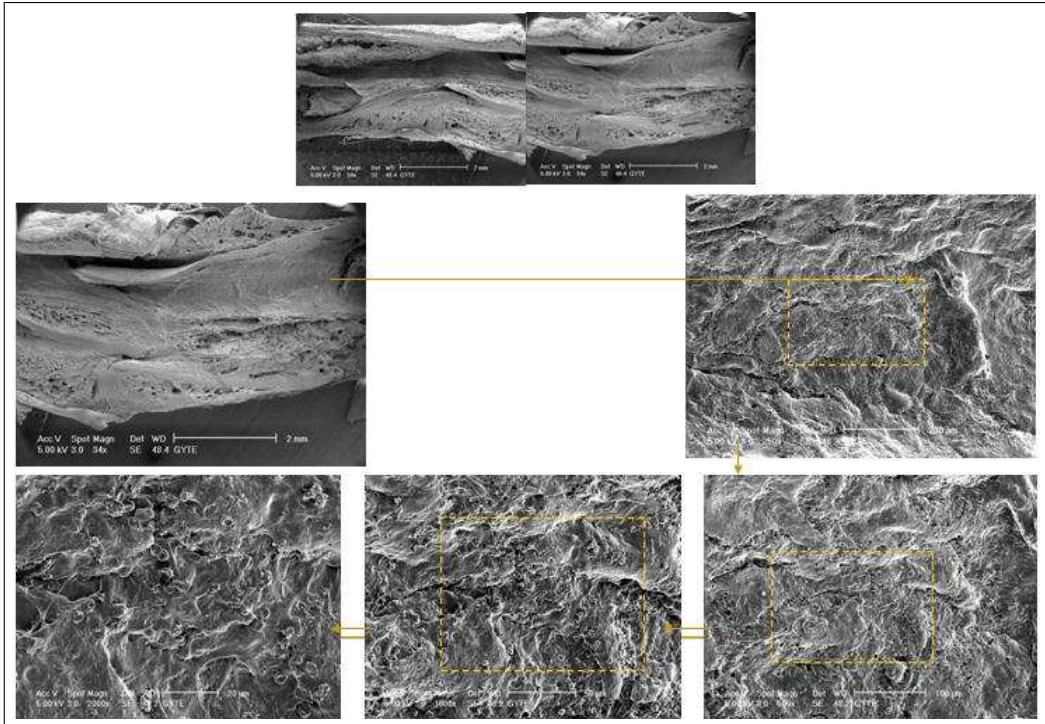


Figure 2.56 The SEM micrographs under various magnifications of the fondaparinux-injected sample 2, obtained almost from healed region of the bone, being fractured and healed.

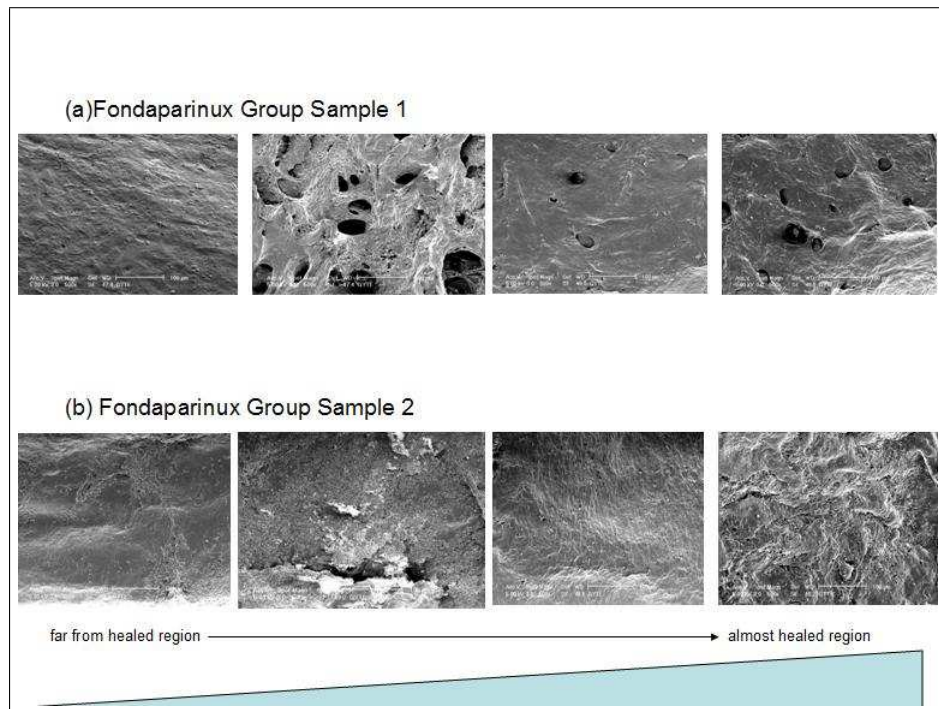


Figure 2.57 The SEM micrographs obtained from similar regions of fondaparinux groups under x500 magnification

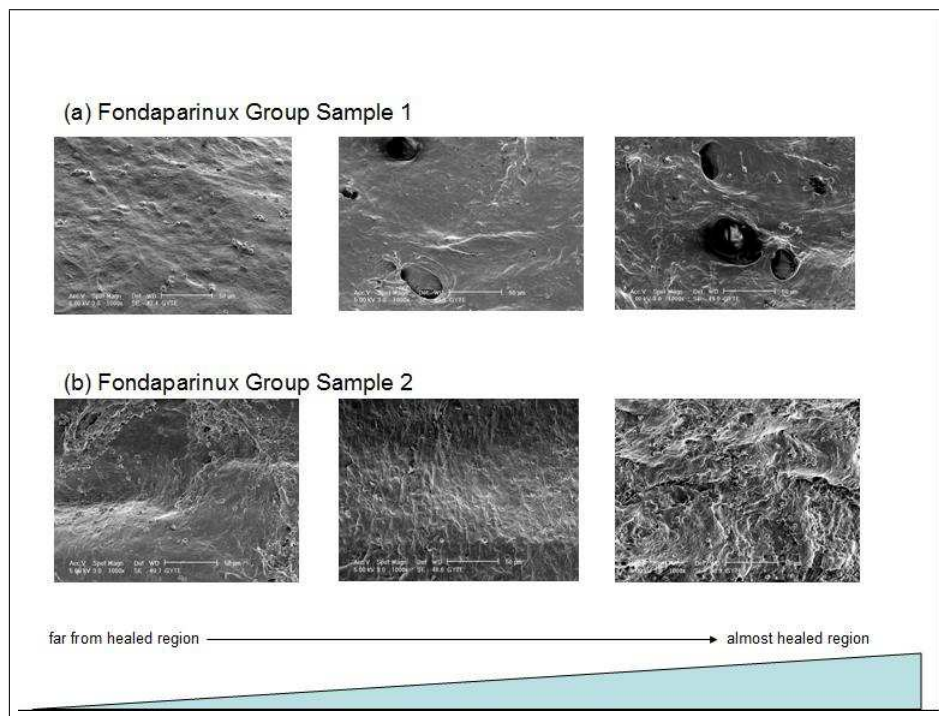


Figure 2.58 The SEM micrographs obtained from similar regions of fondaparinux groups under x1000 magnification

2.4 X- Ray Diffractometry (XRD)

XRD is a well known technique used to determine the degree of crystallinity. XRD provides information about the present phases, the concentration levels of phases and the amorphous content of the samples [96]. To compare the bones and to see the effects of antiembolic agents on the crystallinity of bone and the type of crystallinity XRD studies were performed.

2.4.1 Introduction

Bone has a crystalline microstructure. Three basic crystal structures encountered in most materials are the Body Centered Cubic (BCC), Face Centered Cubic (FCC) and Hexagonal Close-Packed (HCP).

When a crystal is mounted and exposed to an intense beam of X-rays, the X-rays

are diffracted by the crystalline phases in the specimen according to Bragg's law:

$$n\lambda = 2d\sin\theta$$

" n is an integer determined by the order given, " λ is the wavelength of X-rays, and moving electrons, protons and neutrons, " d is the spacing between the planes in the atomic lattice, and " θ is the angle between the incident ray and the scattering planes.

The intensities of these reflections are recorded and displayed on a meter and provide information to determine the arrangement of molecules within the crystal in atomic detail as a continuous trace of intensity versus 2θ [95].

In general, the scattering pattern of amorphous materials display broad, low intensity peaks characteristic of the average local atomic environment. As the crystal size gets smaller, diffraction peaks in the intensity versus 2θ curve get broader [97]. Conversely, if the crystalline portion increases, the peaks become narrower and extend to higher intensities. The areas under the crystalline and amorphous peaks are proportional to their volume fraction in the sample [98].

2.4.2 Materials and Methods

The XRD studies were performed at Materials Laboratories of Gebze Institute of Technology. The experiment was run with Rigaku D-Max 2200 X-ray diffractometer with Cu K-alpha 1 radiation. Conventionally healed and anti-embolic agent injected bone samples were placed into the sample holder and the specimen plane was adjusted with the goniometer. The intensity (count per second) versus diffraction angle 2θ (degrees) were recorded by the PC connected to XRD. The diffractometer was running at 40 kV and 40 mA. The wavelength of the characteristic X-rays of Cu to compute d-spacing was 1.54059 Å. The scanning speed was 4 degree per minute.

2.4.3 Results and Discussion

For materials, that are partially crystalline, the amorphous and crystalline contributions to the X-ray diffraction can be interpreted to determine the degree of crystallinity. The sharpening of the distinct peaks or addition of new peaks to the X-ray diffractograms are associated with the increase in the amount of crystal structure in the bone samples. In general, the scattering pattern of amorphous materials shows broad and low intensity peak characteristics.

The effect of antiembolic agents on fractured and healed bones was studied by microstructure analysis with XRD. The X-ray diffraction pattern of control group, is given as intensity (counts per second) versus 2θ (degrees) in all figures in order to observe the effects of antiembolic agents.

X-ray diffraction pattern of control sample is given in Figure 2.59.

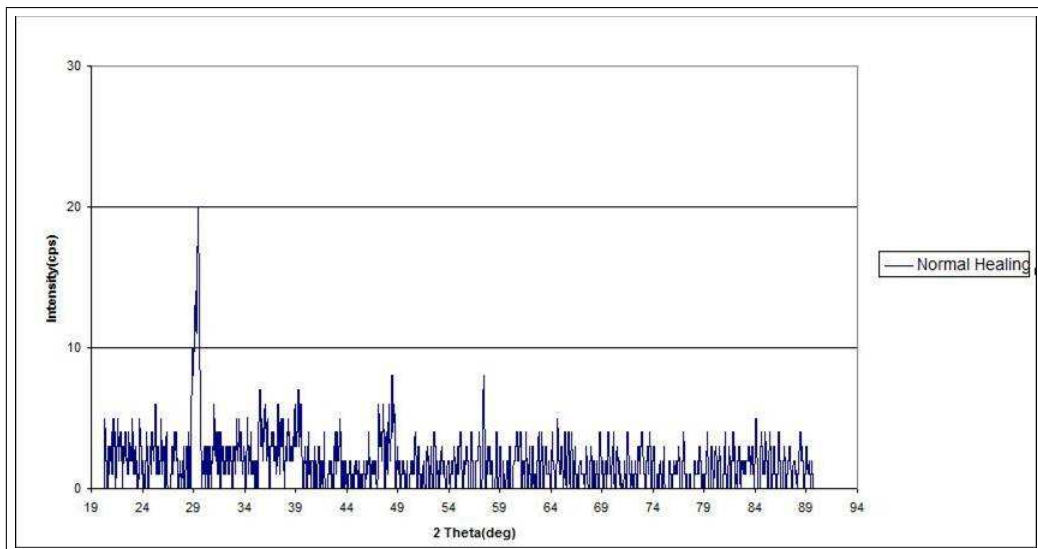


Figure 2.59 The X-ray diffractogram of the fractured and healed control sample

X-ray diffraction pattern of control sample is in the typical trend with a main peak at 2θ of 29.38 degrees and intensity of 20 cps.

X-ray diffraction pattern of heparin-treated fractured and healed bone sample

together with the diffraction pattern of control group is given in Figure 2.60. Figure 2.60 shows the decrease in the contribution of the crystallinity part of the heparin-treated fractured and healed samples. As evidence, the main peak at 2θ of 29.38 is invisible. X-ray diffraction pattern of heparin-treated fractured and healed bone sample shows broad and low intensity peak characteristics like amorphous materials. Additionally, another distinct peak is seen at 2θ of 57.46 in control group, is also disappeared in heparin-treated fractured and healed bone sample.

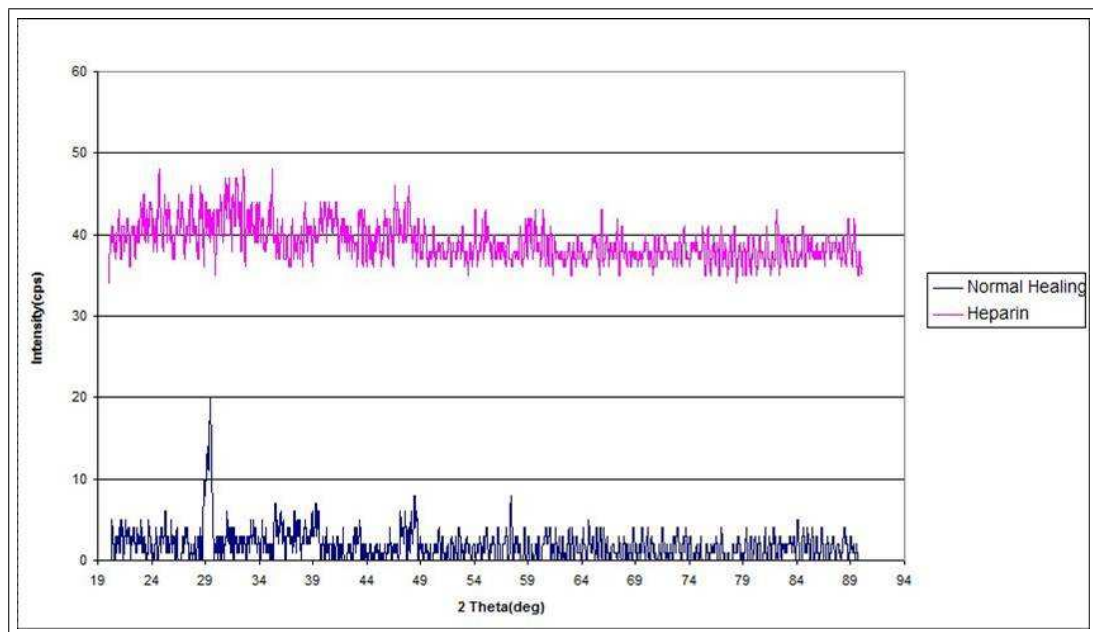


Figure 2.60 The X-ray diffractogram of the fractured and healed control sample and the heparin-treated sample

X-ray diffraction pattern of LMWH-treated fractured and healed bone sample together with the diffraction pattern of control sample is given in Figure 2.61.

The crystallinity pattern of the LMWH-treated fractured and healed bone sample has a main peak at 2θ of 29.38 with a height of 19 cps as in control group. Other distinct peaks at 2θ of 48.48 and 57.46 is invisible in LMWH-treated fractured and healed bone sample, as heparin-treated fractured and healed sample. Therefore, compared to control sample, LMWH-treated fractured and healed sample has less crystalline structure, on the other hand, compared to heparin-treated fractured and healed sample, it is more crystalline.

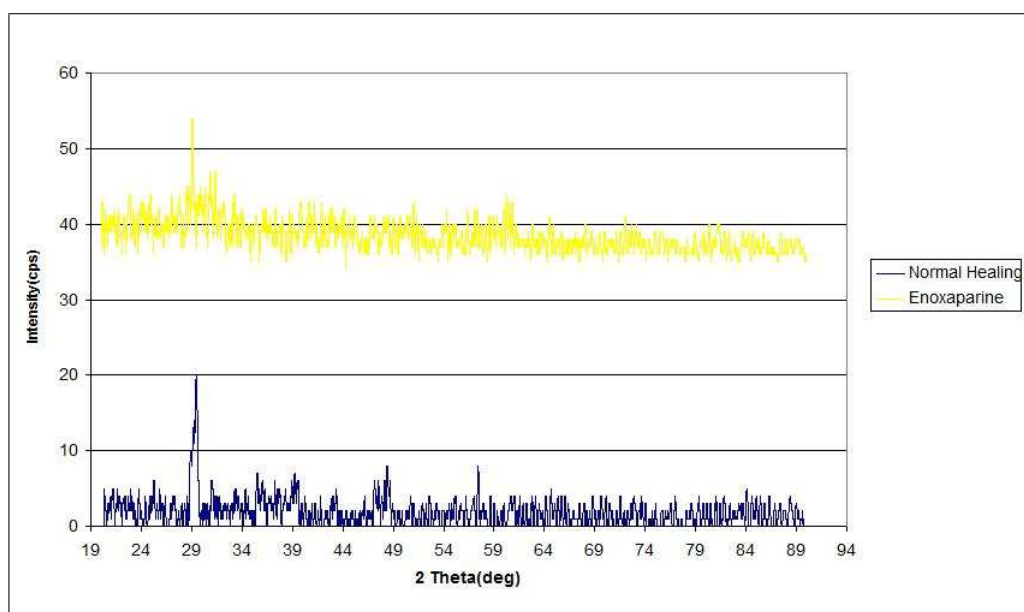


Figure 2.61 The X-ray diffractogram of the fractured and healed control sample and the LMWH-treated sample

The difference between the X-ray diffractograms of fractured and healed control sample and fondaparinux-treated sample is given in Figure 2.62.

The X-ray diffractogram of fractured and healed fondaparinux-treated sample is sharper than the fractured and normally healed sample. The main peak at 2θ of 29.38 is with a height of 34 cps. Additional peak is seen at 2θ of 47.46. The other peaks at 2θ of 48.48 and 57.46 is seen in fractured and healed, fondaparinux-treated sample, as control sample diffractogram with nearly the same intensity.

In order to see the crystallinity difference, X-ray diffractograms of fractured and normally healed sample, heparin-treated sample, LMWH-treated sample and fondaparinux-treated sample is given together in Figure 2.63.

From Figure 2.63, it is remarkable that the diffractogram of fractured and healed, fondaparinux-treated sample gives the highest intensity peaks. That is, has greater contribution of crystalline portion in its structure. At the same time, it has additional crystalline peaks. The diffractogram of heparin-treated sample shows amorphous-like pattern. LMWH-treated sample has less crystalline structure than fractured and nor-

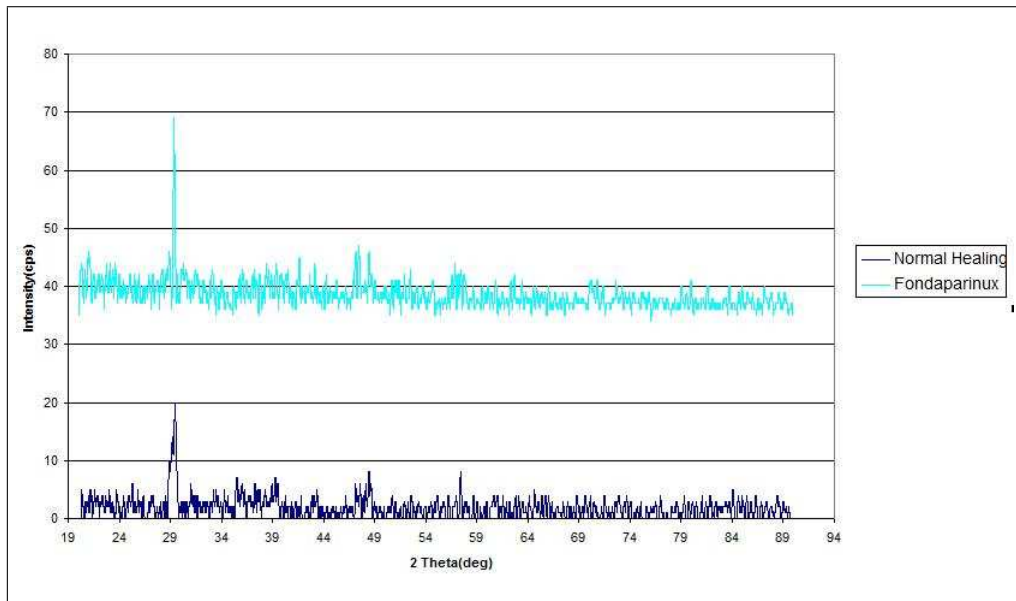


Figure 2.62 The X-ray diffractogram of the fractured and healed control sample and the fondaparinux-treated sample

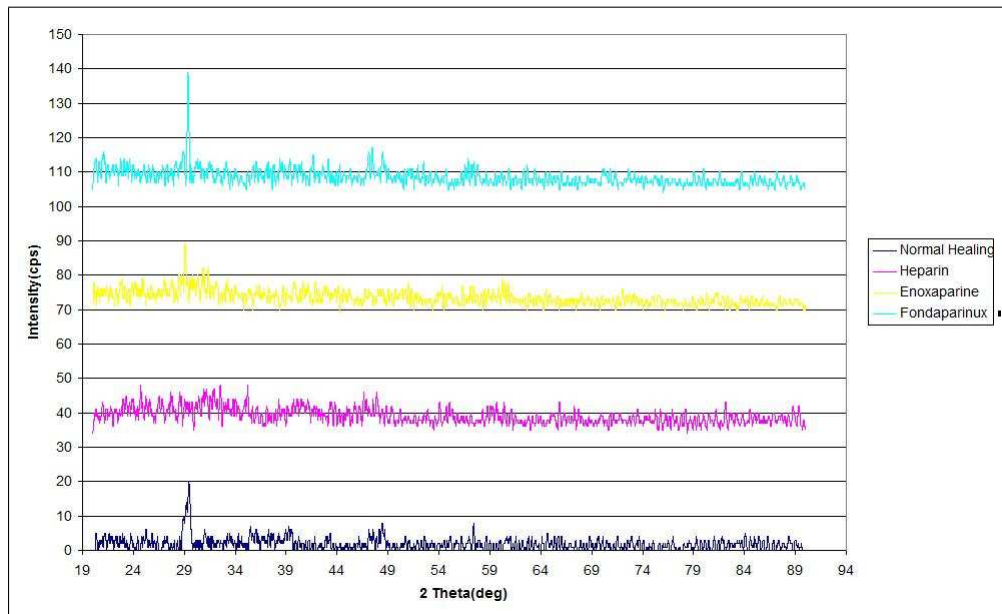


Figure 2.63 The X-ray diffractograms of the control, heparin-treated, LMWH-treated and fondaparinux-treated sample

mally healed sample. In this sense, the chemical effect of antiembolic agents on bone is seen.

3. DISCUSSION

Although anticoagulants must be routinely used in patients presenting risk factors to deep venous thrombosis, as well as in those experiencing fractures at pelvic region, at lower limbs and in the cases of multiple traumas, the effect of antiembolic agents on bone healing mechanism is not a well-known issue for the time being. However material science and engineering knowledge imposes us micro and nano structures, crystallographic structures, the type and distribution of phases and interphases are mostly responsible on the reaction of material against external effects, which include stress, momentum and energy influencing on material directly and/or indirectly. Heparin is an effective [32] antithrombotic agent, but various studies show that it has limitations and side effects on bone such as causing osteoporosis, stimulating bone resorption, increasing calcium loss, decreasing bone mineral density [36, 37, 38]. Some of these limitations of unfractionated heparin are overcome by the use of "low molecular weight heparin" (LMWH) preparations. Nevertheless studies show that they have also negative effect on bone metabolism less than unfractionated heparin [50, 51, 52, 59, 61, 99, 100]. Recently, fondaparinux, at low dosages, is being used for replacing the traditional non-fractionated heparin. Although studies about the fondaparinux are limited, no negative effect on bone metabolism is stated. Besides, in these studies, it is claimed that the negative effects of heparin and similar agents can be prevented by the usage of fondaparinux ([15, 16, 100, 101, 102]).

The effects of antiembolic agents on bone and fracture healing has been studied very much in literature. It is known that heparin has negative effects on bone, nevertheless different views has been proposed about LMWH. In some of studies, it has been suggested that LMWH has also negative effects on bone but not as heparin, and some of them proposed that LMWH has not a clinically meaningful osteoporosis effect. Culture studies on the effects of fondaparinux; a newly coming into synthetic antiembolic agent has been showed that it has not a negative effect on bone.

It has been seen that, there is not enough research on the comparison of the effects of different antiembolic agents on fracture healing in literature (heparin, LMWH and fondaparinux). In this study that evaluates and compares effects of different agents on fracture healing, all animals were injected in the same day by the same surgeon. By daily injection on control group, the stress factor on rats has been standardized.

All information giving in the literature, does not cover on what happens on the inorganic part of the bone. X-ray diffraction studies in this work revealed which kind of compounds and the type of crystallinity formed due to the agents used.

Most probably, whatever is injected into body has more or less effect on the available phases, in the bone. In fact X-ray diffraction studies showed that there is clear interactions between reagent and available phases in terms of phase transition. To our knowledge the type of reaction and thermodynamical and biochemical phenomena of what happens in bone during and after injection of agents is not clear yet. Another type of thermodynamical and biochemical studies are necessary to clarify, why amorphous and crystalline inorganic compounds are obtained.

However, since depending on agents injected, it is clear that different phases are obtained in inside of the fractured and healed bone. Whether phases are amorphous or crystalline, either in micro or nano level, behavior of bone because of that fact would be different;

a) Mass transport and diffusion inside of the phases and on all the interfaces of phases, in that case, would not be same.

b) Crack initiation of any material depends on the type of the crystallinity and the nature of interfaces. Tenacity of interface and deformability of the phases are important parameters, which should not be neglected for the future activities.

Thus, whatever is injected, no matter what the reason is, may alter the structure of the bone, which results in differences in terms of physical, chemical and mechanical

behavior.

Diffusion, phase transformations, mass transport, mechanical relaxations may occur (together with biological activities) in atomic and molecular levels, among atoms, among molecules, among phases being available. Altogether very much complex features are created, new cohesive bondings are obtained, no matter whatever occurs as a result during healing of fracture. Considerations for the future should concentrate on the mechanical stability of the healed bone. To understand, what happens, if the mechanical stability changes, it is necessary to work on from macro until nano level.

We need another extensive researches to understand what is going on inside of the phases and on the interfaces. Because tenacity on the interfaces with respect of insight of the phases gives information on where crack initiation starts and/or, in order to propagate the crack, whether interface or inside of the phase has dragging effect or not.

In this study it is obtained, that inorganic portion of bone is changing whatever anticoagulant agent is injected.

Bone has two main components chemically; 1) organic, 2) inorganic components. In this thesis, it is mainly concentrated on the inorganic part, by the help of XRD technique and SEM. Inorganic part would be crystalline and/or amorphous.

It is well known that inorganic part of bones qualitatively is consisting of apatite, hydroxyapatite, brucide, and calcite in different amounts. Although chemical composition and crystallographic structures are themselves very much important, other things like the amount of each component, designing and alignment of those components with the other word textures of materials play important role in the mechanical behavior and mechanical stability. Addition to considerations given above another kind of researches dealing with:

1. interfaces between inorganic-inorganic (either crystalline or amorphous

2. interfaces between inorganic-organic phases
3. mass transport and diffusion among various organic and inorganic phases including the roles of haversian system
4. osteoclasts-osteoblasts activities and their effect of phases and the distribution of phases
5. partially independent and partially inside of what mentioned above, piezoelectrical activities

However all mentioned cannot be included inside of this thesis. Research proposal should include heavily thermodynamical considerations, kinetics of unknown diffusions activities. Certainly time and rate dependency of the bone should not be ignored in the future research.

It is clear, that agents used have effects on the mass transport and diffusion which are controlling healing process. The role that the agents played, as far as we understand, is not only to avoid from hematoma formation, there that agents cause changing piezoelectrical properties due to structural changes.

XRD studies showed also that heparin injection does not allow atoms to form crystalline structure. It is known amorphous phases are metastable. Therefore one might have curiosity if the amorphous phase obtained via heparin transform into the crystalline phases during reasonable time interval. The agent fondaparinux caused to obtain crystalline phases and also in the capacity of SEM layered structure was observed. Nanomechanical studies in the future works will help to understand nature of layered structure. For the time being on this topic there is no satisfactory information to our knowledge.

SEM studies revealed, that agents used helped healing in terms of not having defects comparing to control group what is obtained in control groups where no agents injected into body. It is well known that defects, in any material accelerate crack

initiation and propagation rate. According to what is obtained in this research via SEM studies bone healed without agents injected during healing are more susceptible to brittle fracture. It is necessary to combine SEM studies with micro and nano morphological structures in order to reach hypothesis which agent is better to avoid from brittle fracture. Partially X-ray diffraction studies are helpful, however detailed structural and morphological studies are imperative.

4. CONCLUSION

Conventional methods for fracture healing on the bone may be successful in many cases. However, micro defects and regions where incomplete crack healing are available cannot be observed by conventional X-ray methods used in hospitals. SEM micrographs make visible defects and incomplete fracture on the bone. SEM studies revealed that antiembolic agent injection into animal helped to obtain no defects on the healed region. Moreover, XRD studies showed that inorganic portion of the bone fractured followed by conventional healing is generally crystalline. Heparin injection results in obtaining almost amorphous inorganic part, so that heparin causes from crystalline to amorphous transition. On the other hand, LMWH and fondaparinux did not allow transition from crystalline to amorphous, however the type and amount of crystallinity were different comparing to the case which does not include antiembolic agent injection. To conclude, antiembolic injection into body results in different constitutions on the bones fractured followed by healing.

REFERENCES

1. Cowin, S., *Bone Mechanics Handbook*, London: CRC, 2nd ed., 2001.
2. Liebschner, M. A. K., and M. A. Wettergreen, *Optimization of Bone Scaffold Engineering for Load Bearing Applications, in Topics In Tissue Engineering*, CRC, 2003.
3. Cruess, R. L., and J. Dumont, *Healing of bone, tendon, and ligament: Fractures*, Lippincott, 2nd ed., 1975.
4. Bronner, F., and R. V. Worrell, *Orthopaedics: Principles of Basic and Clinical Science*, Boca Raton: CRC, 1999.
5. McClintock, F. A., and A. S. Argon, *Mechanical Behavior of Materials*, New York: Addison Wesley, 1996.
6. McMahan, C. J., *Structural Materials*, PA: Merion, 2004.
7. Argon, A. S., *Fracture: Strength and Toughness Mechanisms in Comprehensive Composite Materials*, New York: Pergamon, 2000.
8. Ritchie, R., "How really tough is human cortical bone," Vol. 1, p. 30, New Orleans, USA: TMS Meeting, 2008.
9. Nalla, R. K., J. J. Kruzic, and J. Kinley, "Effect of aging on the toughness of human cortical bone evaluation by r-curves," *Bone*, Vol. 1, no. 35, pp. 1240–1246, 2004.
10. Dökmeçi, M. C., "Recent advances vibrations of piezoelectric crystals," *International Journal of Engineering Science*, Vol. 1, no. 18, pp. 431–448, 1980.
11. Hak, D. J., R. L. Stewart, and S. J. Hazelwood, "Effect of low molecular weight heparin on fracture healing in a stabilized rat femur fracture model," *Journal of Orthopedic Research*, pp. 645–652, 2006.
12. Folwarczna, J., W. Janiec, and L. Sliwinski, "Effects of heparin and low molecular weight heparins on bone mechanical properties in rats," Vol. 2, no. 56, pp. 940–946, 2004.
13. Folwarczna, J., W. Janiec, and M. Barej, "Effects of nadropan on bone histomorphometric parameters in rats," *Pol. J Pharmacol*, Vol. 4, no. 56, pp. 337–343, 2004.
14. Folwarczna, J., W. Janiec, and M. Gawor, "Effects of enoxaparin on histomorphometric parameters of bones in rats," *Pol. J Pharmacol*, Vol. 56, no. 4, pp. 451–457, 2004.
15. Matziolis, G., A. Perka, and H. Disch, "Effects of fondaparinux compared with dalteparin, enoxaparin and unfractionated heparin on human osteoblasts," *Calcif Tissue Int.*, Vol. 73, no. 4, pp. 370–379, 2003.
16. Hanschin, A. E., O. A. Trentz, and S. P. Hoerstrup, "Effect of low molecular weight heparin (dalteparin) and fondaparinux (arietta) on human osteoblasts in vitro," *Br. J. Surgery*, Vol. 92, no. 2, pp. 177–183, 2005.
17. Hansell, M. J., *Fractures and the healing process*, New York: Orthop Nurs, 1988.
18. Baron, R., *Anatomy and Ultrastructure of Bone, in Primer on the Metabolic Bone Diseases and Disorders of Mineral Metabolism*, Philadelphia: Lippincott-Williams and Wilkins, 1999.

19. Park, J. B., and R. S. Lakes, *Biomaterials: An Introduction*, New York: Plenum Press, 2nd ed ed., 1992.
20. Behiri, J., and D. Vashishth, *Biomechanics of Bone*, in *Clinical Biomechanics*, New York: Churchill Livingstone, 2000.
21. Trostle, S. S., and M. D. Markel, "Fracture biology, biomechanics, and internal fixation," *Vet Clin North Am Food Anim Pract*, Vol. 12, no. 1, pp. 19–46, 1996.
22. Vaughan, J., *The Physiology of Bone*, Oxford: Clarendon, third edition ed., 1981.
23. Fleisch, H., *Bisphosphonates in Bone Disease. From the laboratory to the Patient*, New York: The Parthenon Publishing Group, 2nd edition ed., 1995.
24. Kobayashi, D., "Time-dependent expression of bone sialoprotein fragments in osteogenesis induced by bone morphogenetic protein," *J Biochem*, Vol. 119, no. 3, pp. 475–481, 1996.
25. Favus, M. J., "Primer on the metabolic bone diseases and disorders of mineral metabolism," in *An Official Publication of the American Society for Bone and Mineral Research* (Favus, M. J., ed.), New York: Raven, 2nd edition ed., 1993.
26. Childs, S. G., "Stimulators of bone healing. biologic and biomechanical," *Orthop Nurs*, Vol. 22, no. 6, pp. 421–428, 2003.
27. Childs, S. G., "Bone as a collagen-hydroxyapatite composite and its repair," *Trends in Biomaterials Artificial Organs*, Vol. 22, no. 2, pp. 112–120, 2008.
28. Greenbaum, M. A., and I. O. Kanat, "Current concepts in bone healing. review of the literature," *J Am Pediatr Med Assoc*, Vol. 83, no. 3, pp. 123–129, 1993.
29. Remedios, A., "Bone and bone healing," *The veterinary clinics of north america*, Vol. 29, no. 5, pp. 1029–1044, 1993.
30. Mann, F. A., and J. T. Payne, "Bone healing," *Semin Vet Med Surg (Small Anim)*, Vol. 4, no. 4, pp. 312–321, 1989.
31. White, A. A., M. M. Panjabi, and W. O. Southwick, "The four biomechanical stages of fracture repair," *J Bone Joint Surg Am*, Vol. 59, no. 2, pp. 188–192, 1977.
32. Thomas, M. H., "Venous thromboembolism," *American Journal of Respiratory and Critical Care Medicine*, Vol. 159, 1999.
33. Jeffrey, S. F., "Thrombosis-embolism," in *Deep-vein thrombosis: Advancing awareness to protect patient lives*, Washington: Public Health Leadership Conference on Deep-Vein Thrombosis, 2003.
34. Kumar, V., R. S. Cotran, and S. L. Robbins, *Hemodynamic Disorders, Thrombosis and Shock. In Basic Pathology*, Philadelphia: Saunders, 2000.
35. Heit, J. A., M. D. Silverstein, D. N. Mohr, T. M. Petterson, C. M. Lohse, W. M. OFallon, and L. J. Melton, "The epidemiology of venous thromboembolism in the community," *Thrombosis and Haemostasis*, Vol. 86, no. 1, pp. 452–463, 2001.
36. Matzsch, T., D. Bergqvist, U. Hedner, B. Nilsson, and P. Ostergaard, "Heparin induced osteoporosis in rats," *Thromb Haemost.*, Vol. 56, no. 15, pp. 293–294, 1986.

37. Ginsberg, J. S., G. Kowalchuk, J. Hirsh, E. P. Brill, R. Burrows, and G. Coates, "Heparin induced osteoporosis in rats," *Thromb Haemost.*, Vol. 22, no. 64, pp. 286–289, 1990.
38. Ginsberg, J. S., G. Kowalchuk, J. Hirsh, E. P. Brill, R. Burrows, and G. Coates, "Prolonged heparin therapy in pregnancy causes bone demineralization.," *Br J Obstet Gynaecol*, Vol. 12, no. 90, pp. 1129–1134, 1983.
39. Barbour, D. A., S. D. Kick, J. F. Steiner, M. E. Loverde, L. N. Heddleston, and J. L. Lear, "A prospective study of heparin-induced osteoporosis in pregnancy using bone densitometry.," *Am J Obstet Gynaecol*, Vol. 3, no. 170, pp. 862–869, 1994.
40. Dahlman, T. C., "Osteoporotic fractures and the recurrence of thromboembolism during pregnancy and the puerperium in 184 women undergoing thromboprophylaxis with heparin," *Am J Obstet Gynaecol*, Vol. 168, no. 4, pp. 1265–1270, 1993.
41. Douketis, J. D., J. S. Ginsberg, R. F. Burrows, E. K. Duku, C. E. Webber, and E. P. Brill, "The effects of long-term heparin therapy during pregnancy on bone density. a prospective matched cohort study," *Thromb Haemost*, Vol. 75, no. 2, pp. 254–257, 1996.
42. Mandach, U. V., F. Aebbersold, R. Huch, and A. Huch, "Short-term low-dose heparin plus bedrest impairs bone metabolism in pregnant women," *Eur J Obstet Gynaecol Reprod Biol* .10, Vol. 106, no. 1, pp. 25–30, 2003.
43. Gennes, C. C. P. D., and M. M. Samama, "Osteoporosis induced either by unfractionated heparin or low molecular weight heparin," *J Mal Vasc.*, Vol. 21, no. 3, pp. 121–125, 1996.
44. Sivakumaran, M., K. Ghosh, Y. Zaidi, and R. M. H. ., "Osteoporosis and vertebral collapse following low-dose, low molecular weight heparin therapy in a young patient," *Clin Lab Haematol*, Vol. 18, no. 1, pp. 55–57, 1996.
45. Casele, H. L., and S. A. Laifer, "Prospective evaluation of bone density in pregnant women receiving the low molecular weight heparin enoxaparin sodium," *J Matern Fetal Med*, Vol. 9, no. 2, pp. 122–125, 2000.
46. Pettila, V., P. Leinonen, A. Markkola, V. Hiilesmaa, and R. Kaaja, "Postpartum bone mineral density in women treated for thnomboprophylaxis with unfractionated heparin or lmw heparin," *Thromb Haemost*, Vol. 87, no. 2, pp. 182–186, 2002.
47. Wawrzynska, L., W. Z. Tomkowski, J. Przedlacki, B. Hajduk, and A. Torbicki, "Changes in bone density during long-term administration of low-molecular weight heparins or acenocoumarol for secondary prophylaxis of venous thromboembolism," *Thromb Haemost*, Vol. 33, no. 2, pp. 64–67, 2003.
48. Monreal, M., L. Vinas, L. Monreal, S. Lavin, E. Lafoz, and A. M. Angles, "Heparin-related osteoporosis in rats. a comparative study between unfractionated heparin and a low-molecular weight heparin," *Haemostasis*, Vol. 20, no. 4, pp. 204–207, 1990.
49. Hurley, M. M., B. E. Kream, and L. G. Raisz, "Structural determinants of the capacity of heparin to inhibit collagen synthesis in 21-day fetal rat calvariae," . *J Bone Miner Res*, Vol. 5, no. 11, pp. 1127–1233, 1990.
50. Murray, W. J., V. S. Lindo, W. Kakar, and M. E., "Long-term administration of heparin and heparin fractions and osteoporosis in experimental animals," *Blood Coagul Fibrinolysis*, Vol. 6, no. 2, pp. 113–118, 1995.

51. Shaughnessy, S. G., E. Young, P. Deschamps, and J. Hirsh, “. the effectss of low molecular weight and standard heparin on calcium loss from fetal rat calvaria,” *Blood*. 15, Vol. 86, no. 4, pp. 1314–1320, 1995.
52. Muir, J. M., M. Andrew, J. Hirsh, J. I. Weifz, E. Young, and P. Deschamps, “Histomorphometric analysis of the effects of standard heparin on trabecular bone in vivo,” *Blood*. 15, Vol. 88, no. 4, pp. 1314–1320, 1996.
53. Muir, J. M., J. Hirsh, J. I. Weifz, M. Andrew, E. Young, and S. G. Shaughnessy, “A histomorphometric comparison of the effects of heparin and low-molecular weight heparin on cancellous bone in rats,” *Blood*. 1, Vol. 89, no. 9, pp. 3236–3242, 1997.
54. Bhandari, M., J. Hirsh, J. I. Weitz, E. Young, T. J. Venner, and S. G. Shaughnessy, “The effects of standard and low molecular weight heparin on bone nodule formation in vitro,” *Thromb Haemost*, Vol. 80, no. 3, pp. 413–417, 1998.
55. Shaughnessy, S. G., J. Hirsh, M. Bhandari, J. M. Muir, E. Young, and J. I. Weifz, “A histomorphometric evaluation of heparin-induced bone loss after discontinuation of heparin treatment in rats,” *Blood* 15, Vol. 93, no. 4, pp. 1231–1236, 1999.
56. Kock, H. J., and A. E. Handschin, “Osteoblast growth inhibition by unfractionated heparin and by low molecular weight heparins: an in-vitro investigation,” *Clin Appl Thromb Hemost*, Vol. 8, no. 3, pp. 251–255, 2002.
57. Folwarczna, J., W. Janiec, M. Barei, U. Cegiela, M. Pytlik, and K.-I. Sedlak, “Effects of nadroparin on bone histomorphometric parameters in rats,” *Pol J Pharmacol*, Vol. 56, no. 3, pp. 337–343, 2004.
58. Stinchfield, R. A., B. Sankaran, and R. Samilson, “The effect of anticoagulation therapy on bone repair,” *J Bone Joint Surg*, Vol. 38, no. A, pp. 270–282, 1956.
59. Street, J. T., M. McGrath, K. O’Regan, A. Wakai, A. McGuinness, and H. P. Redmond, “Thromboprophylaxis using a low molecular weight heparin delays fracture repair,” *Clin Orthop Relat Res*, Vol. 381, no. A, pp. 278–289, 2000.
60. Kock, H. J., S. Werther, H. Uhlenkott, and G. Taeger, “Influence of unfractionated and low molecular weight heparin on bone healing: an animal model,” *Unfallchirurg*, Vol. 105, no. 9, pp. 91–96, 2002.
61. Hak, D. J., R. L. Stewart, and S. J. Hazelwood, “Effect of low molecular weight heparin on fracture healing in a stabilized rat femur fracture model,” *J Orthop Res*, Vol. 24, no. 4, pp. 645–652, 2006.
62. Mizuno, K., K. Mineo, and T. Tachibana, “The osteogenetic potential of fracture hematoma. subperiosteal and intamuscular transplantation of the haematoma,” *J Bone Joint Surg*, Vol. 72, no. 9, pp. 822–829, 1990.
63. Hawkins, D., and J. Evans, “Minimising the risk of heparin-induced osteoporosis during pregnancy,” *Expert Opin Drug Saf*, Vol. 3, no. 4, pp. 583–590, 2005.
64. Rajgopal, R., M. Bear, M. K. Butcher, and S. G. Shaughnessy, “The effect of heparin and low molecular weight heparins on bone,” *Thromb Res*. Aug 21, 2007.
65. Huo, M. H., and N. M. Troiano, “The influence of ibuprofen on fracture repair: biomechanical, biochemical, histologic and histomorphometric parameters in rats,” *J Orthop Res*, Vol. 9, no. 3, pp. 383–390, 1991.

66. Akman, ., A. Göğüş, N. Şener, B. Bilgiç, and B. Aksoy, "Sıçan tibia kırıkları sonrası uygulanan diklofenak-sodyum'un kırık kaynaması üzerine etkileri," *Hacettepe Ortopedi Dergisi*, Vol. 11, no. 2, pp. 55–60, 2001.
67. Şener, N., . Akman, A. Göğüş, and B. Bilgiç, "Sıçan tibia diafiz kırıklarında kalsiyum sülfatın kırık iyileşmesi üzerine etkileri," *Acta Ortop Traumatol Turc*, Vol. 35, pp. 435–437, 2001.
68. Krischak, G. D., P. Augat, R. Blakytyn, L. Claes, L. Kinzl, and A. Beck, "The nonsteroidal anti-inflammatory drug diclofenac reduces appearance of osteoblasts in bone defect healing in rats," *Arch Orthop Trauma surg*, Vol. 127, no. 6, pp. 453–458, 2007.
69. Giordano, V., M. Giordano, I. G. Kackfuss, M. I. Apfel, and R. D. Gomes, "Effect of tenoxicam on fracture healing in rat tibiae," *Injury*, Vol. 34, no. 2, pp. 85–94, 2003.
70. Beck, A., K. Salem, G. Krischak, L. Kinzl, M. Bischoff, and A. Schmelz, "Nonsteroidal anti-inflammatory drugs (nsaids) in the perioperative phase in traumatology and orthopedics effects on bone healing," *Op orthop Traumatol*, Vol. 17, no. 6, pp. 569–578, 2005.
71. Kellinsalmi, M., V. Parikka, J. Risteli, T. Hentunen, H. V. Leskela, and S. Lehtonen, "Inhibition of cyclooxygenase-2 down regulates osteoclast and osteoblast differentiation and favours adipocyte formation in vitro," *Eur J Pharmacol*. 31, Vol. 572, no. 2-3, pp. 102–110, 2007.
72. Meunier, A., and P. Aspenberg, "Parecoxib impairs early metaphyseal bone healing in rats," *Arch Orthop Trauma Surg*, Vol. 126, no. 7, pp. 433–436, 2006.
73. Leonelli, S. M., B. A. Goldberg, J. Safanda, M. R. Bagwe, and S. J. S. S. K. ., "Effects of a cyclooxygenase inhibitor (rofecoxib) on bone healing," *Med J Orthop*, Vol. 35, no. 2, pp. 79–84, 2006.
74. Saraf, S. K., A. Singh, R. S. Garbyal, and Y. Singh, "Effect of simvastatin on fracture healing: an experimental study," *Indian J Exp Biol*, Vol. 45, no. 5, pp. 444–449, 2007.
75. Adah, F., H. Benghuzzi, M. Tucci, G. Russell, and B. England, ". cholesterol production inhibitor (statin) increased bone healing in surgically created femoral defect in an animal model," *Biomed Sci instrum*, Vol. 43, pp. 95–103, 2007.
76. Erdemli, B., S. S. Kılıçoğlu, and E. Erdemli, "A new approach to the treatment of osteoporosis," *Orthopedics* ., Vol. 28, no. 1, pp. 59–62, 2005.
77. Kılıçoğlu, S., and E. Erdemli, "New addition to the statin's effect," *J Trauma*, Vol. 63, no. 1, pp. 187–191, 2007.
78. Costa, E. R., P. Weinhold, G. A. Tayrose, J. A. Hooker, and L. E. Dahners, "The effect of levodopa or levodopa-carbidopa (sinemet) on fracture healing," . *J Orthop Trauma*, Vol. 20, no. 7, pp. 470–475, 2006.
79. Aslan, M., G. Şimşek, and E. Dayı, "The effect of hyaluronic acid-supplemented bone graft in bone healing: experimental study in rabbits," *J Biomater Appl*, Vol. 29, no. 3, pp. 209–220, 2006.
80. Baldık, Y., U. Talu, L. Altınel, H. Bilge, M. Demiryont, and G. Aykaç-Toker, "Bone healing regulated by nitric oxide: an experimental study in rats," *Clin Orthop Relat Res*, Vol. 404, pp. 343–352, 2002.

81. Türk, C., M. Halıcı, A. Güney, H. Akgün, V. Şahin, and S. Muhtaroglu, "Promotion of fracture healing by vitamin e in rats," *J Int Med Res*, Vol. 32, no. 5, pp. 507–512, 2004.
82. Karaçal, N., P. Koşucu, U. Çobanoğlu, and N. Kutlu, "Effect of human amniotic fluid on bone healing," *J Surg Res*, Vol. 129, no. 2, pp. 283–287, 2005.
83. Dudkiewicz, I., T. Brosh, M. Perelman, and M. Salai, "Colchicine inhibits fracture union and reduces bone strenght-in vivo study," *J Orthop Res*, Vol. 23, no. 4, pp. 877–881, 2005.
84. Aslan, M., G. Şimşek, and U. Yıldırım, "Effects of short-term treatment with systemic prednisone on bone healing: an experimental study in rats," *Dent Traumatol*, Vol. 21, no. 4, pp. 222–225, 2005.
85. Huddleston, P. M., J. M. Steckelberg, A. D. Hanssen, M. S. Rouse, M. E. Bolander, and R. Patel, "Ciprofloxacin inhibition of experimental fracture healing," *J Bone Joint Surg*, Vol. 82, no. A, pp. 161–173, 2000.
86. Perry, A. C., B. Prpa, M. S. Rouse, K. E. Piper, A. D. Hanssen, and J. M. Steckelberg, "Levofloxacin and trovafloxacin inhibition of experimental fracture-healing," *Clin Orthop Relat Res*, Vol. 441, pp. 95–100, 2003.
87. Ince, A., N. Schütze, N. Karl, J. F. Löhr, and J. Eulert, "Gentamicin negatively influenced osteogenic function in vitro," *Int orthop*, Vol. 312, pp. 223–228, 2007.
88. Mammi, G., R. Rocchi, R. Cadossi, and G. Traina, "Effects of pemf on healing of human tibial osteotomies: Double blind study," *Clin Orthop*, Vol. 288, pp. 246–253, 1993.
89. Heckman, J. D., J. Ryaby, and J. McCabe, "Acceleration of tibial fracture healing by non invasive, low intensity pulsed ultrasound," *J Bone Joint Surg*, Vol. 76, no. A, pp. 26–34, 1994.
90. Eckardt, H., K. S. Christensen, M. Lind, E. S. Hansen, and D. W. Hall, "Recombinant human bone morphogenetic protein 2 enhances bone healing in an experimental model of fractures at risk of non-union injury," Vol. 36, no. 4, pp. 494–499, 2005.
91. Kolbeck, S., H. Bail, G. Schmidmaier, M. Alquiza, K. Raun, and A. Kappelgard, "Homologous growth hormone accelerates bone healing, biomechanical and histological study," *Bone*, Vol. 33, no. 4, pp. 628–637, 2003.
92. Bonnarens, F., and T. A. Einhom, "Production of a standard closed fracture in laboratory animals," *J Orhop Res*, Vol. 1, pp. 97–101, 1984.
93. Bart, J. C. J., *Plastics Additives*, Amsterdam, Netherlands: IOS, 2006.
94. Ramakrishna, S., "Introduction to electrospinnig and nanofibers," River Edge NG USA: World Scientific, 2005.
95. Cao, G., "Nanostructures and nanomaterials," Singapore: World Scientific, 2004.
96. Park, J., *Biomaterials Science and Engineering*, New York: Plenum, 1984.
97. Pecsok, R. L., and D. L. Shields, *Modern Methods of Chemical Analysis*, Wiley, international ed., 1968.
98. Treska, M., *Polymer Structure*, Massachusetts Institute of Technology: MIT Open Course Ware, 2006. Available: <http://www.ocw.mit.edu>.

99. Hanschin, A. E., O. A. Trentz, S. P. Hoerstrup, H. J. Kock, G. A. Wanner, and O. Trentz, "Effect of low molecular weight heparin (dalteparin) and fondaparinux (arixtra) on human osteoblasts in vitro," *Br J Surg*, Vol. 92, no. 2, pp. 177–193, 2005.
100. Matziolis, G., C. Perka, A. Disch, and H. Zippel, "Effects of fondaparinux compared with dalteparin, enoxaparin and unfractionated heparin on human osteoblasts," *Calcif Tis sue Int*, Vol. 73, no. 4, pp. 370–379, 2003.
101. Chung, L. T., H. L. Holton, and P. R. Silverman, "The effect of fondaparinux versus enoxaparin in the survival of a congested skin flap in a rabbit model," *Ann Plast Surg*, no. 56, pp. 312–315, 2006.
102. Schlitt, A., M. Buerke, and B. H. D. Peetz, "Fondaparinux and enoxaparin in comparison to unfractionated heparin in preventing thrombus formation on mechanical heart valves in an ex vivo rabbit model," *Thromb Haemost*, no. 90, pp. 245–251, 2003.